UNIVERSITY
OF MICHIGAN

MAR 21 [illegible]

ENGINEERING
LIBRARY

THE AERONAUTICAL QUARTERLY

Volume III NOVEMBER 1951 Part III

CONTENTS

Photoelasticity and Aircraft Design	*H. T. Jessop and C. Snell*
A Note on the Design of Ducted Fans	*Bryan Thwaites*
A New Treatment of Tuned Absorber with Damping	*D. C. Johnson*
A New Approach to Thin Aerofoil Theory	*M. J. Lighthill*
The Profile of Yawed Wings of Infinite Span	*A. D. Young and T. B. Booth*
Beams on Cross Girders with Clamped Ends	*J. M. Klitchieff*
A Direct Aerodynamic Proof of the Biot-Savart Law	*J. Lockwood Taylor*
Review—Laws of Free Turbulence	*Reichardt*

LONDON
ROYAL AERONAUTICAL SOCIETY
4 HAMILTON PLACE W1

10/-

THE AERONAUTICAL QUARTERLY

Editorial Board

Dr. H. ROXBEE COX, D.I.C., F.R.Ae.S., F.I.Ae.S.

Professor S. GOLDSTEIN, F.R.S., F.R.Ae.S.

Sir GEOFFREY TAYLOR, F.R.S.

G. H. DOWTY, F.R.Ae.S. (Chairman of the JOURNAL Committee of the Royal Aeronautical Society)

J. SMITH, C.B.E., F.R.Ae.S., A.M.I.Mech.E. (Chairman of the Technical Board and Executive Committee of the Society of British Aircraft Constructors)

Joint Editors

Dr. A. M. Ballantyne, T.D., A.F.R.Ae.S.
Joan Bradbrooke, A.R.Ae.S.

Editorial Referees

Aerodynamics

(a) General

Prof. L. Bairstow
Dr. G. P. Douglas
Prof. A. A. Hall
Sir B. Melvill Jones
Mr. D. Keith-Lucas
Dr. N. A. V. Piercy
Mr. E. F. Relf
Prof. E. J. Richards

(b) Fluid Motion

Mr. A. Fage
Prof. S. Goldstein
Prof. L. Howarth
Mr. W. P. Jones
Prof. M. J. Lighthill
Dr. J. W. Maccoll
Dr. J. H. Preston
Mr. L. F. G. Simmons
Mr. H. B. Squire
Sir Geoffrey Taylor
Prof. G. Temple
Prof. A. D. Young

(c) Stability and Control

Mr. L. W. Bryant
Mr. S. B. Gates
Mr. G. T. R. Hill
Mr. H. B. Irving
Mr. G. H. Lee
Mr. M. B. Morgan

Helicopters and Propellers

Dr. J. A. J. Bennett
Mr. L. G. Fairhurst
Mr. R. Hafner
Capt. R. N. Liptrot
Mr. J. Mullin

Instruments and Electrical Equipment

Dr. G. E. Bairsto
Mr. G. W. H. Gardner
Mr. C. S. Hudson
Mr. A. N. Irens
Mr. C. N. Jaques
Mr. F. W. Meredith

Aircraft Design

Mr. R. Boorman
Mr. R. M. Clarkson
Mr. A. N. Clifton
Mr. W. S. Farren
Mr. H. H. Gardner
Mr. H. Knowler
Mr. W. E. W. Petter
Mr. F. H. Pollicutt
Mr. A. E. Russell
Mr. R. S. Stafford

Radio and Radar

Mr. J. F. Atherton
Mr. B. G. Gates
Mr. R. L. Smith Rose
Dr. A. M. Uttley
Sir Robert Watson Watt

Aviation Medicine

Dr. A. Buchanan Barbour

Meteorology

Prof. D. Brunt
Mr. J. K. Hardy
Prof. P. A. Sheppard

Sound

Mr. N. Fleming
Mr. W. Makinson

Aircraft Propulsion

Mr. H. Constant
Sir A. H. Roy Fedden
Dr. S. Hooker
Mr. A. R. Howell
Mr. P. Lloyd
Dr. A. W. Morley
Dr. E. S. Moult
Mr. N. S. Muir
Mr. F. Nixon
Mr. F. M. Owner
Mr. H. Pearson
Dr. D. Pye
Mr. H. Sammons
Prof. O. A. Saunders

Air Transport

Mr. P. G. Masefield
Mr. N. E. Rowe
Mr. W. Tye

Aircraft Accessories

Mr. W. C. Clothier
Mr. H. G. Conway
Mr. G. H. Dowty
Mr. R. Graham

Vibration and Flutter

Prof. A. R. Collar
Prof. W. J. Duncan
Mr. R. A. Frazer
Dr. A. Robinson
Mr. H. Temperton

Performance

Mr. H. Davies
Mr. D. R. Newman
Mr. A. H. Yates

Structures

Mr. A. C. Brown
Mr. H. L. Cox
Mr. D. J. Farrar
Dr. H. Roxbee Cox
Prof. W. S. Hemp
Mr. H. B. Howard
Mr. E. D. Keen
Mr. F. A. Kerry
Dr. D. M. A. Leggett
Prof. R. L. Lickley
Prof. A. J. Sutton Pippard
Prof. A. G. Pugsley
Prof. S. C. Redshaw
Mr. R. H. Sandifer
Sir Richard Southwell

Fuels and Oils

Mr. E. L. Bass
Mr. J. W. Drinkwater
Prof. F. H. Garner
Prof. W. E. Garner
Dr. K. E. W. Ridler
Dr. C. G. Williams

Materials

Prof. L. Aitchison
Dr. N. P. Allen
Prof. N. F. Mott
Mr. L. Rotherham
Dr. H. Sutton
Dr. C. Sykes

Flight Testing

Mr. P. A. Hufton
Mr. E. T. Jones
Mr. S. Scott Hall
Mr. H. L. Stevens

Photoelasticity and Aircraft Design

H. T. JESSOP, T.D., M.Sc. and C. SNELL, M.Sc.
(Reader in Photoelasticity, and Lecturer, Civil Engineering Department, University College, London)

1. Introduction

It is now more than 25 years since Coker and Filon first developed photoelasticity as a practicable method of exploring the stress distribution in certain types of engineering components. All engineers must be familiar with the striking photographs of fringe patterns obtained by their method in stressed plates of various shapes viewed in a polariscope. In those early days observations were made on Xylonite models and the method was only applicable to components in which stress distribution was of a two-dimensional type. Moreover, with the apparatus then available investigations were somewhat difficult and many engineers at that time were very distrustful of the results obtained from what was, to them, a little understood laboratory technique.

Since then, however, conditions have changed greatly in many respects. The discovery in 1938 of the "frozen stress" properties of some of the new synthetic resins opened the way to the application of the photoelastic method to three-dimensional stress distributions, the development of new materials has greatly increased the scope and accuracy of the method, experience has confirmed the reliability of results obtained, and engineers have become accustomed to the use of the techniques of the physics laboratory in their research problems. Today, in many branches of engineering, photoelasticity is recognised as one of the most valuable design tools, and new techniques are continually being developed for the application of the method to fresh problems.

The Aircraft Industry is perhaps one of those in which the value of the method is least appreciated; this is probably because so many of the problems of aircraft design are of types which are unsuited to photoelastic investigation. For the photoelastic method, like all other practical methods of stress exploration, is not by any means of universal application. In some cases the shape of a component renders it unsuitable, while in others it may be found impossible to reproduce in a model the system of loading to which the prototype is subjected. Thus the thin panels which form the skin of wings or fuselage could not be investigated by this method because scale models of such parts made in photoelastic material could not support the necessary loads without buckling. It might be noted, however, that the trend towards thicker skins, if it should continue, would probably bring some of these parts within the scope of the photoelastic method. Again, a considerable part of

Paper received November 1951.
[The Aeronautical Quarterly, Vol. III, November 1951]

the stress in some aeroplane parts is due to vibrations of the parts themselves, and it would be impossible to freeze such dynamic stresses into a photoelastic model. Electric resistance strain gauges applied to the actual structure are very properly used for the exploration of stress in such parts.

There are, however, many aeroplane components eminently suitable for photoelastic investigation; components whose form is compact and for which the type of loading applied in service may be very clearly defined. Examples of such components may be found in the short spars and spar attachments connecting sections of the aircraft, in mounting brackets for engine or undercarriage assemblies, and in hinge brackets taking the reactions from control surfaces. All of these are vital to the safety of the aircraft, all are from time to time subject to failure, and in none of them is the stress distribution at all well known. These are, moreover, parts which are not well adapted to exploration by strain gauges, for the stress concentrations in them almost invariably occur in fillets and around holes and cut-outs where the use of gauges is extremely difficult. Granted that the loads to which such parts are subjected vary in both magnitude and direction, and that the failures are almost always due to fatigue—neither of which conditions can be reproduced in a frozen-stress model—but fatigue failures are very closely related to the peak values of the stresses at points of greatest stress concentration, and these points may be identified, and the stresses for any specified load distribution assessed, by the examination of a photoelastic model under a system of static loading. The photoelastic method therefore provides a rapid and simple means of comparing the relative strengths of different designs in such components for any defined load.

2. Outline of the Method

A scale model of the part to be examined is first made in one of the optically active plastics. This model may be machined from a solid block or cast in a mould, the method chosen depending upon the plastic employed and the form of the part. The model is then subjected to a system of dead weight loads reproducing qualitatively one of the systems of loading known to occur in service. It is then placed in an oven and heated to its "critical temperature" (varying from 85°C. to 120°C. for different plastics) and allowed to cool slowly. After cooling the loads are removed and the stresses are then found to be "frozen" into the model.

One method of investigating these models is to cut thin slices from them and to examine the slices in the polariscope using the two-dimensional technique. In order to localise the observations these slices are cut as thin as possible (a thickness as small as 0.04 in. can be obtained without the machining process affecting the frozen stresses), and the optical effect upon light passing through a slice is not large. The close fringe patterns, therefore, which generally characterise the two-dimensional problems are not obtained, the maximum effect at a point of stress concentration rarely producing more than about the first "fringe," but modern apparatus and

methods allow measurement of even this small effect to an accuracy generally better than one per cent. Examination of such a slice will yield the mean value through its thickness of the difference of what are called the "secondary principal stresses" in the plane of the slice, and if the slice is sufficiently thin such a mean value will give a good approximation to the actual value at any point. The determination of the principal stresses from observations of these secondary stress differences, however, can only be achieved in practice at points where the direction of one principal stress is known, and it is fortunate, from the point of view of practical application of the method, that the stress concentrations in which the designer is interested almost invariably occur in regions in which this is the case; that is, on the free surface of the component or in a plane of symmetry.

A second method of examination, the technique for which has only recently been developed, is known as the "scattered light" method. This consists in passing a very narrow beam of polarised light through the solid model and viewing it from a direction perpendicular to that of the beam. For this method the model must be made in a photoelastic material which has the property of scattering light well. This is ensured by incorporating in the material during casting a small quantity of very finely divided solid. The material then has a slightly misty appearance, and the path of the light through it is clearly visible as a narrow illuminated pencil. When there are stresses in the model this pencil is seen to be crossed by dark interference bands or fringes, and if a graph is plotted of the positions of these fringes, the slope of the graph at any point gives a measure of the optical effect of the stresses in the material at that point. Thus in this method, instead of measuring the mean effect of the stresses through a slice of finite thickness, a measure of their effect at any point on the beam is obtained and, since the beam itself may be of a width less than 0.01 in., the method gives a high degree of localisation to the observations and may be used with quite small models.

This method is subject to the same limitations as the slicing method in that the stresses recorded at any point are only principal stresses when the direction of the light beam is that of one principal stress at the point. This condition, however, can always be fulfilled in the most important region, *i.e.* at a point on the free boundary of a model, by allowing the beam to enter the model normal to the surface. Measurement of the fringes seen in such a beam enables a graph to be drawn, and the slope of the graph at the point corresponding to the point of entry of the beam gives a measure of the difference of the principal stresses in the plane of the surface of the model at that point. The approximate directions of these principal stresses are also determined by observing the inclination of the model necessary to give the sharpest definition of the fringes, so that when the slicing technique is used at a later stage to measure the separate stresses, the direction in which slices should be cut is known. Observations by the scattered light method are also used for preliminary exploration of the surface stresses in cases where the location of the points of stress concentration is not immediately obvious. This enables the investigation to be made without having to cut a large number of slices.

There are other methods of examination which may be needed in certain special cases, but for most components of the type mentioned earlier, a combination of the two techniques which have been outlined here will give all the information the designer needs.

3. Two-Dimensional Analogies

While the accurate determination of the stresses in a component may require the use of the three-dimensional techniques outlined, there are many cases in which a large amount of useful qualitative information may be obtained from the examination of models which reproduce in two dimensions some of the characteristics of the actual component. Such models may be cut quickly and inexpensively from polished sheets of suitable photoelastic material, subjected to load, and examined directly in the polariscope. This preliminary investigation is frequently useful in enabling a qualitative comparison to be made between various modifications of a design, for although the stress distributions in such plane models are not identical with those in the prototypes, they indicate with a considerable degree of reliability which type of modification is likely to be most effective in reducing dangerous stress concentrations.

In some cases it is possible that these two-dimensional analogies may yield evidence which is sufficiently conclusive to make the examination of a three-dimensional model unnecessary. In others it may not be possible in the model to reproduce conditions sufficiently close to those in the prototype, and a fuller investigation will then be needed.

4. Illustration of the Photoelastic Method

As an example, an investigation has been made of the stress concentrations in an elevator hinge-bracket from a Spitfire. While this component may not be of special current interest, as it is understood that this particular design is now obsolete, the stress problems involved in its design are of the same type as those occurring in similar components of more modern aircraft, and the methods described here would be equally applicable to such components.

The loading of this particular bracket in service is very simple and is indicated in Fig. 1. The load (estimated at 600 lb.), is applied through a steel pin fitting in a bushed hole in the lug of the bracket, and acts in the plane of the lug. The base of the bracket is secured to the channel-section rear spar of the tailplane by four 2 B.A. bolts, recesses (A) $\frac{1}{2}$ in. in diameter, being machined in the base to provide parallel bearing surfaces for the securing nuts. The bush (B) is secured to the lug by four countersunk rivets through its flange.

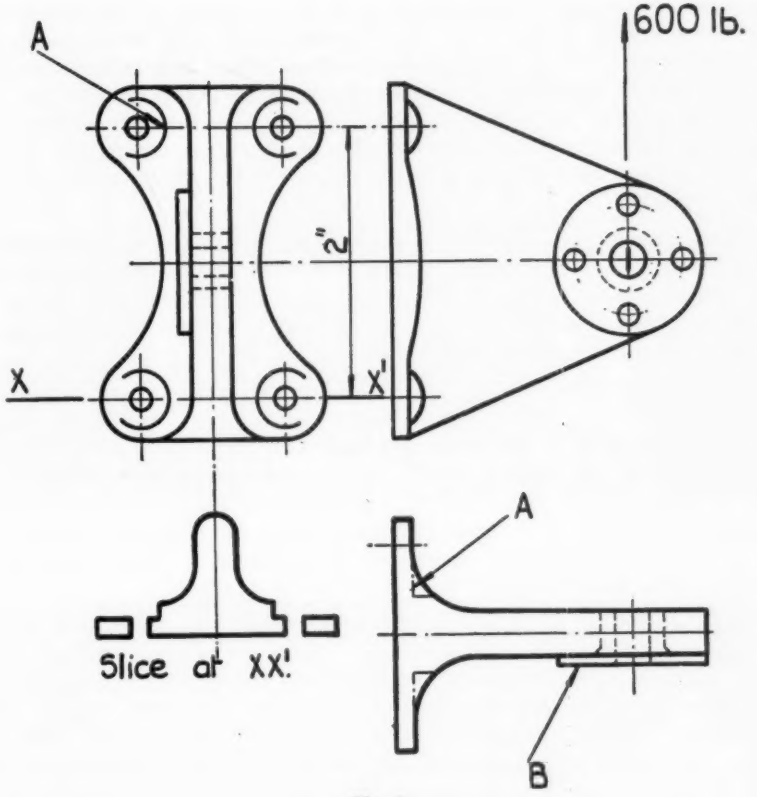

Fig. 1.
Drawings of bracket.

Inspection of the design suggested that the two regions of greatest stress concentration would be found, (*i*) at some point on the boundary of the hole where the load is transmitted from the bush to the lug, and (*ii*) in the neighbourhood of the two securing bolts which are in tension under the load. There were indications that the stress in the second region would prove to be the more serious, for the sharp re-entrant angle produced by machining the recesses would cause a further concentration of tension very close to the area of load application under the nut. A preliminary two-dimensional test was made to study the effect of variation of design in this region.

Figure 2(*a*) shows the fringe pattern in a plate cut to represent a section of the bracket through the two upper bolt-holes. The model was lightly secured to a fixed horizontal plate by two clamps, the jaws of which correspond to the nuts in the

machined recesses, and a vertical load of 10 lb. was applied to the vertical arm. Fig. 2(*b*) represents in two dimensions the effect of providing bosses which form seatings for the nuts and which may be machined without introducing a re-entrant angle. The load on this model was 12 lb. An inspection of the fringe pattern shows that while the 10 lb. load in the first model produced more than three fringes in the angle, the 12 lb. load in the second model produced less than three fringes. A more accurate measurement gave the ratio of the peak stresses per unit load in the two cases as 5 to 3.

The fringe pattern in Fig. 2(*a*) is characteristic of a sharp angle under tension. At first sight it would appear that the boundary stress is higher on either side of the angle than it is at the vertex, but examination of a much enlarged image shows that the highest stress actually occurs at the vertex, but is confined in that region to an extremely narrow strip along the boundary (*see* Fig. 7).

For the three-dimensional investigation a full-size model was cast in "Marco" resin using a "Vinamold" mould, with an actual bracket, supplied by Vickers-Armstrongs, as pattern. The bush was turned from another block of resin and fitted into the lug after casting. Fig. 3 is a photograph of the finished model in its loading frame. The inverted loading was adopted to allow for the model being immersed in a tank of glycerine and water during the "freezing" process, this precaution being necessary to prevent the formation of a "rind" stress in the material due to loss of moisture from the surface on heating.

Special care has to be taken in the method of applying loads when freezing stresses into these models, especially when it is required to investigate the stresses near to load points, for the yield of the photoelastic material is large compared with that of the material of the prototype, and this may lead to serious changes in load distribution if suitable precautions are not taken. In this model the method of bolting the bracket to its support needed special attention. To ensure that local yield of the plastic round the bottom bolts did not allow the base of the bracket to lose contact with its support, these bolts were provided with spring washers (*P*, Fig. 3) whose strength was just sufficient to maintain contact under the load. Also, thick washers of the "Marco" resin were inserted under all the nuts to prevent the edges of the nuts cutting into the softer material of the model. One feature of the prototype which was not reproduced in the model was the riveting of the bush flange to the lug. To obtain a satisfactory reproduction of this, using rivets of the same material as the lug, would have necessitated making a larger scale model, and since the observations on the first model showed conclusively that this was not the critically stressed region, it was thought unnecessary to undertake this.

It may be noted, however, that the way in which the load is shared between rivets and bush in such a construction as this might be important in other similar components. The distribution will obviously be related to the amount of initial tension in the rivets, and tests would have to be made using some method of varying this factor. This problem might well be the subject of a future investigation.

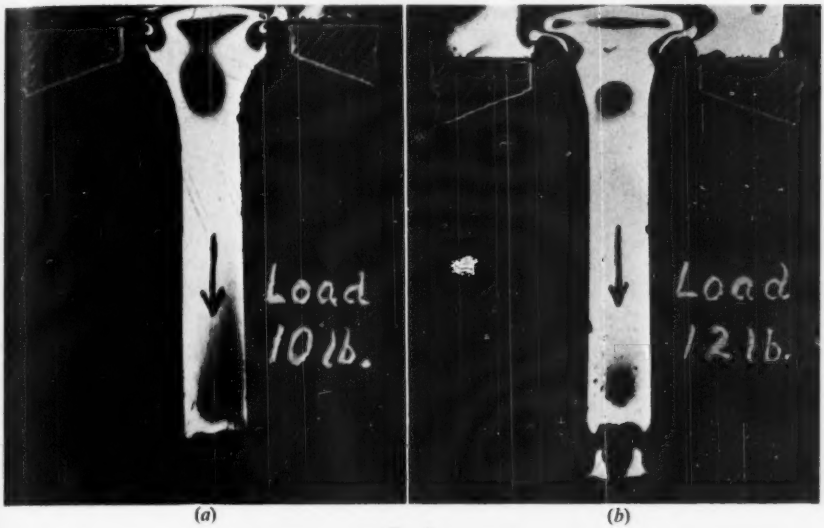

(*a*) (*b*)

Fig. 2.
Fringe patterns in two-dimensional models.

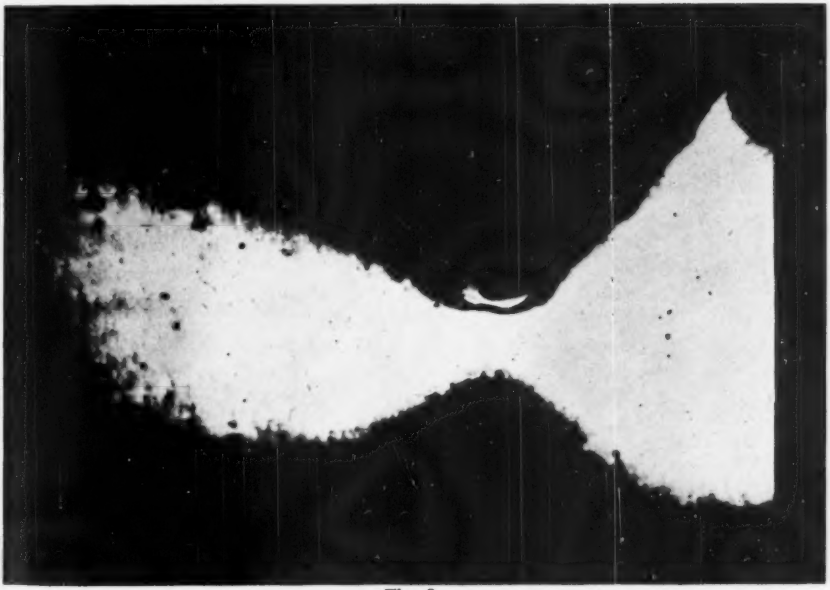

Fig. 8.
Enlarged photograph of fringes in corner of slice cut along XX' (Fig. 1).

Fig. 4
Fringe pattern in lug.

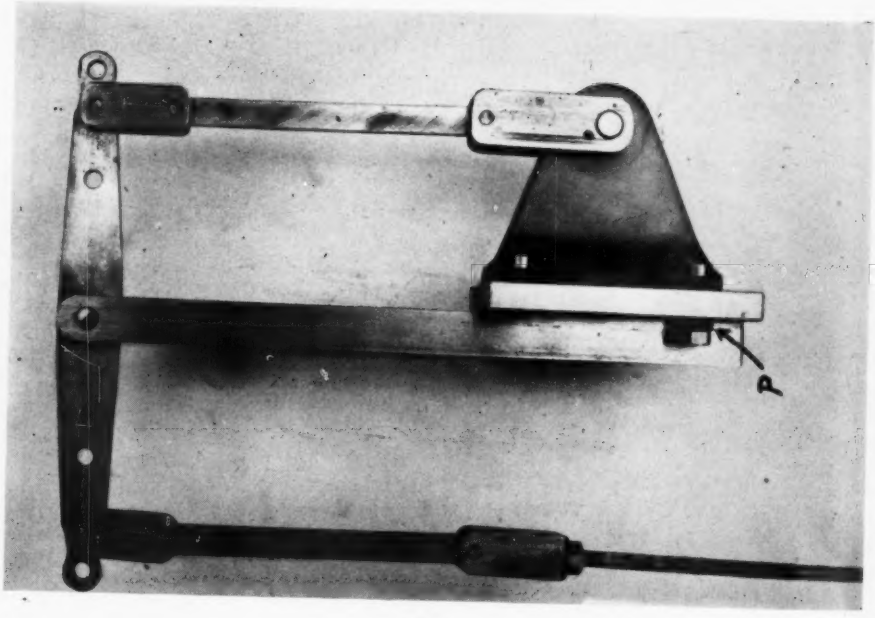

Fig. 3 *(left).*
Photoelastic model in its loading rig.

Photoelastic model in its loading rig.

The model was subjected to a load of 3 lb. and heated in its glycerine and water bath to 90°C., at which temperature it remained for half an hour before being allowed to cool to room temperature in about 15 hours. The load was then removed and the model taken from its frame for examination. The bush was first removed and the lug of the bracket examined in the standard polariscope. Under the loading conditions of this test the greater part of the lug has approximately a simple two-dimensional stress distribution, and the principal stress differences may be deduced directly from the fringe pattern seen through the thickness of the lug. Fig. 4 is a photograph of these fringes taken in monochromatic mercury green light, and Fig. 5 shows the distribution of lines of principal stress in this region as deduced from the isoclinic fringes.

At points on the "free" boundary the fringes indicate the actual magnitude of the boundary stress (the stress normal to the boundary being zero), and this is seen to be a maximum at *A* (Fig. 4) where the stress in the model produces 1.3 fringes through the thickness of the lug. The relation between optical effect and stress is found from a calibration test-piece cast from the same mix as the model and heated with it under a simple load. From this the "fringe value" of the material is found. This is the stress difference in lb./in.² which would produce one fringe in light passing through one inch thickness of the stressed material. For the material of this model the fringe value was found to be 4.47 lb./in.² per fringe per inch, and from this the tension at *A* was calculated as 19.3 lb./in.² in the model, which corresponds to approximately 3,900 lb./in.² in the prototype under a load of 600 lb.

On the boundary of the hole at *B* the stress difference indicated by the fringe pattern is the algebraic difference between an approximately tangential tensile stress and the compressive stress due to the load transmitted by the bush. The 2.86 fringes recorded at *B* correspond to a stress difference of 9,600 lb./in.² in the prototype, or 4,800 lb./in.² shear stress. To obtain the magnitudes of the separate stresses in this region, observations by the scattered light method were made. The end of the lug was cut off to allow a beam of polarised light to be passed into the model normal to the boundary of the hole at various points around the portion *AB* of the circumference (Fig. 6). The graph of the fringes at the point *C* where the circumferential stress was found to be a maximum is shown in Fig. 7. The slope of the graph at *O* shows a fringe gradient of 6.5 fringes per inch, and this corresponds to a tension in the boundary of 29 lb./in.² in the model or 5,800 lb./in.² in the prototype. The normal thrust due to the bush is then deduced as 3,800 lb./in.²

To examine the stresses in the region of the securing bolts a thin slice was cut from the frozen model, the mid-plane of the slice corresponding to the section across *XX'* (Fig. 1). The slice was 1/16 in. thick, and when examined in the ordinary polariscope showed less than one fringe over most of its area, although at least one fringe was discernible in the sharp angle corresponding to the inner edge of the recess *A*. When examined with a magnification of 15 times, however, the second fringe was seen at the extreme point of the angle. Fig. 8 is a photograph taken with

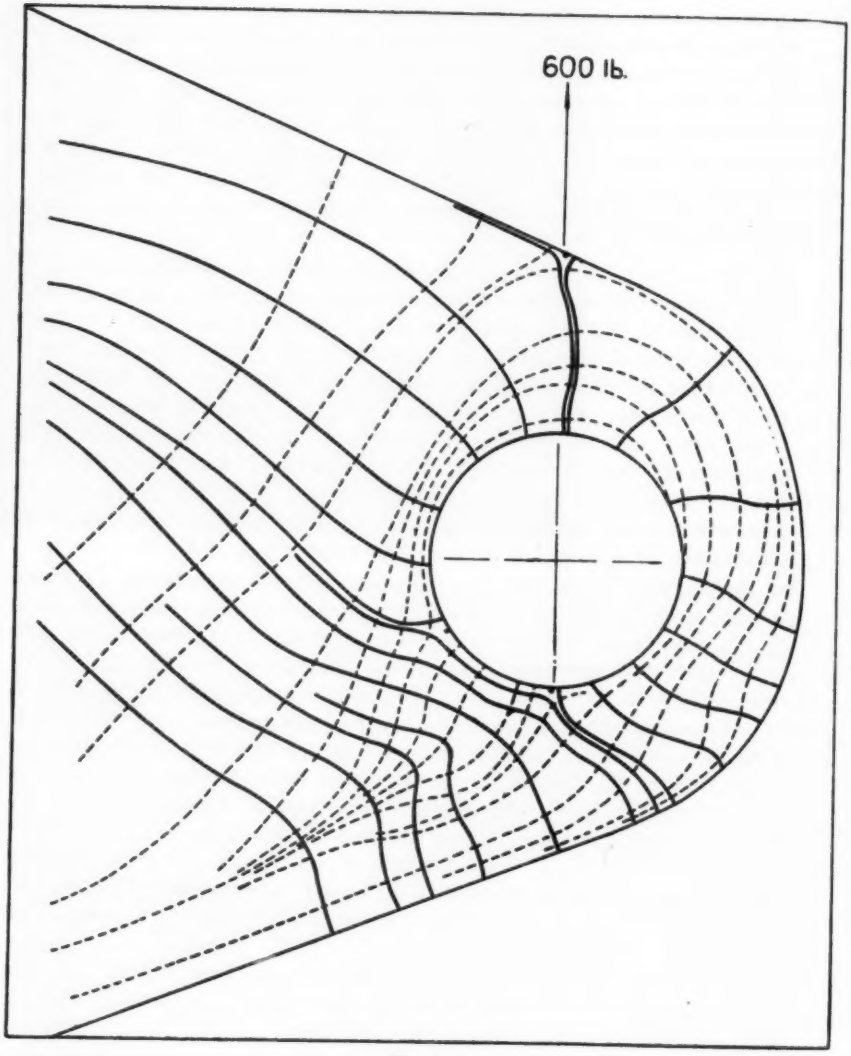

Fig. 5.
Lines of principal stress in lug.

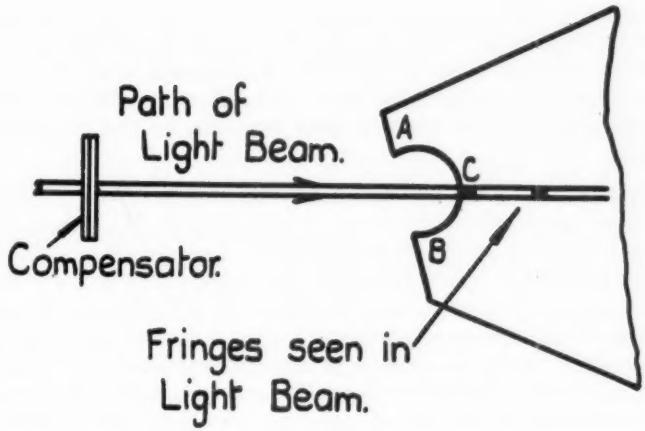

Fig. 6.
Method of examination by scattered light.

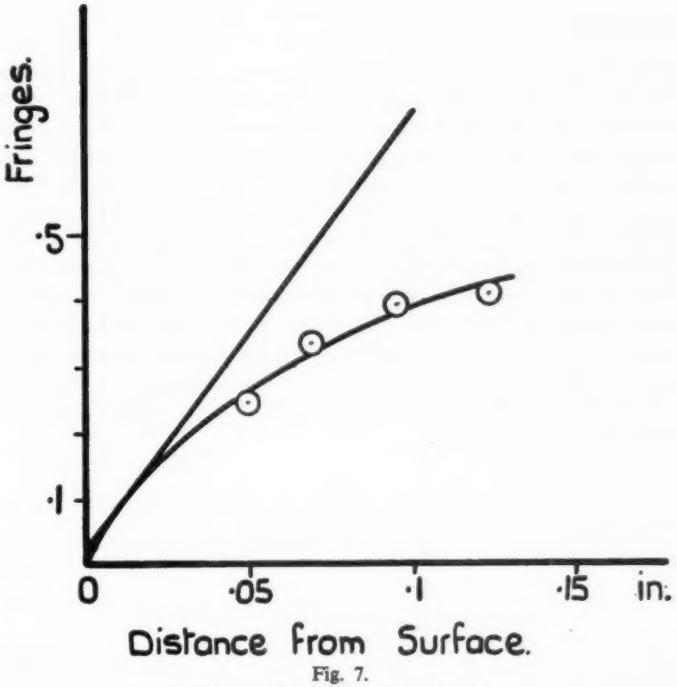

Fig. 7.
Graph of fringes in scattered light.

this magnification. Thus the stress concentration at this point produces two fringes through a thickness of 1/16 in. and this corresponds to a stress of over 28,000 lb./in.^{2} in the prototype under 600 lb. load. Examination of the slice in a tilting stage microscope confirmed that the plane of the slice is a principal plane in the region of the angle, and this stress therefore represents the true maximum tension in the corner.

The original bracket was then modified by the addition of four cylindrical plugs which fitted into the machined recesses and projected slightly to form bosses on which bearing surfaces for the nuts could be machined. A new model was cast from this and stresses were frozen into it as before. The modification produced no change in the stresses around the bush, but examination of a thin slice corresponding to that cut from the previous model showed no trace of the high stress concentration. The optical effect through a thickness of 1/16 in. was too small to produce the first fringe, and so gave nothing which could be photographed. Measurement by a compensation method showed that the maximum stress in this region produced about 0.9 fringe, corresponding to a tension of about 12,500 lb./in.^{2} in the prototype.

5. Conclusion

The investigation described, while by no means comprehensive, has shown the capabilities of the photoelastic method in obtaining information as to the stress distribution in such components as this. In this example it shows that while the lug of the bracket is amply strong, there is a very high, although localised, stress concentration in the sharp corners of the machined recesses in the base. How the material of the bracket will react under this concentration is a question for the metallographist, but it seems likely that repeated application of the specified load would lead to the formation of fatigue cracks and ultimately to failure. In any case the existence of such high concentrations is obviously undesirable. It may be noted also that the abnormally high sensitivity to fatigue shown by some of the new light alloys makes it more than ever necessary for the aircraft designer to know the magnitudes of the stress concentrations in all components. The photoelastic method is at present the only means of determining exactly how high such local stresses are.

A Note on the Design of Ducted Fans

BRYAN THWAITES, M.A., Ph.D., A.F.R.Ae.S.

Summary: The design of ducted fans, and the estimation of their performance for conditions other than those of the design, are usually based on the equations of the so-called strip-theory. Existing methods of solution invariably employ some form of iteration which is more or less rapidly convergent according to the experience of the computer and the detail of the method.

In this note, a solution is given which, although it is strictly an iteration, is explicit in the sense that in practice no iteration is necessary. It is shown how both design for a given performance and performance for a given fan can be calculated in one direct step.

Conditions for maximum efficiency are considered in an Appendix. Here a suggestion of R. Baldur's is used to give a simple approximate solution of the strip-theory equations which can be developed to give conditions for maximum efficiency, for the special case of a constant pressure rise through the fan.

Notation

Suffix "0" denotes an approximate value (except for r_0, a_0 and α_0).

r	radial distance
r_0	root radius
R	tip radius
q	r_0/R
A	duct area $=\pi(R^2-r_0^2)$
Q	torque
T	thrust
P	power
Ω	angular velocity
N	number of blades
c	chord
F	$\pi u(R^2-r_0^2)$, flux through fan per second

Paper received November 1950.

[The Aeronautical Quarterly, Vol. III, November 1951]

ρ	air density
u	axial velocity
p	pressure difference
a_0	slope of two-dimensional lift curve
α	incidence
$-\alpha_0$	no-lift angle
C_L	lift coefficient
C_D	drag coefficient
γ	$\tan^{-1}(C_D/C_L)$
a_2	inflow factor
η	efficiency
η_1	efficiency of blade element
θ	blade angle
ϕ	$\theta-\alpha$
β	defined by equation (12)
δ	defined by equation (19)
G, H	defined in equation (1)

1. Strip Theory Equations

Let P, T, N, Ω and η be respectively the motor power, thrust, number of blades, angular velocity and efficiency of a fan which occupies the annular space $r_0 \leqslant r \leqslant R$. Let u, c, a_2, θ, α, p, C_L and C_D be respectively the axial velocity, chord, axial inflow factor, blade angle, incidence, pressure difference, lift coefficient and drag coefficient, these eight quantities being functions of r. Then if $(dT/dr)\,\delta r$ and $(dQ/dr)\,\delta r$ are respectively the thrust and torque due to the annulus between r and $r+\delta r$, the strip theory equations may be written

$$\left.\begin{aligned} &\frac{dT}{dr}=\tfrac{1}{2}\rho Ncu^2 G\cot\phi\,; \qquad \frac{dQ}{dr}=\tfrac{1}{2}\rho Ncu^2 Hr\cot\phi \\ &G=\frac{C_L}{\sin\phi}-\frac{C_D}{\cos\phi}=\frac{C_L\cos(\phi+\gamma)}{\sin\phi\,\cos\phi\,\cos\gamma}\,; \quad H=\frac{C_D}{\sin\phi}+\frac{C_L}{\cos\phi}=\frac{C_L\sin(\phi+\gamma)}{\sin\phi\cos\phi\cos\gamma} \\ &\tan\gamma=\frac{C_D}{C_L}\,; \quad 2\pi rp=\frac{dT}{dr}\,; \quad \phi=\theta-\alpha\,; \quad \tan\phi=\frac{u}{r\Omega}\frac{1}{(1-a_2)}=\frac{u}{r\Omega}\left(1+\frac{Nc}{8\pi r}H\right) \end{aligned}\right\} \quad (1)$$

Before showing the method of solution of these equations to give certain required results, it may be shown briefly how the requirements of the fan determine the values of some of the parameters at the beginning.

There are two usual methods of approach. In the first, the power of the fan and the flux through it are known and it is desired to design a fan of the maximum efficiency. This involves determining the values of u, R, r_0, p and Ω to give maximum efficiency, which is an impossible task generally, although it may be done to a good approximation in the special case $p=$ constant, as is shown in the Appendix.

The second approach is the more usual in which some of u, R, r_0, p and Ω are fixed at the beginning. In the choice of these values, previous experience will naturally be used to avoid values which might lead to a particularly low efficiency. There are many possible procedures but the following are points which usually arise:

(*i*) u is assumed known and also the required down-stream values of pressure and velocity. This implies a knowledge of the power output of the fan and hence, by using a reasonable value of the efficiency, of the power input. This leads to a choice of motor of which the power P is fixed (but the angular velocity will be determined from the following criteria). P is therefore taken as a fixed quantity.

(*ii*) R will probably be fixed by non-aerodynamic considerations. The aerodynamic conditions on r_0 are that the C_L at r_0 is allowable, with possibly a condition for non-interference between the blades and that r_0/R should not be too small for the sake of efficiency.

(*iii*) An upper limit on Ω is fixed by the Mach number at the tips, $r=R$, and by the centrifugal stresses which may also impose condition on c.

(*iv*) N and c are fixed in conjunction to ensure allowable values of C_L and sufficiently high values of Reynolds number, while ensuring non-interference.

More detailed information concerning these preliminaries may be found in previous papers on fan design. For the present purposes, the above considerations enable us to regard P, Ω, N, u, as fixed, and a good approximation (according to the accuracy of the efficiency estimate) of p known.

The value of θ, the blade angle, is required.

2. General Process when u and p are given arbitrarily

From equations (1),

$$\left.\begin{aligned} p &= \frac{1}{2\pi r}\frac{dT}{dr} = \frac{\rho N c u^2}{4\pi r} C_L \frac{\cos(\phi+\gamma)}{\sin^2\phi\,\cos\gamma} \\ \text{and } \tan\phi &= \frac{u}{r\Omega}\left\{1+\frac{Nc\,C_L}{8\pi r}\frac{\sin(\phi+\gamma)}{\sin\phi\,\cos\phi\,\cos\gamma}\right\} \end{aligned}\right\} \quad . \quad . \quad (2)$$

Elimination of C_L between these two equations gives

$$\frac{r\Omega}{u} = \cot\phi + \frac{p}{2\rho u^2}\tan(\phi+\gamma), \quad . \quad . \quad . \quad . \quad . \quad (3)$$

which can be rearranged as

$$\phi = \tfrac{1}{2}\left\{\beta - \gamma + \sin^{-1}\left[\cos\beta\left\{\frac{u}{r\Omega}\cos\gamma\left(1+\frac{p}{2\rho u^2}\right)+\sin\gamma\right\}\right]\right\} \quad . \quad (4)$$

$$\text{where } \tan\beta = \frac{u}{r\Omega}\left(1-\frac{p}{2\rho u^2}\right). \quad . \quad . \quad . \quad (5)$$

The desired form of p but not its scale, will have been determined. Now

$$P = \frac{2\pi}{\eta}\int_{r_0}^{R} pur\,dr \quad . \quad . \quad . \quad . \quad . \quad (6)$$

and on a reasonable value, η_0, of η being chosen, a first approximation to p, $p=p_0$, may be made which satisfies (6). The error in p_0 will be one or two per cent. and it is easily verified that in usual cases the change in ϕ due to that possible change in p, from (4), is practically insignificant.

Similarly it can be verified that small changes in γ do not affect the value of ϕ given in (4). γ is regarded as a function of C_L (and Reynolds number) and an approximation C_{L_0} to C_L is obtained from equations (2) in the form

$$C_{L_0} = \frac{4\pi P_0}{\rho Ncu\Omega}\sin\phi_0, \quad \tan\phi_0 = \frac{u}{r\Omega} \quad . \quad . \quad . \quad (7)$$

All quantities on the right hand side of equations (4) and (5) have now been found to a degree of accuracy sufficient to determine the final value of ϕ.

Before going on to calculate C_L and so α and θ, it must be ensured that the torque is Q. If suffix "0" denotes an approximate value,

$$P_0 = \Omega Q_0 = 2\pi\Omega\int_{r_0}^{R} p_0 r^2\tan(\phi+\gamma)\,dr \quad . \quad . \quad . \quad (8)$$

and the better the choice of η_0, the closer will P_0 be to P. If now p is taken equal to $(P/P_0)p_0$, ϕ will be unaltered, the torque will be exactly Q, the efficiency will be $\eta = \eta_0 P/P_0$ and the thrust will be exactly ηP. Thus C_L is given from (2) as

$$C_L = \frac{4\pi r p_0}{\rho Ncu^2}\frac{P}{P_0}\frac{\sin^2\phi\cos\gamma}{\cos(\phi+\gamma)} \quad . \quad . \quad . \quad . \quad (9)$$

from which α and finally $\theta = \phi + \alpha$ follow.

The design has been accomplished therefore in a direct manner. The only awkwardness is the inevitable numerical integrations for Q_0 and P, and one of these can be avoided in the special case u=constant, p=constant, considered in Section 3. An arbitrary initial choice of η is also inevitable, but a good choice can usually be made and it is noteworthy that the error in the initial choice does not involve any recalculation.

3. The Usual Case, u=constant, p=constant

In this case, the work can be considerably simplified and a direct estimate of η_0 made at the beginning.

From (6),
$$p=\frac{\eta P}{Au} \quad . \quad . \quad . \quad . \quad . \quad . \quad (10)$$

where the area of the duct is $A=\pi(R^2-r_0^2)$. Substitution for p in (4) and (5) gives

$$\phi=\tfrac{1}{2}\left\{\beta-\gamma+\sin^{-1}\left[\cos\beta\left\{\frac{u}{r\Omega}\left(1+\frac{\eta P}{2\rho Au^2}\right)\cos\gamma+\sin\gamma\right\}\right]\right\} \quad . \quad (11)$$

where
$$\tan\beta=\frac{u}{r\Omega}\left[1-\frac{\eta P}{2\rho Au^2}\right] \quad . \quad . \quad . \quad . \quad . \quad (12)$$

γ is given sufficiently accurately from the approximate value of C_L given, from (7), by

$$C_{L0}=\frac{4\pi\eta P\sin\phi_0}{\rho Nc\Omega Au^2}, \quad \tan\phi_0=\frac{u}{r\Omega} \quad . \quad . \quad . \quad . \quad (13)$$

η may be estimated as follows. From (1), and (10) $dQ/dr=[2\pi\eta Pr/(uA)]\,r\tan(\phi+\gamma)$. Now $r\tan(\phi+\gamma)$ does not vary greatly across the duct, and if

$$r\tan(\phi+\gamma)=L_0+L_1(r-r_1)+O(r-r_1)^2,$$

where
$$r_1=\frac{R+r_0}{2},$$

then
$$Q=\frac{\eta PL_0}{n}\left[1+O(R-r_1)^2\right]$$

in which the implied constant in the O is itself small. A good approximation to the power P is therefore $(\eta P\Omega/u)\,[r\tan(\phi+\gamma)]_{r=r_1}$ and the approximation, η_0, to η is therefore chosen as

$$\eta_0=\frac{u}{r_1\Omega}[\cot(\phi+\gamma)]_{r=r_1} \quad . \quad . \quad . \quad . \quad (14)$$

in which a guessed value of η may be taken in the calculation of ϕ.

ϕ can now be calculated from (11), and then Q_0 is given by

$$Q_0 = \frac{2\pi\eta_0 P}{uA}\int_{r_0}^{R} r^2 \tan(\phi+\gamma)\,dr\,.$$

The true efficiency is then $\eta=\eta_0 P/(\Omega Q_0)$ and so C_L is given by (2) and (10) in the form

$$C_L = \frac{4\pi r\eta_0 P}{\rho N c A u^3}\,\frac{P}{\Omega Q_0}\,\frac{\sin^2\phi\cos\gamma}{\cos(\phi+\gamma)}. \qquad . \quad . \quad . \quad (15)$$

From this, α and lastly θ can be evaluated.

4. A Worked Example

A ducted fan is required to absorb 15 h.p. in a duct of area 11.5 ft.^{2} in which $u=77$ ft./sec. The motor to be used runs at 1,500 r.p.m., r_0 is chosen reasonably as $\frac{1}{2}R$, and this fixes R. $2\pi r_0=7.47$ ft. and so $Nc=3$ ft. is taken. The tip speed is 353 ft./sec. and so there will be no compressibility effects. From (13) it is found that C_L varies approximately from 0.55 at the root to 0.22 at the tips. An aerofoil section with a design C_L approximately equal to 0.4 and a low-drag range of, say, $0<C_L<0.8$ is suitable, and N.A.C.A. 65_3-418 is chosen. To obtain a low drag coefficient, the section Reynolds number should be at least 10^6, and so $N=3$, $c=1$ ft. are taken. The efficiency η_0 is given by $[u/(r_1\Omega)]\,[\cot(\phi+\gamma)]_{r=r_1}$; $r_1=1.72$ ft., and with η taken as 0.87 in this calculation for ϕ, and γ as 1.30 to correspond with a C_L of about 0.4, η_0 equals 0.89. C_{L_0} is then given from (13) and using the value of the Reynolds number, γ_0 can be written down. With $\eta=\eta_0=0.89$, β and ϕ follow from (12) and (11), and then dQ_0/dr. Integration of this gives the torque Q_0 and so the power $P_0=\Omega Q_0$ which, it is noticed, is near 8,250. C_L is then calculated from (15) and then α and θ. It is not necessary to do any more calculation since the whole process is self-checking. The input power is now 8,250 ft. lb./sec., and the efficiency is $\eta_0 P/(\Omega Q_0)=0.892$. The whole work is set out in Table I.

5. The Inverse Problem

A fan having been designed for one condition may operate at other conditions and it is desirable to be able to calculate speedily the case of θ given. A relation between Q and Ω must be assumed (the motor characteristics for a fixed control setting).

TABLE I

$P=8{,}250$, $A=11.5$, $u=77$, $\Omega=157$, $R=2.25$, $r_0=1.189$
$r_1=1.719$, $N=3$, $c=1.0$, $\frac{P}{2\rho A u^3}=0.3304$, $\alpha^\circ=9.96\,C_L-3.06$.

r	$u/(r\Omega)$	$\frac{\text{R.N.}}{10^6}$	C_{L_0}	γ_0°	β°	ϕ°	$\frac{dQ_0}{dr}$	C_L	α°	θ°
1.189	0.4125	1.27	0.46	1.04	16.24	23.60	33.78	0.517	2.09	25.7
1.366	0.3590	1.43	0.41	1.13	14.22	20.54	38.62	0.446	1.39	21.9
1.543	0.3179	1.60	0.37	1.23	12.65	18.19	43.72	0.393	0.85	19.0
1.719	0.2853	1.76	0.33	1.33	11.39	16.34	49.05	0.352	0.45	16.8
1.896	0.2587	1.93	0.30	1.43	10.35	14.82	54.60	0.319	0.12	14.9
2.073	0.2366	2.10	0.28	1.55	9.48	13.55	60.41	0.291	−0.16	13.4
2.250	0.2180	2.27	0.26	1.63	8.75	12.49	66.33	0.268	−0.40	12.1

At $r=r_0$, if $\eta=0.87$, $\gamma=1.3^\circ$ $\quad Q_0=52.45$, $\quad \Omega Q_0=P_0=8{,}235$;
$\beta=11.50^\circ$, $\phi=16.33^\circ$, $\eta_0=0.89$. $\quad P/P_0=1.002$; $\quad \eta=0.892$.

From equations (1)

$$H=\frac{C_L\sin(\phi+\gamma)\sec\gamma}{\sin\phi\cos\phi},\quad \tan\phi=\frac{u}{r\Omega}\left(1+\frac{Nc}{8\pi r}H\right),\quad \text{and}\quad \phi=\theta-\alpha \quad . \tag{16}$$

and if

$$C_L=a_0\sin(\alpha+\alpha_0) \quad . \quad . \quad . \quad . \tag{17}$$

is assumed, $-\alpha_0$ being the no-lift angle of the blades, elimination of H, α and C_L from (16) and (17) gives, after some working,

$$\phi=-\frac{\delta}{2}+\tfrac{1}{2}\sin^{-1}\left\{\cos\delta\left[1+\frac{u}{r\Omega}\left(-1+\frac{Nc\,a_0}{8\pi r\cos\gamma}\cos(\theta+\alpha_0+\gamma)\right)\right]\right\} \quad . \tag{18}$$

where

$$\tan\delta=\cot(\theta+\alpha_0-\gamma)+\left(1+\frac{r\Omega}{u}\right)\frac{8\pi r\cos\gamma}{Nc\,a_0}\operatorname{cosec}(\theta+\alpha_0-\gamma) \quad . \tag{19}$$

Equation (18) therefore gives ϕ, and α and C_L follow immediately. dQ/dr can then be evaluated, and hence Q. This calculation is performed for a few values of Ω, so that a value of Ω can be chosen for the fan's performance to suit the motor.

APPENDIX

Equation (4) gives ϕ in terms of u, r, Ω, p, ρ and γ.

The author is indebted to R. Baldur for pointing out that a rather simpler formula can be obtained for ϕ by using the local blade efficiency, η_1, as a parameter in place of γ. For from equations (1),

$$\tan(\phi+\gamma)=\frac{H}{G}=\frac{1}{r}\frac{dQ}{dr}\Big/\frac{dT}{dr}=\frac{u}{r\Omega\,\eta_1} \quad . \quad . \quad . \quad (20)$$

and so equation (3) can be written as

$$\cot\phi=\frac{r\Omega}{u}\left[1-\frac{p}{2r^2\Omega^2\rho\,\eta_1}\right]. \quad . \quad . \quad . \quad . \quad . \quad (21)$$

For this formula to give as accurate a value of ϕ as equation (4), a good estimate of η_1 must be made. This value of η_1 inevitably involves γ, which, however, it is easy to estimate. Elimination of ϕ between (20) and (21) gives

$$\eta_1=1-\frac{p}{2r^2\Omega^2\rho}-\tan\gamma\left(\frac{u}{r\Omega}+\frac{r\Omega}{u}\right) \quad . \quad . \quad . \quad (22)$$

which is true to $O(\gamma^2)$ and $O[p^2/(4r^4\Omega^4\rho^2)]$. γ and $p/(2r^2\Omega^2\rho)$* rarely take values greater than 0.1 and are usually much less, and so approximations to the order of the square and product of these quantities are likely to be good enough. Thus, using (22), (24) and (20), a solution to this order of approximation can easily be found of the basic equations (1); in particular, equations (8) and (9) become

$$P_0=\Omega Q_0=2\pi u\int_{r_0}^{R}p_0 r\left[1+\frac{p_0}{2r^2\Omega^2\rho}+\tan\gamma\left(\frac{r\Omega}{u}+\frac{r\Omega}{u}\right)\right]dr \quad . \quad (23)$$

and

$$C_L=\frac{4\pi p_0 u^2}{\rho r^2\Omega^2 Nc}\frac{P}{P_0}\left[1+\frac{p_0}{2r^2\Omega^2\rho}\frac{1+\dfrac{u^2}{r^2\Omega^2}}{2+\dfrac{u^2}{r^2\Omega^2}}+\gamma\frac{u}{r\Omega}\right]\frac{1}{\sqrt{(u^2+r^2\Omega^2)}} \quad . \quad (24)$$

(24) therefore gives C_L and so α and $\theta=\phi+\alpha$ directly from p_0.

The original formulae (4) to (9) do not involve much more computation than those of this Appendix and are probably preferable by being exact. However, the approximation given here enables the integration in the case $p=$constant, $u=$constant, to be performed, a direct estimate of the efficiency to be made and conditions for maximum efficiency to be formulated.

*$\eta_1=[1/(2J)]\,[J+\sqrt{(J^2-J)}]+O(\gamma)$, where $J=r^2\Omega^2\rho/(2p)$. Therefore, $J\geqslant 1$ and so $p/(2r^2\Omega^2\rho)$ must be less than $\frac{1}{2}$.

If p is constant, and a mean value for γ is taken,

$$P=\frac{\pi up(R^2-r_0^2)}{\eta}=\Omega Q=2\pi up\int_{r_0}^{R}\left[\gamma\frac{u}{\Omega}+r+\gamma\frac{r^2\Omega}{u}+\frac{p}{2\Omega^2\rho r}\right]dr,$$

whence
$$\eta=1-\frac{1}{R^2-r_0^2}\left[\frac{2\gamma u}{\Omega}(R-r_0)+\frac{2}{3}\frac{\gamma\Omega}{u}(R^3-r_0^3)+\frac{p}{\rho\Omega^2}\log\frac{R}{r_0}\right] \quad . \quad . \quad (25)$$

In any problem the power P will be fixed, and also probably the flux $F=\pi u(R^2-r_0^2)$ of air through the fan. (25) can therefore be rewritten as

$$\eta=1-\frac{1}{1-q^2}\left[\frac{2\gamma F}{\pi R^3\Omega(1+q)}+\frac{2\gamma\pi R^3\Omega(1-q^3)(1-q^2)}{3F}+\frac{P}{F\rho R^2\Omega^2}\log\frac{1}{q}\right],$$

where
$$q=r_0/R$$

and the problem now is: given F and P, what values of R, q, γ and Ω give a maximum value for η? First, the smaller γ, the greater η. A clue to the answer is given by taking $\gamma=0$, when $R\Omega$ must be as big as possible (and the limitation will be imposed by the tip Mach number) and q as near unity as possible. Thus if $q=1-\Delta$ and working to $O(\Delta^3)$ in η, the value of q which makes η a maximum is

$$q=1-\left[\frac{3}{4}+\frac{PR\pi}{\Omega F^2\gamma\rho}+\frac{4\pi^2R^6\Omega^2}{F^2}\right]^{-\frac{1}{4}} \quad . \quad . \quad . \quad . \quad (26)$$

and the resulting expression η shows that both R and Ω should be as large as possible. It should be remembered that γ has taken a constant value, but this is consistent with the analysis being to $O(\gamma^2)$. For high efficiency, the design consists therefore of choosing large values of R and Ω, and of then finding p and hence r_0 from (26). An incompatibility may arise if u is also fixed by the design, for F, q and u are related by $F=\pi uR^2(1-q^2)$: if the value of q given in (26) is incompatible with this, a value as near as possible should be chosen.

A New Treatment of the Tuned Absorber with Damping

D. C. JOHNSON, M.A.
(Department of Engineering, Cambridge University)

Summary: The design of the damped tuned vibration absorber, which has previously been treated algebraically, is studied by the use of a three-dimensional admittance diagram. The advantages of this method are that the basic principles can be more easily understood and that it is not necessary to simplify the vibrating system so much. The results obtained by the use of the method show that under some conditions the algebraic treatment does not give the optimum tuning, but that the differences in performance of dampers which have been designed by the two methods will not be large. It is shown how the method may be extended to more complex problems.

1. Introduction

The damped tuned absorber is a device which is used for reducing torsional vibration in engine crankshafts. It is convenient to discuss the problem of damper design in terms of the idealised dynamic system which is used for calculating the natural frequencies of torsional vibration of crankshafts. Such a system is shown

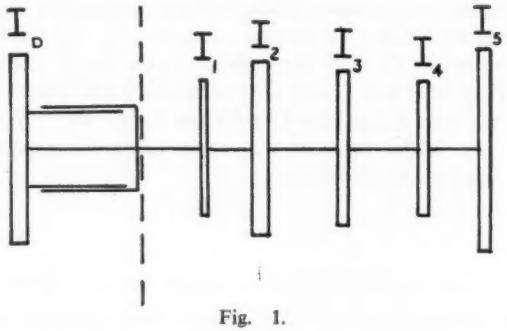

Fig. 1.

in Fig. 1 to the right of the broken line. It consists of a number of rigid discs, which have moments of inertia I_1, I_2, ... and so on, and which are connected by light shafts having torsional stiffness λ_1, λ_2 .... and so on. The discs will be acted on by

Paper received February 1951.
[The Aeronautical Quarterly, Vol. III, November 1951]

torques $P_1 e^{j(\omega t+\phi_1)}$, $P_2 e^{j(\omega t+\phi_2)}$, ... and so on, respectively, due to the gas and inertia forces on the pistons. These torques produce torsional vibration of the system. The absorber consists of an additional disc, moment of inertia I_D, attached to the crankshaft by a member of torsional rigidity λ_D; some arrangement for dissipating energy is connected across this member so that energy is absorbed if there is relative motion between I_D and I_1. Such an arrangement may use dry or fluid friction, or it may consist of a rubber cylinder which absorbs energy because of its elastic hysteresis. The absorber is represented to the left of the broken line in Fig. 1. In this paper it is assumed that the energy absorbing mechanism has a linear characteristic, so that the torque T_D is related to the relative angular velocity of I_D to I_1 by an equation

$$T_D = \mu(\dot{\theta}_D - \dot{\theta}_1)$$

where μ is a constant, and θ_D is the displacement of I_D. The problem is to choose values for I_D, λ_D and μ which will prevent excessive torsional vibration of the crankshaft throughout the range of variation of ω, the pulsatance of the applied torques.

Notation

The numbers and suffixes 1, 2, ... refer to the discs.

I	moment of inertia
λ	torsional stiffness
P	amplitude of applied torque
ω	pulsatance of applied torque
ϕ	phase angle of applied torque
T_D	absorber torque
μ	damping constant
α_{11}	direct admittance at 1
α_{12}	cross admittance from 1 to 2
θ_1	amplitude of motion at 1
α_D	absorber admittance
X and Y	real and imaginary parts of $1/\alpha_D$
Q	quality factor for absorber
K	ratio of applied frequency to damper's natural frequency
F	force exerted by the system on the absorber
P_2	force applied at 2 (in Section 9).

2. Previous Treatment of the Problem

An algebraic solution of the problem is given by Timoshenko[1]. In order to simplify the mathematics he replaces the dynamic system of Fig. 1 by that of Fig. 2(*a*). He then shows that, if values of I_D and λ_D are chosen, a family of curves relating amplitude of I with ω may be drawn for different values of μ. All the curves of the family pass through two points; that is to say, there are two values of ω for which the amplitude of I is independent of the damping. The surprising result may be used for choosing the values for the constants. I_D and λ_D are chosen so that the two particular amplitudes are equal and μ is then chosen so that the amplitude-frequency curve has these values as maxima.

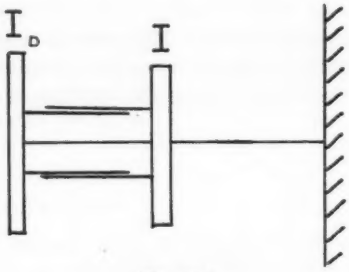

Fig. 2(*a*).

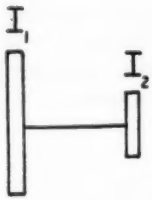

Fig. 2(*b*).

It is stated by Zdanowich and Moyal[2] that Timoshenko's treatment is not always satisfactory, presumably because of the simplification involved. This simplification is not only the replacement of the dynamic system by one which has a single degree of freedom; it also involves the assumption that the torque is applied at the point where the absorber is attached and that the amplitude at this point is the criterion of the severity of torsional vibration. The design method used by Zdanowich and Moyal does not require any of these assumptions to be made. The reason for the development of the treatment given in the present paper is that a method was required which would help engineering students to understand the fundamental ideas upon which any full treament, such as that of Zdanowich and Moyal, must be based.

3. Outline of New Treatment

The treatment depends upon the use of mechanical admittances (Duncan[3]). The principle is to replace the algebraic problem by a geometrical one; this is done by considering certain characteristic curves of the absorber and of the engine to which it is to be fixed. The simplified problem, when the torque is applied and

the amplitude is measured at I_1, will be solved first. The method will then be extended to cover the case when torques may be applied at any point, or when the severity of vibration is gauged by the torque amplitude at some other point in the system, rather than by the amplitude of displacement of I_1. The presence of both these effects simultaneously leads to a more difficult problem.

Writing α_{11} for the direct admittance of the crankshaft for torsional motion of I_1, and α_D for the direct admittance of the absorber at the same point, then we obtain

$$\theta_1\left(\frac{1}{\alpha_{11}}+\frac{1}{\alpha_D}\right)=P_1$$

where θ_1 is the amplitude of I_1. The admittances will be complex quantities, but it is assumed throughout that the imaginary part of α_{11} is negligible; that is to say that the damping forces within the engine are sufficiently small to be neglected. The maximum values of θ_1 will be those for which $1/\alpha_{11}+1/\alpha_D$ is a minimum, assuming that P_1 is independent of ω. Curves of $1/\alpha_D$ and $-1/\alpha_{11}$ will be plotted together, so that, for any given ω, the distance between the curves will be equal to $1/\alpha_{11}+1/\alpha_D$. The maximum value of θ_1 will then correspond to the value of ω for which the curves are closest together.

Because α_D is complex a space curve is required to represent its variation with ω; writing

$$\frac{1}{\alpha_D}=X+iY$$

the values of X, Y, ω are then plotted on the rectangular axes as shown in Fig. 3. The curve of $-1/\alpha_{11}$ will lie in the $X\omega$ plane.

4. Form of the $1/\alpha_D$ Curve

The damper admittance is given by

$$\alpha_D=\frac{-1}{I_D\omega^2}+\frac{1}{\lambda_D+i\omega\mu}.$$

It is convenient to introduce some auxiliary variables, so that the curve may be plotted in dimensionless quantities. Writing

$$\omega_D{}^2=\frac{\lambda_D}{I_D},\quad \frac{\omega}{\omega_D}=K \quad \text{and} \quad \frac{\omega_D I_D}{\mu}=Q$$

gives

$$\alpha_D=\frac{1}{-\lambda_D K^2}+\frac{1}{\lambda_D\left(1+\dfrac{iK}{Q}\right)}$$

which may be written

$$\frac{1}{\alpha_D} = \lambda_D \frac{K^2\left\{(K^2-1)-\dfrac{K^2}{Q^2}\right\}+\dfrac{iK^5}{Q}}{(K^2-1)^2+\dfrac{K^2}{Q^2}}.$$

This means that for a given ratio of the applied frequency to the natural frequency of the damper and for a given value of Q, the quality factor, the reciprocal of the admittance may be expressed as a complex multiple of λ_D.

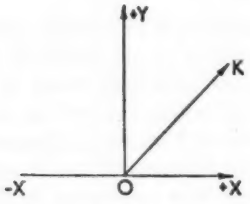

Fig. 3(*a*).

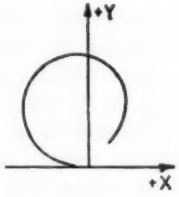

Fig. 3(*b*).

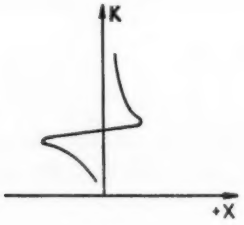

Fig. 3(*c*).

It will be found that X and Y, the real and imaginary parts of $1/\alpha_D$ are connected by the relation

$$X^2+Y^2+X\left(\frac{2-K^2}{1-K^2}\right)+\frac{1}{1-K^2}=0$$

for all values of Q. This shows that the locus of the point (X, Y) in any K plane, is a circle of which the centre lies in the ωX plane. The circles in all the planes form a surface upon which lie the family of curves of $1/\alpha_D$ which is obtained for different values of Q.

If a three-dimensional model of the curves is constructed, it is possible, if $-1/\alpha_{11}$ is first plotted to a suitable scale, to obtain the curves of $1/\alpha_{11}+1/\alpha_D$ by

measurement of the distances between the two curves. Such a model has been made in which the circles have been fixed to a transparent base; three wires, which represent the curves for $Q=2$, 5 and 10, have been fixed to the circles. This arrangement may be placed on top of a piece of paper upon which the curve of $-1/\alpha_{11}$ for any particular engine has been drawn. The distances between the wires and the graph may be measured directly.

The shape of a typical $1/\alpha_D$ curve is shown by Figs. 3(*a*), 3(*b*) and 3(*c*).

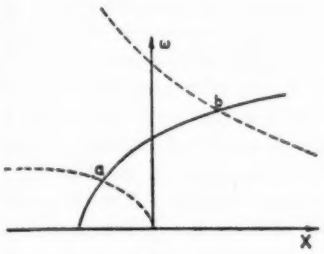

Fig. 4.

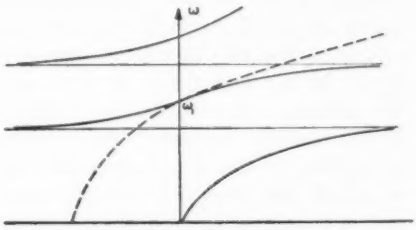

Fig. 5.

5. Use of the Model to Select a Damper for a System with One Degree of Freedom

The curve of $-1/\alpha_{11}$ for the system discussed by Timoshenko is shown by the full line in Fig. 4. If the natural frequency of the system is fairly close to that of the absorber then the existence of two minimum values for $1/\alpha_D+1/\alpha_{11}$ can be seen by inspection of the curves of Fig. 3 and Fig. 4. The selection of a damper which will make these two minima as large as possible is the geometrical equivalent of Timoshenko's algebraic method. The ratio I_D/I_1 is first decided because the magnitude of I_D is limited by available space at the end of the engine crankshaft. For any given ratio of damper frequency to crank frequency a curve of $1/\alpha_{11}$ may be drawn to the correct scale. It is then necessary to select the damper frequency by trial and error, but the procedure may be shortened if a new curve is drawn on the base of the model. This curve, shown dotted in Fig. 4, passes through the centres of all the circles of the model. It will cut the $-1/\alpha_{11}$ line at two points *a* and *b* as seen in Fig. 4. These points give the values of ω for which $1/\alpha_D+1/\alpha_{11}$ is independent of μ; they are the two points used by Timoshenko. The trial and error process now consists of making equal the radii of the two circles of which the centres are *a* and *b*. It is not necessary to draw a large number of trial curves. If one curve is drawn for an engine frequency of, say, 1.1 × absorber frequency, then it will give a good approximation to any engine curve corresponding to a frequency in the range 1.0 to 1.2 × absorber frequency; it is only necessary to move the curve

bodily. The value of μ can then be found by choosing the $1/\alpha_D$ curve for which the radii of the two equal circles correspond to minimum values of $1/\alpha_D + 1/\alpha_{11}$. It so happens that the two required minima are given by about the same value of μ.

6. Extension to System with Several Degrees of Freedom

The $-1/\alpha_{11}$ curve for the dynamic system of Fig. 1 will be of the form shown by the full lines in Fig. 5. Suppose an absorber is to be designed to reduce the vibration in the region of the first natural frequency ω_1 of Fig. 5. The approximation involved in the method discussed consists of replacing the curve of Fig. 5 by one of the shape of that in Fig. 4, the simple curve being chosen to cut the vertical axis at ω_1 and also to have the correct slope at this point; such a curve is shown by the broken line of Fig. 5. It is now necessary to examine how the results of this treatment are modified by the difference between the curves of Figs. 4 and 5. First it is useful to compare the admittance lines of the anchored one-mass system with those of a free two-mass system, Fig 2(*b*); such a comparison is made in Fig. 6 in which the line 1 is for the anchored one-mass system. The two-mass system lines have an asymptote below the natural frequency ω_1. If this asymptote is much nearer to the origin than it is to ω_1, then the admittance line in the region of

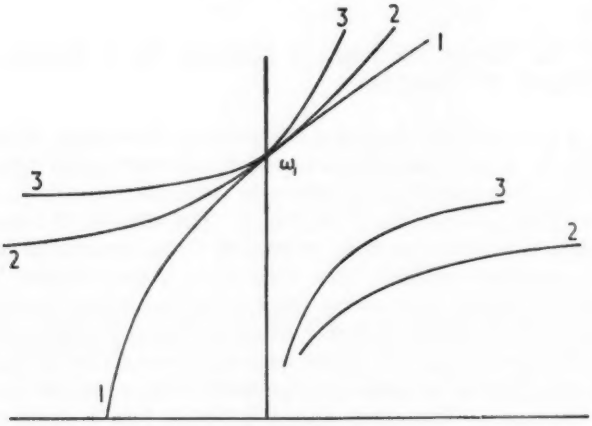

Fig. 6.

ω_1 is close to that of the one-mass system; but if the asymptote is closer to ω_1, then the two lines depart from one another appreciably both above and below ω_1. The position of the asymptote is fixed by the ratio of the two moments of inertia; Curve 2 of Fig. 6 corresponds to a ratio of 5 : 1 between the disc remote from the absorber and the disc to which the absorber is fixed; Curve 3 is for a ratio of 0.5 : 1 between these two. In the following these discs will be referred to as I_2 and I_1 respectively.

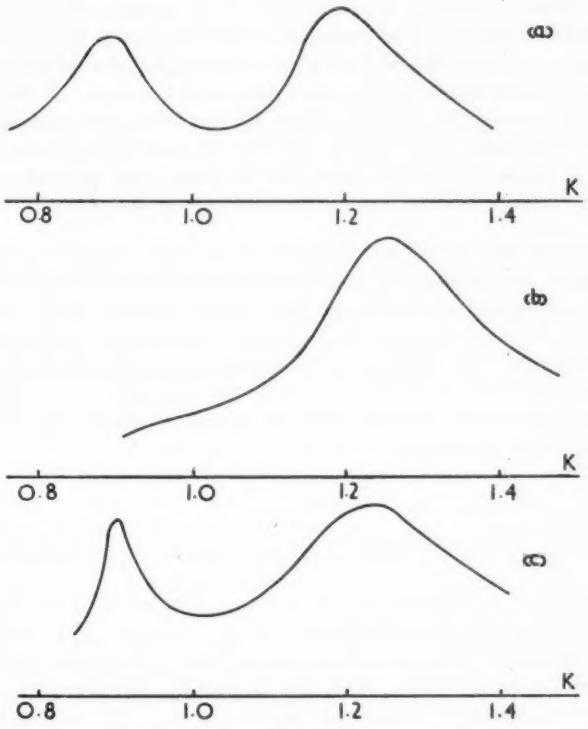

Fig. 7.

Now if an absorber tuning is chosen to give two equal circles in conjunction with Curve 1, it will be found that with Curve 3 the lower frequency circle will be increased in radius and the upper frequency circle will be reduced. This follows by consideration of the curves of Figs. 3, 4 and 6. This means that the greatest amplitudes above the damper frequency exceed the greatest amplitudes below it. This effect will be overcome if the damper frequency is slightly reduced; the geometrical treatment shows therefore that if a two-mass system is replaced by a one-mass system, and if the Timoshenko design method is then used, the damper frequency that is calculated will be too high.

It has been found by measurement that this effect is not likely to be serious. The effect is greatest when the damper mass is small, that is to say when it is about 10 per cent. or less of the effective engine mass. The effect would also be more pronounced if, for any reason, it were necessary to use rather less damping than the optimum. In Fig. 7(*a*) a curve of $\alpha_{11}\,\alpha_D/(\alpha_{11}+\alpha_D)$ against ω is plotted for a single-mass system. The ratio of absorber mass to system mass is 1 : 10 and the tuning, absorber

frequency : system frequency, is 1.1 : 1. This is the optimum tuning as calculated by Timoshenko's method. The damping in the absorber is for $Q=5$. Fig. 7(*b*) shows the curve which is obtained for a two-mass system, for which the asymptote is at 0.8 of the natural frequency, the other data being the same. It will be seen that the upper peak is about 20 per cent. higher, but the lower peak vanishes altogether. Fig. 7(*c*) is for the same system as Fig. 7(*b*) but the absorber tuning is 1.01 : 1. The upper peak is reduced to the first value and the lower peak is present and of equal height. Thus there is some advantage in the lower tuning ratio.

If the system has more than two discs the general conclusions are not greatly changed Again, the difference between the admittance curves of the real system and those of an equivalent anchored one-mass system depends upon how close the asymptotes of the real system are to the natural frequency to which the equivalent system corresponds. The presence of an asymptote just below this frequency has an exactly similar effect as in the case of the two-disc system. If there is also an asymptote just above this frequency then the difference between the two admittance curves in this region is reduced.

7. Variation of Amplitude at Other Points of the System

The amplitude of vibration at the point of attachment of the damper is not necessarily the true criterion of the severity of vibration. For example. in the two-mass system which has been discussed previously, the torque amplitude in the shaft may be the factor which limits the permissible vibration; the ratio of the torque to the amplitude of motion at the damper end will vary with frequency. A general expression, in terms of the admittances, may be derived for the amplitude at any point of the system when the damper is attached, and the exciting force is applied, at another point. Referring to the latter point by the suffix 1 and to the former by the suffix 2, the amplitude at 2, due to an applied force P at 1, will be $P\alpha_{12}$ where α_{12} is the "cross admittance"; similarly the amplitude at 1 will be $P\alpha_{11}$.

Both these admittances are to be taken to apply to the system alone, without the damper. Now when the damper is attached, the ratio of the amplitude at 2 to that at 1 will not be changed. The amplitude at 1 will be obtainable from the diagram as before. The amplitude at 2 will be obtained by multiplying by the factor α_{12}/α_{11} so that

$$\text{amplitude} = \frac{\alpha_{12}}{\alpha_{11}} \frac{\alpha_{11}\alpha_{D}}{\alpha_{11}+\alpha_{D}}.$$

Thus if α_{12}/α_{11} is plotted against ω it will show how the damper frequency should be chosen to give the lowest value of the amplitude at 2.

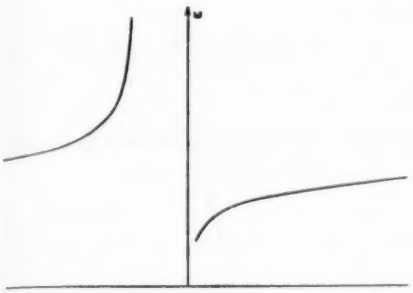

Fig. 8.

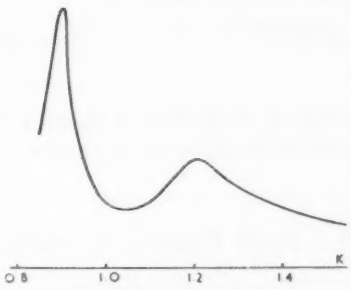

Fig. 9.

For the two-mass system of Fig. 2(*b*)

$$\frac{\alpha_{12}}{\alpha_{11}} = \frac{\lambda}{\lambda - I_2\,\omega^2}$$

where the points 1 and 2 are taken to correspond with the discs I_1 and I_2. The torque in the shaft will be $I_2\,\omega^2\,\theta_2$ so that if $\alpha_{11}\,\alpha_D/(\alpha_{11}+\alpha_D)$ is multiplied by $\lambda\omega^2/(\lambda - I_2\,\omega^2)$ then a curve can be obtained giving the torque in the shaft for unit torque applied at 1. The function $\lambda\omega^2/(\lambda - I_2\,\omega^2)$ is plotted in Fig. 8; the torque curve deduced from it, in conjunction with the curve of Fig. 7(*c*), is shown in Fig. 9. The difference between this curve and that of Fig. 7(*c*) is very noticeable; the heights of the peaks may be made more equal by changing the damper tuning to 1:1, but in this case it will be found that the smaller peak is increased and the larger peak is not reduced.

It may be mentioned here that if the magnitude of the exciting force varies with frequency, as, for instance, when inertia forces are present, then the amplitude curve may be modified in the same manner and again it may be found to be advantageous to change the tuning of the absorber.

8. Excitation at Other Points of the System

It has been shown how the amplitude at 2 may be found when the exciting force and the damper are at 1. The reciprocal theorem, applied to the system and damper together, shows that, by the same process, the amplitude at 1 may be found when the exciting force acts at 2. Further, if several exciting forces, of the same frequency but not necessarily in phase with one another, act at points 2, 3, 4, ... then the amplitude at 1 may again be found. It will be necessary to find

$$\alpha_{12}/\alpha_{11},\quad \alpha_{13}/\alpha_{11},\quad \alpha_{14}/\alpha_{11}$$

and to obtain thence a curve of the amplitude of

$$\left(\frac{\alpha_{12}}{\alpha_{11}}\right)P_2+\left(\frac{\alpha_{13}}{\alpha_{11}}\right)P_3+\ldots$$

where P_2 is the force at 2, and so on, and where the expression denotes the vector sum of the quantities, because P_2, P_3, and so on, may not be in phase.

9. More General Problems

If the absorber is attached at a point 1, the exciting force applied at 2 and the amplitude required at 3, then the process becomes more complex. Writing θ_1 for the amplitude at 1, and so on, P_2 for the applied force at 2, and F for the force exerted by the system on the absorber

$$\theta_3=P_2\,\alpha_{23}-F\,\alpha_{13}$$

$$\theta_1=\alpha_D F$$

$$\theta_1=P_2\,\alpha_{21}-F\,\alpha_{11}.$$

Eliminating F and θ_1 *gives*

$$\theta_3=P_2\left\{\alpha_{23}-\frac{\alpha_{21}\,\alpha_{13}}{\alpha_D+\alpha_{11}}\right\}.$$

In order to obtain θ_3 in terms of the measured vector $\dfrac{1}{\{\alpha_D\,\alpha_{11}/(\alpha_D+\alpha_{11})\}}$ the expression can be rewritten

$$\theta_3=P_2\left\{\frac{\alpha_{11}\,\alpha_{22}-\alpha_{21}\,\alpha_{31}}{\alpha_{11}}+\frac{\alpha_{21}\,\alpha_{31}}{\alpha_{11}^{\,2}}\,\frac{\alpha_{11}\,\alpha_D}{\alpha_{11}+\alpha_D}\right\}.$$

The first term inside the bracket depends upon the system only and is real; the second term is a multiple of the distance measured and is complex.

References

1. Timoshenko, S. (1937). *Vibration Problems in Engineering*, Constable, 2nd Edition, 1937, p. 245.
2. Zdanowich, R. W. and Moyal, J. E. (1945). Some Practical Applications of Rubber Dampers for the Suppression of Torsional Vibration in Engine Systems. *Proceedings of the Institution of Mechanical Engineers*, Vol. 153, 1945.
3. Duncan, W. J. (1947). Mechanical Admittances and Their Application to Oscillation Problems. R. & M. 2000.

A New Approach to Thin Aerofoil Theory

M. J. LIGHTHILL

(Professor of Applied Mathematics, The University, Manchester)

Summary: The general technique[5] for rendering approximate solutions to physical problems uniformly valid is here applied to the simplest form of the problem of correcting the theory of thin wings near a rounded leading edge. The flow investigated is two-dimensional, irrotational and incompressible, and therefore the results do not materially add to our already extensive knowledge of this subject, but the method, which is here satisfactorily checked against this knowledge, shows promise of extension to three-dimensional, and compressible, flow problems.

The conclusion, in the problem studied here, is that the velocity field obtained by a straightforward expansion in powers of the disturbances, up to and including either the first or the second power, with coefficients functions of co-ordinates such that the leading edge is at the origin and the aerofoil chord is one of the axes, may be rendered a valid first approximation near the leading edge, as well as a valid first or second approximation away from it, if the whole field is shifted downstream parallel to the chord for a distance of half the leading edge radius of curvature ρ_L. It follows that the fluid speed on the aerofoil surface, as given on such a straightforward second approximation as a function of distance x along the chord, similarly is rendered uniformly valid (*see* equation (52)) if the part singular like x^{-1} is subtracted and the remainder is multiplied by $[x/(x+\frac{1}{2}\rho_L)]^{\frac{1}{2}}$.

1. Introduction

Although the author's new approach to thin aerofoil theory will be applied here only to the two-dimensional flow at negligible Mach number, it is brought forward principally in the hope that its use may later be extended to three-dimensional flow over wings, and to flow at general subsonic and (in the case of swept-back wings) supersonic Mach numbers. In all cases it is only the potential flow which is considered, but it is known how this can be used, together with the theory of the boundary layer, to predict the real motion of the fluid.

The existing theory of the two-dimensional incompressible potential flow about thin aerofoils (*see* Goldstein's Wright Brothers Lecture[2] and other references there quoted, the basic work being by Theodorsen[6]) is completely satisfactory for the practical purpose of obtaining a sufficiently accurate answer in a sufficiently short

Paper received July 1951.

[The Aeronautical Quarterly, Vol. III, November 1951]

time. However, being based on the theory of conformal mapping, it offers no possibility of extension to three-dimensional problems, or to problems involving compressibility.

In contrast, the lifting-surface theory of flow over wings cannot be called completely satisfactory, particularly near the leading edge. This theory consistently neglects the squares of the disturbances to the main stream, and so is a direct extension of the two-dimensional theory called Approximation I by Goldstein (which, especially as applied to flow over the camber line only, has a long history, not worth recalling here, *see*, for example, Ref. 1, p. 87). Since in both theories squares of disturbances are neglected, the boundary conditions may be satisfied on a plane surface, parallel to the main stream, with the same plan form as the wing, because the difference between the values of disturbance velocities on such a plane surface and on the wing is of the order of the squares of the disturbances. The theory is not strictly logical, since for no wing, however thin, is the square of the disturbance negligible, at any rate near the leading edge stagnation point, and indeed the behaviour predicted in this neighbourhood is manifestly incorrect.

It is generally believed that the lifting surface theory gives a fair approximation to the pressure distribution on a thin wing at moderate incidence, except near the leading edge, and part of the evidence for this belief is that the Goldstein higher approximations show it to be correct for two-dimensional flow. What is needed is a simple method of modifying lifting-surface theory so that it becomes a good approximation even near to the leading edge.

Passing to compressible flow, we may call the theory of two-dimensional subsonic potential flow about thin aerofoils, below the shock stall, nearly but not quite satisfactory from the practical point of view. The Kármán-Tsien approach (in its practical engineering form, where no deformation of the boundary is contemplated) gives results which have been checked satisfactorily with experiment in many cases, but its foundations are too obscure to inspire confidence in applying it to any case widely different from those checked. The method of Hantzsche and Wendt[3], on the other hand, which is a step-by-step method based on the Prandtl-Glauert theory as a first approximation, is very sound and useful where it is applicable, but is limited in practice to special shapes, such as Joukowsky aerofoils and elliptic cylinders. This is because, although the method involves essentially an expansion in powers of the disturbances, it was found necessary at every stage to apply the boundary conditions on the surface of the aerofoil, not on a plane surface, owing to errors in the higher approximations which otherwise result from the total want of accuracy near the leading edge.

Thus the first approximation, in this method, is not, and must not be, "Approximation I" as modified by the Prandtl-Glauert transformation, even though this is the solution obtained by consistently neglecting the squares of the disturbances. To get tolerable accuracy in the second approximation it is essential to use a first approximation which is valid even near the leading edge. Even in

obtaining the second approximation the great simplification which would be achieved by applying the boundary conditions on a plane surface is not permissible.

A parallel difficulty arises in the theory of supersonic flow past wings swept back beyond the Mach angle (so that the flow normal to their leading edges is still subsonic). In this problem the wave drag cannot be calculated from the ordinary completely linearised theory of supersonic flow because of its inaccuracy near the leading edge. R. T. Jones[4] has shown how the wave drag can be corrected, but it would be desirable to be able to predict the complete pressure distribution near the leading edge, for example in order to detect stalling.

Thus it is seen that in all these problems involving the flow over thin wings with rounded leading edges the mathematically natural method of solution, namely expansion in powers of some parameter defining the size of the disturbances, has two objections to it:—

(*i*) Neither the first nor any subsequent approximation is valid uniformly; in fact they are worthless near the leading edge.

(*ii*) The inaccuracy due to this increases with successive approximations, so that, sufficiently near the leading edge, the process diverges.

Now in what follows this method of series expansion will be slightly modified, in accordance with the author's general theory of rendering approximate solutions to physical problems uniformly valid[5], by introducing, with each approximation to the velocity field, a slight *straining* of the co-ordinate system. This is determined progressively with the successive approximations to ensure uniform convergence near the leading edge.

Actually, in the problem of two-dimensional incompressible flow which alone is considered here, the straining becomes, to a first approximation, a pure translation. The velocity field given by the first or second approximation is found to be valid uniformly, even near the leading edge, if the field is shifted bodily downstream (parallel to the chord) through a distance equal to half the leading edge radius of curvature. This radius is itself a multiple of the square of the parameter which defines the size of the disturbances, and so the shift makes a difference to the equations for the coefficients of successive powers of this parameter in the velocity field. As a result of the shift the region of divergence of the process disappears altogether, and the singularity, previously at the leading edge, is moved *inside* the aerofoil contour. Here it represents a real feature of the analytical continuation of the flow field within the aerofoil contour, of which the dominant singularity is approximated by this one at the mid-point of the leading edge radius of curvature. But the flow field outside the aerofoil is perfectly regular. To higher approximations a real straining, not a pure translation, of the co-ordinate system would be required; it might be guessed that this will prove true even to a first approximation when the analogous problems of three-dimensional and/or compressible flow are investigated on these lines.

The work described is novel from the point of view of method insofar as the general technique[5] is for the first time applied to an elliptic problem. Thus it is an isolated singularity which has to be tackled, not a singularity spread along a whole characteristic.

The "natural" process of a series expansion of the velocity field is set out in Section 2, and the deduction of a uniform approximation in Section 3. The formulae for the velocity distribution on the surface, taking into account the incidence, fairing and camber line to a second approximation and uniformly valid even near the leading edge, are obtained in Section 4. These are of some general aerodynamical interest, even though the problem may be considered previously solved for practical purposes.

For simplicity the author has applied the Kutta-Joukowsky condition at the trailing edge, instead of adopting the rather more accurate procedure of using an experimentally determined value of the lift-curve slope. This is a modification which could easily be made, although it would add to the complication of the formulae.

Notation

(Dashes denote differentiation with respect to x)

ρ_L	leading edge radius of curvature
x	distance along aerofoil chord from leading edge
ε	parameter defining the size of the disturbances
c	aerofoil chord
$C(x), F(x)$	functions defining the shape of the aerofoil (*see* the beginning of Section 2)
y	co-ordinate of aerofoil surface perpendicular to chord
α	defined by $\varepsilon\alpha$ = angle of incidence
u, v	velocity components in directions of x and y respectively
U	main stream velocity
$u_1, u_2, \ldots, u_n, \ldots$	coefficients in the expansion of u in powers of ε
$v_1, v_2, \ldots, v_n,$	coefficients in the expansion of v in powers of ε
u_{11}, u_{12}	defined by equations (17)
$U(x), V(x)$	defined by equations (19)
$W(x), Z(x)$	defined by equations (22)
q	fluid speed at aerofoil surface
q_{max}	maximum value of q
A_1, k_0, k_1	constants in equation (36)

$\mathscr{R}, \mathscr{I}$	real and imaginary parts of
n	an integer
α_{opt}	optimum value of α, defined in equation (46)
ρ	fluid density
A	value of u at infinity (in Lemma 1)
V_0	value of $V(x)$ at $x=0$
w	variable of integration
$F_0, F_1, \ldots$ $C_1, C_2, \ldots$	coefficients in the expansions of $F(x)$ and $C(x)$ (*see* equation (24))
X, Y	co-ordinates in the strained system (*see* equation (26))
$x_1, x_2, \ldots$ $y_1, y_2, \ldots$	functions of X and Y in the expansion of x and y in powers of ε (*see* equation (26))

2. Expansion of the Velocity Field in Series

In this section the problem of determining the two-dimensional incompressible potential flow past a thin aerofoil of moderate camber at a moderate angle of incidence is treated by expanding the velocity field in a power series in powers of a parameter ε defining the size of the disturbances.

To do this let the upper surface of the aerofoil have the equation $y=\varepsilon[C(x)+F(x)]$ for $0<x<c$, and the lower surface the equation $y=\varepsilon[C(x)-F(x)]$, also for $0<x<c$; where $F(0)=C(0)=F(c)=C(c)=0$. Then the straight segment $y=0$, $0<x<c$ is the *chord* of the aerofoil as usually defined; the origin and the point $(c, 0)$ are the leading and trailing edges respectively, and the equations of the fairing and camber line of the aerofoil are $y=\pm\varepsilon F(x)$ and $y=\varepsilon C(x)$ respectively. Now let the angle of incidence be $\varepsilon\alpha$. Then the velocity components u, v in the x and y directions take the values

$$u=U\cos\varepsilon\alpha,\quad v=U\sin\varepsilon\alpha \qquad . \quad . \quad . \quad . \quad (1)$$

at infinity, while on the aerofoil surface $y=\varepsilon[C(x)\pm F(x)]$ they satisfy (with either the upper or the lower sign taken throughout)

$$\frac{v}{u}=\varepsilon[C'(x)\pm F'(x)]. \qquad . \quad . \quad . \quad . \quad (2)$$

Outside the aerofoil surface they satisfy the equations of irrotationality and continuity; in the suffix derivative notation*

$$u_y-v_x=0,\quad u_x+v_y=0. \qquad . \quad . \quad . \quad . \quad (3)$$

*u_y denotes $\partial u/\partial y$, u_{xx} denotes $\partial^2 u/\partial x^2$ and so on.

If now the velocity field be expanded in powers of ε as

$$u=U(1+\varepsilon u_1+\varepsilon^2 u_2+\ldots), \quad v=U(\varepsilon v_1+\varepsilon^2 v_2+\ldots), \qquad (4)$$

then by (1)

$$u_1=0,\ u_2=-\tfrac{1}{2}\alpha^2,\ u_3=0,\ \ldots,\quad v_1=\alpha,\ v_2=0,\ v_3=-\tfrac{1}{6}\alpha^3,\ \ldots, \qquad (5)$$

at infinity; clearly also the equations (3) are satisfied by each pair (u_n, v_n) of coefficients in (4). But since u_n, v_n do not depend on ε their boundary conditions derived from (2) must be expressed not on the surface $y=\varepsilon[C(x)\pm F(x)]$ itself but on a surface independent of ε, evidently the two sides $y=\pm 0$ of the plane surface $y=0,\ 0<x<c$. Transformation of equation (2) to this surface (which may involve analytical continuation of the coefficients u_n, v_n through the surface of the aerofoil) is effected by Taylor's theorem, giving

$$\frac{v+v_y\,\varepsilon[C(x)\pm F(x)]+\frac{1}{2}v_{yy}\,\varepsilon^2[C(x)\pm F(x)]^2+\ldots}{u+u_y\,\varepsilon[C(x)\pm F(x)]+\frac{1}{2}u_{yy}\,\varepsilon^2[C(x)\pm F(x)]^2+\ldots}=\varepsilon[C'(x)\pm F'(x)], \qquad (6)$$

on $y=\pm 0,\ 0<x<c$.

When the series (4) is inserted for u and v on the left hand side of (6) and terms of higher order than ε^3 are neglected, it becomes

$$\{\varepsilon v_1+\varepsilon^2(v_2+[C(x)\pm F(x)]v_{1y})+\varepsilon^3(v_3+[C(x)\pm F(x)]v_{2y}+\tfrac{1}{2}[C(x)\pm F(x)]^2 v_{1yy})\}\times$$
$$\times\{1-\varepsilon u_1-\varepsilon^2(u_2+[C(x)\pm F(x)]u_{1y})+\varepsilon^2 u_1^2\}. \qquad (7)$$

Equating this to the right hand side of (6), and isolating the coefficients of ε, ε^2, ε^3 in the resulting equation, we obtain that, on $y=\pm 0,\ 0<x<c$

$$v_1=C'(x)\pm F'(x), \qquad (8)$$

$$v_2=u_1 v_1-[C(x)\pm F(x)]v_{1y}=\frac{d}{dx}\{u_1[C(x)\pm F(x)]\}, \qquad (9)$$

$$v_3=v_1(u_2+[C(x)\pm F(x)]u_{1y}-u_1^2)+u_1(v_2+[C(x)\pm F(x)]v_{1y})-[C(x)\pm F(x)]v_{2y}-$$
$$-\tfrac{1}{2}[C(x)\pm F(x)]^2 v_{1yy}$$
$$=\frac{d}{dx}\{u_2[C(x)\pm F(x)]+\tfrac{1}{2}[C(x)\pm F(x)]^2[C''(x)\pm F''(x)]\}, \qquad (10)$$

The evaluation of irrotational solenoidal fields (u_n, v_n) satisfying these boundary conditions, with the conditions at infinity (5), depends on a certain well-known lemma, which can be interpreted physically in terms of the outflow due to a plane distribution of sources.

Lemma 1. If u, v satisfy equations (3) outside the strip $y=0$, $0<x<c$, and if $u=A$, $v=0$ at infinity, while on the two sides $y=\pm 0$ of the strip $v=\pm V(x)$, and if u as well as v is integrable from 0 to c for $y=\pm 0$, then

$$u-iv=A+\frac{1}{\pi}\int_0^c \frac{V(w)\,dw}{x+iy-w}. \qquad (11)$$

It is worth remarking that this lemma, being equivalent to the properties of source distributions, is essentially trivial, does not depend on the theory of analytic functions, and has simple extensions to three-dimensional and compressible flow problems. Also it is sufficient by itself to treat all problems arising in the flow at zero incidence about a symmetrical aerofoil, which are therefore those for which the theory will be most readily extended to other problems (*see* Section 1). Thus if $\alpha=0$ and $C(x)\equiv 0$, then by (5), (8) and Lemma 1,

$$u_1-iv_1=\frac{1}{\pi}\int_0^c \frac{F'(w)\,dw}{x+iy-w} \qquad (12)$$

But for dealing with the effect of camber and incidence on u_1 and v_1 it is necessary to apply the lemma to the function

$$(u_1-iv_1)\left[\frac{x+iy}{c-x-iy}\right]^{\frac{1}{2}}, \qquad (13)$$

where that branch of the complex square root is taken which is positive on $y=+0$, $0<x<c$ and negative on $y=-0$, $0<x<c$. This branch is equal to $+i$ at infinity. It follows that for a wing with $F(x)\equiv 0$, the function (13) would satisfy the conditions of the lemma, by (5) and (8), and therefore

$$u_1-iv_1=\left(\frac{c-x-iy}{x+iy}\right)^{\frac{1}{2}}\left\{\alpha+\frac{1}{\pi}\int_0^c \frac{C'(w)}{x+iy-w}\left(\frac{w}{c-w}\right)^{\frac{1}{2}}dw\right\}. \qquad (14)$$

For the general case of flow about an aerofoil the complete solution for (u_1, v_1) is evidently the sum of (12) and (14), namely

$$u_1-iv_1=\frac{1}{\pi}\int_0^c \frac{F'(w)\,dw}{x+iy-w}+\left(\frac{c-x-iy}{x+iy}\right)^{\frac{1}{2}}\left\{\alpha+\frac{1}{\pi}\int_0^c \frac{C'(w)}{x+iy-w}\left(\frac{w}{c-w}\right)^{\frac{1}{2}}dw\right\}. \qquad (15)$$

In this work the position of numerator and denominator in the square root has been chosen so that the Kutta-Joukowsky condition of finite velocity at the trailing

edge be satisfied. The arguments by which the effect of camber and incidence are obtained are not easily extended to three-dimensional problems. The formula (15) constitutes Goldstein's Approximation I for the whole velocity field.

Letting $y \longrightarrow 0$ in (15), it follows that

$$u_1 = u_{11}(x) \pm u_{12}(x) \text{ on } y = \pm 0,\ 0 < x < c, \quad . \quad . \quad (16)$$

where

$$u_{11} = \frac{1}{\pi}\int_0^c \frac{F'(w)\,dw}{x-w},\ u_{12} = \left(\frac{c-x}{x}\right)^{\frac{1}{2}} \left\{ \alpha + \frac{1}{\pi}\int_0^c \left(\frac{w}{c-w}\right)^{\frac{1}{2}} \frac{C'(w)\,dw}{x-w} \right\}, \quad (17)$$

and these integrals are to be interpreted as Cauchy principal values. Hence by (7)

$$v_2 = U'(x) \pm V'(x) \text{ on } y = \pm 0,\ 0 < x < c, \quad . \quad . \quad . \quad . \quad (18)$$

where
$$U(x) = u_{11} C(x) + u_{12} F(x),\quad V(x) = u_{11} F(x) + u_{12} C(x). \quad . \quad (19)$$

The problem of finding an irrotational solenoidal field (u_2, v_2) satisfying (18) is identical with the problem already solved for (u_1, v_1); the only difference is in the conditions at infinity (5). The solution is readily obtained as

$$u_2 - iv_2 = -\tfrac{1}{2}\alpha^2 + \frac{1}{\pi}\int_0^c \frac{V'(w)\,dw}{x+iy-w} + \left(\frac{c-x-iy}{x+iy}\right)^{\frac{1}{2}} \frac{1}{\pi}\int_0^c \frac{U'(w)}{x+iy-w}\left(\frac{w}{c-w}\right)^{\frac{1}{2}} dw$$
$$. \quad . \quad . \quad . \quad . \quad . \quad . \quad (20)$$

To carry the process one stage further, not because anyone would consider using the third order coefficients u_3, v_3 in a practical calculation, but simply for the purpose of investigating the analytical nature of the successive approximations, (10) is finally written in the form

$$v_3 = W'(x) \pm Z'(x) \text{ on } y = \pm 0,\ 0 < x < c, \quad . \quad . \quad (21)$$

where

$$\left.\begin{aligned} W(x) &= \frac{C(x)}{\pi}\int_0^c \frac{V'(w)\,dw}{x-w} + \frac{F(x)}{\pi}\left(\frac{c-x}{x}\right)^{\frac{1}{2}} \int_0^c \left(\frac{w}{c-w}\right)^{\frac{1}{2}} \frac{U'(w)\,dw}{x-w} + \\ &\quad + \tfrac{1}{2}[C^2(x) + F^2(x)]\,C''(x) + C(x)F(x)F''(x), \\ Z(x) &= \frac{F(x)}{\pi}\int_0^c \frac{V'(w)\,dw}{x-w} + \frac{C(x)}{\pi}\left(\frac{c-x}{x}\right)^{\frac{1}{2}} \int_0^c \left(\frac{w}{c-w}\right)^{\frac{1}{2}} \frac{U'(w)\,dw}{x-w} + \\ &\quad + \tfrac{1}{2}[C^2(x) + F^2(x)]\,F''(x) + C(x)F(x)C''(x). \end{aligned}\right\} \quad . \quad (22)$$

Then, exactly as before, u_3 and v_3 must be given by the equation

$$u_3 - iv_3 = \frac{1}{\pi}\int_0^c \frac{Z'(w)\,dw}{x+iy-w} + \left(\frac{c-x-iy}{x+iy}\right)^{\frac{1}{2}} \left\{ -\tfrac{1}{6}x^3 + \frac{1}{\pi}\int_0^c \frac{W'(w)}{x+iy-w}\left(\frac{w}{c-w}\right)^{\frac{1}{2}} dw \right\}. \quad . \quad . \quad . \quad . \quad . \quad . \quad (23)$$

The nature of the singularities of the coefficients u_n, v_n at the leading and trailing edges will now be considered for $n=1, 2, 3$. In this investigation it will be assumed that the aerofoil contour is an analytic arc except at the trailing edge, which is a cusp. This means that $C(x)$ is regular in $0 \leqslant x \leqslant c$ (*i.e.* has derivatives of all orders in this interval), and also that $x^{-\frac{1}{2}}(c-x)^{-\frac{3}{2}}\,F(x)$ is regular in $0 \leqslant x \leqslant c$. For example at the rounded leading edge $x=0$, series expansions of the form

$$F(x) = x^{\frac{1}{2}}(F_0 + F_1 x + \ldots),\ C(x) = C_1 x + C_2 x^2 + \ldots \quad . \quad . \quad (24)$$

must hold, while at the cusp F must fall to zero at least as rapidly as $(c-x)^{\frac{3}{2}}$, but C only like $(c-x)$.

It is now easy to find the analytic form of u_n, v_n for $n=1, 2, 3$ by means of a second trivial lemma.

Lemma 2. If $f(w)\,w^{\frac{1}{2}}(c-w)^{\frac{1}{2}}$ is regular in $0 \leqslant w \leqslant c$ then so is

$$\int_0^c \frac{f(w)\,dw}{x-w} \quad (\text{in } 0 \leqslant x \leqslant c).$$

It follows from Lemma 2 and (17) that u_{11} is regular in $0 \leqslant x \leqslant c$, and so is $u_{12}\,x^{\frac{1}{2}}(c-x)^{\frac{1}{2}}$. Hence by (19) both $U(x)$ and $V(x)\,x^{-\frac{1}{2}}(c-x)^{-\frac{3}{2}}$ are regular in $0 \leqslant x \leqslant c$. In this respect $U(x)$ and $V(x)$ are completely parallel to $C(x)$ and $F(x)$, and it follows that the singularity of (u_2, v_2) at either leading edge or trailing edge is no worse than that of (u_1, v_1). Notice how it proved essential to the truth of this important first conclusion that $C(x)$ should vanish at both leading and trailing edges; otherwise $V(x)\,x^{-\frac{1}{2}}\,(c-x)^{-\frac{3}{2}}$ could not have been concluded regular in $0 \leqslant x \leqslant c$. *Thus it is necessary as a first step, before any expansion in powers of the disturbances is attempted, that the chord of the aerofoil be selected as x-axis* (so that all adjustments of incidence have to be made by changing the velocity at infinity).

However, the analytic behaviour of (u_1, v_1) and (u_2, v_2) is by no means satisfactory, at least at the leading edge, where (15) and (20) show that all four coefficients become infinite whereas in fact the velocity, even on potential theory, must remain finite. Some modification of the theory must be made, and (as Section 3 will show) it is the analytic behaviour of (u_3, v_3), now to be investigated, which suggests the modification which is necessary.

Now (u_3, v_3) are given by Equation (23) in terms of functions $W(x)$, $Z(x)$ defined in (22). Lemma 2 shows that all the integrals in (21) and (22) are regular in $0 \leqslant x \leqslant c$, in virtue of the information concerning $U(x)$ and $V(x)$ just obtained. It follows that $W(x)$ is regular, using the form of $F(x)$ at the singularities and the fact that $C(x)$, as well as being regular, vanishes at both singularities. However, $Z(x)x^{-\frac{1}{2}}(c-x)^{-\frac{3}{2}}$ is *not* regular in $0 \leqslant x \leqslant c$, unlike the corresponding products involving $F(x)$ or $V(x)$. The contributions to this product from the first three terms of $Z(x)$ in (18), and from the term $\frac{1}{2}C^2(x)F''(x)$, are regular. However, the term $\frac{1}{2}F^2(x)F''(x)$ in $Z(x)$, while of satisfactory order $(c-x)^{\frac{3}{2}}$ at the trailing edge, is of order $x^{-\frac{1}{2}}$ at the leading edge. In fact, as a result of this term,

$$Z(x) \sim -\tfrac{1}{8}F_0^3 x^{-\frac{1}{2}} \text{ as } x \longrightarrow 0. \quad . \quad . \quad . \quad (25)$$

Thus it follows at once by (21) that v_3 has a higher order of infinity on $y=0$ as $x \longrightarrow 0$ than v_1 or v_2, namely $v_3 \sim \pm \frac{1}{16}F_0^3 x^{-\frac{3}{2}}$. It is clear from this that the singularity of the whole vector field (u_3, v_3) at $x=0$ is of a similar order, namely $u_3 - iv_3 \sim -\frac{1}{16}iF_0^3(x+iy)^{-\frac{3}{2}}$ (although actually the conditions of Lemma 1 are not satisfied and the expression (23) for $u_3 - iv_3$ contains a divergent integral).

To sum up, there is a single term $\pm \frac{1}{16}F_0^3 x^{-\frac{3}{2}}$ on the right hand side of the boundary condition for v_3 ((10) or (21)), in view of which the third order terms $\varepsilon^3 u_3$ and $\varepsilon^3 v_3$ in the series (4) for the velocity field are even more singular at the leading edge than the first and second order terms.

3. Deduction of a Uniformly Valid Approximation

From the results of Section 2 a uniformly valid approximation will now be deduced, following ideas of an earlier paper[5], which will first be briefly summarised.

If there is a singularity near which successive terms in a series solution are each still more singular than the last, so that sufficiently near the singularity the series diverges, the divergence can be removed by *straining the co-ordinate system*, and hence considering each coefficient of the series solution as a function of new independent variables. The required transformation of the independent variables may also (like the solution itself) be put in the form of series expansions in powers of the small parameter (here ε), say

$$\left.\begin{aligned} x &= X + \varepsilon x_1(X,Y) + \varepsilon^2 x_2(X,Y) + \ldots, \\ y &= Y + \varepsilon y_1(X,Y) + \varepsilon^2 y_2(X,Y) + \ldots, \end{aligned}\right\} \quad . \quad . \quad . \quad (26)$$

and may be determined progressively as the coefficients in the series for the solutions are found. If it is desired only to use the latter series up to and including terms of order ε^n then the series (26) may similarly be stopped at this point; here n would

be 1 or 2 in practice. The transformation of independent variables alters the differential equations or boundary conditions for the coefficients of powers of ε in the solutions, and can in fact be determined so that the increase in order of magnitude of these coefficients near the singularity no longer occurs. In many cases a singularity remains but it is pushed outside the domain of physical interest, in which the process now converges to a non-singular solution.

In the problems treated in Ref. 5 the partial differential equation was usually hyperbolic, so that the singularity lay along a whole characteristic. The kind of transformation required to shift this singular curve (this is necessary, for it is essentially a misplacing of the singularity, owing to not letting its position be a function of ε, that causes the divergence) then necessarily took the form of a small alteration to that "characteristic variable" which vanished on the said curve. But in the present elliptic problem, for which the singularity is confined to a single point (the leading edge $x=y=0$), as it will be generally in elliptic problems, there is more freedom in the choice of what variable may conveniently be given a small change so as to shift the singularity to the appropriate position, although probably a good choice may lead to greater simplicity in the analysis.

In the present problem it is evident that a straining of order ε^2 in the independent variables will be sufficient since it is only in (u_3, v_3), not in (u_2, v_2), that an increase in order of magnitude near the singularity first becomes apparent, whence there is no need to do anything that will change the field (u_2, v_2). Further, it is not proposed that any more terms in the series for the velocity field than $\varepsilon u_1+\varepsilon^2 u_2$, $\varepsilon v_1+\varepsilon^2 v_2$ be used, and therefore it will be sufficient to terminate the series (26) at the terms in ε^2. Hence all that is required is to determine a transformation

$$x=X+\varepsilon^2 x_2(X,Y), \quad y=Y+\varepsilon^2 y_2(X,Y), \qquad (27)$$

such that, when u, v are expanded in series of powers of ε whose coefficients are functions of X and Y, the coefficients of ε^3 are no more singular at the origin than those of ε and ε^2. It is assumed without proof, as a result of the careful analysis of analogous problems in Ref. 5, that the process could be continued indefinitely and that with further, even smaller, modifications to x, y all subsequent increases in the order of the singularity could also be prevented. In consequence it is inferred that the process converges uniformly within the field of flow.

The deduction of a suitable form for x_2 and y_2 could be made by substituting (27) in the equations of motion and boundary conditions, with the coefficients in the series (4) for the velocity field regarded as functions of X, Y rather than of x, y, and equating coefficients of ε, ε^2 and ε^3. Evidently u_1, v_1, u_2 and v_2 would be the same functions of X, Y as they were found to be of x, y in Section 2. But u_3, v_3 would have a different expression, involving the unknown functions $x_2(X,Y)$ and $y_2(X,Y)$, and these would then be selected so that no singularity in u_3, v_3 of worse than inverse square root type occurred at the origin $X=Y=0$.

However, in the present instance it was not necessary to go through this process, because the preliminary study of a simple case (the Joukowsky aerofoil), for which the exact solution is known, indicated that the simple transformation, obtained from (27) by taking $y_2=0$ and x_2 a mere constant, might suffice. The verification that this is true in general was very simple, proceeding as follows.

Since the co-ordinates are changed by a mere constant shift, the vector fields (u_n, v_n) must still be irrotational and solenoidal even in the new co-ordinates. The conditions at infinity (5) are also unaltered. But the boundary condition (2) takes the form

$$\left[\frac{v(X,y)}{u(X,y)}\right]_{y=\varepsilon[C(X+\varepsilon^2 x_2)\pm F(X+\varepsilon^2 x_2)]} = \varepsilon\,[C'(X+\varepsilon^2 x_2)\pm F'(X+\varepsilon^2 x_2)]\,, \quad . \quad (28)$$

and when this is expanded in series in the form (6), the left hand side is evidently modified only to order ε^4, while the right hand side is changed, even though terms of order ε^4 be neglected, to

$$\varepsilon\,[C'(X)\pm F'(X)]+\varepsilon^3 x_2\,[C''(X)\pm F''(X)]\,. \quad . \quad . \quad (29)$$

Hence the equations (8), (9) and (10) remain true, with X written for x throughout, except that there is an additional term $x_2\,[C''(X)\pm F''(X)]$ on the right of (10). Hence u_1, v_1, u_2, v_2 are (as foreshadowed above) the same functions of X and y as they were previously of x and y. But the boundary condition for v_3 in the form (21), again with X for x, is correct only if $W(X)$ be increased by $x_2 C'(X)$ and $Z(X)$ by $x_2 F'(X)$. As a result of this change $W(X)$ remains regular in $0\leqslant X\leqslant c$, but the part of $Z(X)$ which is infinite at $X=0$, namely $-\frac{1}{8}F_0{}^3 X^{-\frac{1}{2}}$ (*see* (25)), disappears provided that

$$x_2=\tfrac{1}{4}F_0{}^2. \quad . \quad . \quad . \quad . \quad . \quad (30)$$

With the cancellation of this infinite part, what remains satisfies (like $F(X)$ and $V(X)$) the condition that $X^{\frac{1}{2}}(c-X)^{\frac{1}{2}}\,Z(X)$ be regular in $0<X<c$, and therefore the field (u_3, v_3) is no more singular as a function of (X, y) than (u_1, v_1) or (u_2, v_2).

Once x_2 has been determined in this way no further notice need be taken of the cumbersome u_3 and v_3. The approximation which has been discovered to be valid if the cubes of the disturbances are neglected is

$$\left.\begin{aligned} u&=U\,[1+\varepsilon u_1(x-\tfrac{1}{4}F_0{}^2\varepsilon^2,\ y)+\varepsilon^2 u_2(x-\tfrac{1}{4}F_0{}^2\varepsilon^2,\ y)]\,,\\ v&=U\,[\varepsilon v_1(x-\tfrac{1}{4}F_0{}^2\varepsilon^2,\ y)+\varepsilon^2 v_2(x-\tfrac{1}{4}F_0{}^2\varepsilon^2,\ y)]\,, \end{aligned}\right\} \quad . \quad (31)$$

where the functions u_1, v_1, u_2 and v_2 were determined in Section 2 by equations (15) and (20). A uniformly valid first approximation would still remain if the terms in u_2, v_2 in (31) were omitted; but the shift of the origin to the point $(\frac{1}{4}F_0{}^2\varepsilon^2, 0)$ cannot be omitted if the approximation is to have any value at all near the leading edge.

This new position of the singularity of the approximate velocity field (31) is inside the aerofoil contour, being at the mid-point of the radius of curvature of the leading edge. This is evident from the equation of the aerofoil contour $y=\varepsilon[\pm F_0 x^{\frac{1}{2}}+C_1 x+\ldots]$ and Newton's formula $\lim[y^2/(2x)]$ for radius of curvature at the origin.

This justifies the conclusion in the form stated in the Introduction, that the velocity field given by the first or second approximation is valid uniformly, even near the leading edge, if it is shifted bodily downstream (parallel to the chord) through a distance equal to half the leading edge radius of curvature.

Some departure from the extreme simplicity of this conclusion is to be expected when the work is extended to three-dimensional or compressible flow fields. It might be found, for example, that a shift in x by an amount depending (at least) on z (the distance along the span) was necessary in the three-dimensional case, and that it was necessary to take non-zero values for x_1 and y_1 in the series (26) in compressible flow. Unfortunately the author cannot at present work on these suggested extensions, but hopes that some reader may be interested enough to achieve them, at least in part.

4. Formulae for the Velocity Distribution on the Surface

In this section the formulae of Section 3 are specialised to give approximations to the distribution of q/U, the ratio of the fluid speed to its value at infinity, over the surface of the aerofoil. This is done partly because it makes possible a check of the theory against Goldstein's Approximations II and III, partly because one or two new facts of interest emerge, and partly because the simplifications used in the process will be helpful as indicating how to proceed when the work is generalised as indicated in Section 1.

On the surface

$$q=(u^2+v^2)^{\frac{1}{2}}=u\{1+\varepsilon^2[C'(x)\pm F'(x)]^2\}^{\frac{1}{2}} \quad . \quad . \quad (32)$$

by (2), and either of these forms may be useful in calculating q. It is evident that, to an approximation in which squares of ε are neglected throughout, q may be taken as $U(1+\varepsilon u_1)$ and also the surface value of u_1 may be equated to its value on $y=\pm 0$, and therefore

$$\frac{q}{U}=(1+\varepsilon u_1)_{y=\pm 0}=1+\varepsilon\{u_{11}(x)\pm u_{12}(x)\} \quad . \quad . \quad (33)$$

on the surface, with u_{11}, u_{12} defined by (17). This is Goldstein's Approximation I. Going to the next approximation but without yet making any effort to make it

accurate at the leading edge, so that cubes of ε^3 are neglected throughout, we have

$$\frac{q}{U} = (1+\varepsilon u_1+\varepsilon^2 u_2)_{y=\pm 0} + \varepsilon^2 \left(\frac{\partial u_1}{\partial y}\right)_{y=\pm 0} [C(x) \pm F(x)] + \tfrac{1}{2}\varepsilon^2 [C'(x) \pm F'(x)]^2$$

$$= 1 - \tfrac{1}{2}\varepsilon^2 \alpha^2 + \frac{1}{\pi}\int_0^c \frac{\varepsilon F'(w) + \varepsilon^2 V'(w)}{x-w}\, dw +$$

$$+ \left(\frac{c-x}{x}\right)^{\frac{1}{2}} \left\{ \varepsilon\alpha + \frac{1}{\pi}\int_0^c \frac{\varepsilon C'(w) + \varepsilon^2 U'(w)}{x-w} \left(\frac{w}{c-w}\right)^{\frac{1}{2}} dw \right\} +$$

$$+ \varepsilon^2 \{ [C(x) \pm F(x)][C''(x) \pm F''(x)] + \tfrac{1}{2}[C'(x) \pm F'(x)]^2 \}, \qquad . \quad (34)$$

on the surface, where use has been made of (15), (20) and the fact that, by (8), $\partial u_1/\partial y = \partial v_1/\partial x = C''(x) \pm F''(x)$ on $y = \pm 0$. It should be noticed that although the first and second approximations u_1, u_2, v_1, v_2 to the velocity *components* on the surface are only infinite like $x^{-\frac{1}{2}}$ at $x=0$, the magnitude (34) of the velocity on the surface, as expanded up to and including terms in ε^2, is infinite like $-\frac{1}{8}\varepsilon^2 F_0^{\,2} x^{-1}$, which arises from the terms $\varepsilon^2 [F(x)F''(x) + \frac{1}{2}\{F'(x)\}^2]$ therein.

The correction of (33) and (34) near the leading edge is performed by an identical process and it will be sufficient here to do it for the more inclusive formula (34). The velocity field (15) behaves like

$$u_1 - iv_1 \sim \left[c^{\frac{1}{2}} \left(\alpha - \int_0^c \frac{C'(w)\, dw}{w^{\frac{1}{2}}(c-w)^{\frac{1}{2}}} \right) - \tfrac{1}{2} i F_0 \right] (x+iy)^{-\frac{1}{2}} \qquad . \quad (35)$$

near the origin, and $u_2 - iv_2$ has a similar behaviour. Thus the velocity field, after the translation of axes found to be necessary in Section 3 has been applied, is given by

$$\frac{u-iv}{U} = 1 + \varepsilon(u_1 - iv_1) + \varepsilon^2 (u_2 - iv_2)$$

$$= [A_1 - \tfrac{1}{2} i(\varepsilon F_0 + \varepsilon^2 V_0)](x - \tfrac{1}{4}F_0^{\,2}\varepsilon^2 + iy)^{-\frac{1}{2}} + 1 + k_0 + k_1 (x - \tfrac{1}{4}F_0^{\,2}\varepsilon^2 + iy)^{\frac{1}{2}} + \ldots .$$

$$. \quad . \quad . \quad . \quad . \quad . \quad . \quad (36)$$

in some neighbourhood of the singularity $(\frac{1}{4}F_0^{\,2}\varepsilon^2, 0)$ into which the leading edge is shifted by the translation; here A_1, k_0, k_1, ... are constants, each containing a portion of order ε and a portion of order ε^2. Equation (36) must be approximated, for $y = \varepsilon[C(x) \pm F(x)]$, so that it is correct to within $O(\varepsilon^3)$ for $x >> \frac{1}{4}F_0^{\,2}\varepsilon^2$, and correct at least to within $O(\varepsilon)$ for all x. (The latter condition could hardly be improved while the first term of (36) contains the translation of x only to the first approximation $\frac{1}{4}F_0^{\,2}\varepsilon^2$).

In all the terms in (36) $(x-\frac{1}{4}\varepsilon^2 F_0{}^2+iy)^{\frac{1}{2}}$ may be replaced by $x^{\frac{1}{2}}+\frac{1}{2}iy\,x^{-\frac{1}{2}}$, because the squares of these expressions differ only by $\frac{1}{4}(y^2x^{-1}-\varepsilon^2F_0{}^2)=O(\varepsilon^2x^{\frac{1}{2}})$ which is in the ratio ε^2 to the terms retained when x is not small, and for all x is at most in the ratio ε to them, this maximum being achieved for $x=O(\varepsilon^2)$. Hence

$$\frac{u}{U}=\mathscr{R}\left[\frac{A_1-\frac{1}{2}i(\varepsilon F_0+\varepsilon^2V_0)}{x^{\frac{1}{2}}+\frac{1}{2}iyx^{-\frac{1}{2}}}+1+k_0+k_1(x^{\frac{1}{2}}+\tfrac{1}{2}iyx^{-\frac{1}{2}})+\right.$$
$$\left.+\,k_2(x+iy)+k_3(x^{\frac{3}{2}}+\tfrac{3}{2}iyx^{\frac{1}{2}})+\dots\right], \qquad (37)$$

where the higher powers of $x^{\frac{1}{2}}+\frac{1}{2}yx^{\frac{1}{2}}$ have been replaced by the first two terms of their binomial expansion, with an error uniformly $O(\varepsilon^3)$. Hence

$$\frac{u}{U}=\frac{A_1x^{\frac{1}{2}}-\frac{1}{4}yx^{-\frac{1}{2}}(\varepsilon F_0+\varepsilon^2V_0)}{x+\frac{1}{4}y^2x^{-1}}+1+\mathscr{R}k_0+\mathscr{R}k_1x^{\frac{1}{2}}+\mathscr{R}k_2x+\dots+$$
$$+y\{-\tfrac{1}{2}\mathscr{I}k_1x^{-\frac{1}{2}}-\mathscr{I}k_2-\tfrac{3}{2}\mathscr{I}k_3x^{\frac{1}{2}}-\dots\}. \qquad (38)$$

Now if the cube of ε had been neglected without *any* exception in (38), so that the term $\frac{1}{4}y^2x^{-1}$ in the denominator of the fraction had been neglected, the straightforward second approximation

$$1+(\varepsilon u_1+\varepsilon^2u_2)_{y=\pm0}+y\,\varepsilon\left(\frac{\partial u_1}{\partial y}\right)_{y=\pm0} \qquad (39)$$

to u on the surface would have been obtained. Comparing the two (and replacing the said $\frac{1}{4}y^2x^{-1}$ in the denominator by $\frac{1}{4}F_0{}^2\varepsilon^2$, which it equals in the only region where it is important) we obtain

$$\frac{u}{U}=\frac{A_1x^{\frac{1}{2}}-\frac{1}{4}yx^{-\frac{1}{2}}\varepsilon F_0}{x+\frac{1}{4}F_0{}^2\varepsilon^2}+1+(\varepsilon u_1+\varepsilon^2u_2)_{y=\pm0}-A_1x^{-\frac{1}{2}}+y\left[\varepsilon\left(\frac{\partial u_1}{\partial y}\right)_{y=\pm0}+\tfrac{1}{4}\varepsilon F_0x^{-\frac{3}{2}}\right]$$
$$=\frac{x}{x+\frac{1}{4}F_0{}^2\varepsilon^2}\{A_1x^{-\frac{1}{2}}-\tfrac{1}{4}yx^{-\frac{3}{2}}\varepsilon F_0+1+\tfrac{1}{4}F_0{}^2\varepsilon^2x^{-1}+(\varepsilon u_1+\varepsilon^2u_2)_{y=\pm0}-$$
$$-A_1x^{-\frac{1}{2}}+y[\varepsilon(\partial u_1/\partial y)_{y=\pm0}+\tfrac{1}{4}\varepsilon F_0x^{-\frac{3}{2}}]\}, \qquad (40)$$

where in all the terms $(\mathscr{R}k_n)x^{\frac{1}{2}n}$ and $(\mathscr{I}k_n)\frac{1}{2}nx^{\frac{1}{2}n-1}$ it has been permissible to multiply by $x/(x+\frac{1}{4}F_0{}^2\varepsilon^2)$ because the error is a factor $1+O(\varepsilon^2)$ for ordinary x and is only 100 per cent. for $x\longrightarrow0$, while the terms involved are uniformly $O(\varepsilon)$. Simplifying (40) and making use of the value of $\partial u_1/\partial y$ on $y=\pm0$ as was done in (34), we obtain

$$\frac{u}{U}=\frac{x}{x+\frac{1}{4}F_0{}^2\varepsilon^2}\{(1+\varepsilon u_1+\varepsilon^2u_2)_{y=\pm0}+$$
$$+\varepsilon^2[C(x)\pm F(x)][C''(x)\pm F''(x)]+\tfrac{1}{4}F_0{}^2\varepsilon^2x^{-1}\}. \qquad (41)$$

It should be noted that this surface value of u is obtained from the "natural" second approximation by the two simple steps of (*i*) removing the term of order x^{-1} by adding $\frac{1}{4}F_0^2\varepsilon^2 x^{-1}$, and (*ii*) multiplying by a factor $x/(x+\frac{1}{4}F_0^2\varepsilon^2)$. Thus the zero value at the leading edge is achieved exactly.

Finally, to obtain q/U, (32) shows that into (41) must be inserted a factor, which may be written

$$(1+\tfrac{1}{4}F_0^2\varepsilon^2 x^{-1})^{\frac{1}{2}}\{1+\tfrac{1}{2}\varepsilon^2[C'(x)\pm F'(x)]^2-\tfrac{1}{8}\varepsilon^2 F_0^2 x^{-1}\}. \quad . \quad (42)$$

to the order of approximation used here, giving

$$\frac{q}{U}=\left(\frac{x}{x+\frac{1}{4}F_0^2\varepsilon^2}\right)^{\frac{1}{2}}\{(1+\varepsilon u_1+\varepsilon^2 u_2)_{y=\pm 0}+\varepsilon^2[C(x)\pm F(x)][C''(x)\pm F''(x)]+$$
$$+\tfrac{1}{2}\varepsilon^2[C'(x)\pm F'(x)]^2+\tfrac{1}{8}\varepsilon^2 F_0^2 x^{-1}\}. \quad . \quad . \quad . \quad (43)$$

Again, this is obtained from the "natural" second approximation (34) by (*i*) removing the term of order x^{-1}, this time by adding $\frac{1}{8}\varepsilon^2 F_0^2 x^{-1}$, and (*ii*) by multiplying by a factor $[x/(x+\frac{1}{4}F_0^2\varepsilon^2)]^{\frac{1}{2}}$. These are very simple corrections, and it is consoling that the labour involved in obtaining the "natural" second approximation would not have to be followed by much additional work to make it uniformly valid.

If the terms in ε^2 were not retained, the approximation (43) would become

$$\frac{q}{U}=\left(\frac{x}{x+\frac{1}{4}F_0^2\varepsilon^2}\right)^{\frac{1}{2}}\left(1+(u_1)_{y=\pm 0}\right), \quad . \quad . \quad . \quad (44)$$

so that equation (33) (Goldstein's Approximation I) is rendered uniformly valid simply by multiplication by a factor. This is in agreement with Goldstein's Approximation II. The factors are not identical, but they agree to within the approximation used.

The calculation of the second approximation (34), which is so easily modified to become uniformly valid, would probably be done numerically, in terms of values of $C(x)$ and $F(x)$ given at, say 40 points round the aerofoil. The integrals occurring in (34), as well as in the definition (17), (19) of U and V, would be computed by the convenient Germain-Thwaites-Watson method[7]. (Of course for a wide range of aerofoils given by algebraic formulae, u_{11}, u_{12} and hence U, V can be calculated analytically, but the part of the integrals in (34) involving U, V would probably be too complicated for this approach to be used).

It is evident from the approximation (44), with the behaviour of $(u_1)_{y=\pm 0}$ at $x=0$ deducible from (35), that near the leading edge the surface velocity is given approximately by

$$\frac{\pm x^{\frac{1}{2}}+c^{\frac{1}{2}}\varepsilon(\alpha-\alpha_{opt})}{(x+\frac{1}{4}F_0^2\varepsilon^2)^{\frac{1}{2}}} \quad . \quad . \quad . \quad . \quad . \quad (45)$$

where
$$\alpha_{opt}=\int_0^c \frac{C'(w)\,dw}{w^{\frac{1}{2}}(c-w)^{\frac{1}{2}}} \quad . \quad . \quad . \quad . \quad . \quad (46)$$

is the angle of incidence for which the leading edge is itself the stagnation point. For other angles of incidence the stagnation point is at $x=c\,\varepsilon^2(\alpha-\alpha_{opt})^2$; also the peak velocity (if there is one near the leading edge) is achieved at $x=\frac{1}{16}\,\varepsilon^2 F_0^4/\{c(\alpha-\alpha_{opt})^2\}$, being equal to

$$q_{max}=U\left[1+\frac{4c}{F_0^2}(\alpha-\alpha_{opt})^2\right]^{\frac{1}{2}} \quad . \quad . \quad . \quad . \quad (47)$$

This demonstrates the well-known fact that stalling for ordinary aerofoils sets in, to a very rough approximation, when the incidence departs from the optimum incidence by the square root of the ratio $\frac{1}{2}\,\varepsilon^2 F_0^2/c$ of leading edge radius of curvature to chord (this incidence gives $q_{max}=U\sqrt{3}$).

The second order formula (34) for surface velocity (which needs modification as in (43)) is particularly simple if second order terms due only to the effect of high incidence are taken into account, for then, by (19), U and V are simply given by

$$U(x)=\alpha\left(\frac{c-x}{x}\right)^{\frac{1}{2}}F(x),\quad V(x)=\alpha\left(\frac{c-x}{x}\right)^{\frac{1}{2}}C(x). \quad . \quad . \quad (48)$$

The resulting formula may be compared with Goldstein's Approximation III, which makes no assumption of small incidence, and it agrees to within the order of approximation.

Finally the lift of a thin aerofoil is investigated. This is equal to $2\pi\rho U$ times the imaginary part of the coefficient of $(x+iy)^{-1}$ in $u-iv$ at infinity. Clearly this coefficient will not be affected by the translation of axes. Hence, by (15) and (20), the lift is

$$2\pi\rho U^2\left[\tfrac{1}{2}c\varepsilon\alpha-\frac{1}{\pi}\int_0^c\left(\varepsilon C'(w)+\varepsilon^2 U'(w)\right)\left(\frac{w}{c-w}\right)^{\frac{1}{2}}dw\right], \quad . \quad (49)$$

and the lift coefficient is

$$C_L=2\pi\varepsilon\alpha-\frac{4}{c}\int_0^c\left(\varepsilon C'(w)+\varepsilon^2 U'(w)\right)\left(\frac{w}{c-w}\right)^{\frac{1}{2}}dw \quad . \quad . \quad (50)$$

Equation (50) gives at once a second order approximation to the no-lift angle, which is not generally known. Also the lift curve slope appears as

$$\frac{dC_L}{d(\varepsilon\alpha)} = 2\pi - \frac{4}{c}\varepsilon \int_0^c \left(\frac{w}{c-w}\right)^{\frac{1}{2}} d\left[F(w)\left(\frac{c-w}{w}\right)^{\frac{1}{2}}\right] = 2\pi + 2\varepsilon \int_0^c \frac{F(w)\,dw}{w(c-w)}. \quad . \quad . \quad . \quad . \quad . \quad . \quad (51)$$

This agrees, to the approximation considered, with the value given by Goldstein's theory when the Kutta-Joukowsky condition is assumed.

This section, and the paper, may be concluded by giving the second approximation to the surface velocity distribution, rendered a valid approximation as in (41) even near the leading edge, in a notation free of tiresome epsilons, which are really only convenient for the purpose of explaining the theory. If then the aerofoil surface is $y = C(x) \pm F(x)$, $0 \leqslant x \leqslant c$, where $C(0) = C(c) = 0$ and $F(x) \sim (2\rho_L x)^{\frac{1}{2}}$ as $x \to 0$, so that ρ_L is the leading edge radius of curvature, and if α is the angle of incidence, and if the functions $U(x)$ and $V(x)$ are defined by equations (17) and (19), then the ratio q/U of the fluid speed on the surface to its value at infinity is given by the formula

$$\frac{q}{U} = \left(\frac{x}{x+\frac{1}{2}\rho_L}\right)^{\frac{1}{2}} \left\{1 - \tfrac{1}{2}\alpha^2 + \frac{1}{\pi}\int_0^c \frac{F'(w)+V'(w)}{x-w}\,dw \pm \right.$$

$$\pm \left(\frac{c-x}{x}\right)^{\frac{1}{2}} \left[\alpha + \frac{1}{\pi}\int_0^c \frac{C'(w)+U'(w)}{x-w}\left(\frac{w}{c-w}\right)^{\frac{1}{2}} dw\right] +$$

$$\left. + [C(x) \pm F(x)]\,[C''(x) \pm F''(x)] + \tfrac{1}{2}[C'(x) \pm F'(x)]^2 + \tfrac{1}{4}\frac{\rho_L}{x}\right\} \quad . \quad (52)$$

where the upper and lower signs refer to the upper and lower surfaces respectively.

References

1. Glauert, H. (1925). *Aerofoil and Airscrew Theory*. Cambridge, 1925.
2. Goldstein, S. (1948). Low-Drag and Suction Airfoils. *Journal of the Aeronautical Sciences*, Vol. 15, pp. 189-220, April 1948.
3. Hantzsche, W. and Wendt, H. (1942). The Effect of Compressibility on Thin Slightly Cambered Profiles at Subsonic Speeds. *Z.A.M.M.*, Vol. 22, pp. 72-90, April 1942.
4. Jones, R. T. (1950). Leading-Edge Singularities in Thin-Airfoil Theory. *Journal of the Aeronautical Sciences*, Vol. 17, pp. 307-310, May 1950.
5. Lighthill, M. J. (1949). A Technique for Rendering Approximate Solutions to Physical Problems Uniformly Valid. *Phil. Mag.*, Vol. 40, pp. 1179-1201, December 1949.
6. Theodorsen, T. (1931). Theory of Wing Sections of Arbitrary Shape. N.A.C.A. Report 411, 1931.
7. Watson, E. J. (1945). Formulae for the Computation of the Functions Employed for Calculating the Velocity Distribution about a Given Aerofoil. R. & M. 2176, May 1945.

The Profile Drag of Yawed Wings of Infinite Span*

A. D. YOUNG, M.A., F.R.Ae.S.

and

T. B. BOOTH, B.A., D.C.Ae.

(*Department of Aerodynamics, College of Aeronautics*)

Summary: A method is developed for calculating the profile drag of a yawed wing of infinite span, based on the assumption that the form of the spanwise distribution of velocity in the boundary layer, whether laminar or turbulent, is insensitive to the chordwise pressure distribution. The form is assumed to be the same as that accepted for the boundary layer on an unyawed plate with zero external pressure gradient. Experimental evidence indicates that these assumptions are reasonable in this context. The method is applied to a flat plate and the N.A.C.A. 64-012 section at zero incidence for a range of Reynolds numbers between 10^6 and 10^8, angles of yaw up to 45°, and a range of transition point positions. It is shown that the drag coefficients of a flat plate varies with yaw as $\cos^{\frac{1}{2}}\Lambda$ (where Λ is the angle of yaw) if the boundary layer is completely laminar, and it varies as $\cos^{\frac{4}{5}}\Lambda$ if the boundary layer is completely turbulent. The drag coefficient of the N.A.C.A. 64-012 section, however, varies closely as $\cos^{\frac{1}{2}}\Lambda$ for transition point positions between 0 and 0.5 *c*. Further calculations on wing sections of other shapes and thicknesses and more detailed experimental checks of the basic assumptions at higher Reynolds numbers are desirable.

1. Introduction and Review

The increasing use of sweepback to delay compressibility troubles has aroused interest in the behaviour of boundary layers on yawed and swept-back wings, for an understanding of this behaviour is required if the characteristics of swept-back wings are to be predicted and controlled satisfactorily. This paper is concerned only with a limited and relatively simple aspect of the problem, namely the profile drag of a yawed wing of infinite span. It is hoped that apart from the intrinsic interest of the results, the discussion will add to the basic store of data and ideas needed to tackle the more general problem.

*Part of this paper appeared in the Thesis presented by T. B. Booth for the Diploma of the College of Aeronautics, 1949.

Paper received October 1950.

[The Aeronautical Quarterly, Vol. III, November 1951]

The treatment begins with the development of the boundary layer equations and the momentum integral equations for laminar and turbulent flow. The development of the laminar boundary layer equations is not new, having been given in essentials elsewhere[1, 2, 3, 4], but it is included here for completeness. It is shown that the chordwise flow is independent of the spanwise flow and hence the corresponding boundary layer equation can be solved by any of the accepted methods. A method for solving the spanwise flow equation is suggested which is approximate but sufficiently accurate for the purpose in mind. For a flat plate at zero incidence it is found that the spanwise velocity profile is strictly similar at all points to that in the chordwise direction, and the resultant direction of flow is everywhere that of the free stream. The skin friction coefficient at any point, as well as the overall drag coefficient, is reduced by the factor $\cos^{\frac{1}{2}}\Lambda$ due to yaw, and thus the skin friction at a point is the same as that on an unyawed plate at the same distance measured parallel to the undisturbed stream direction downstream from the leading edge. This result is peculiar to laminar flow in the boundary layer.

The turbulent boundary layer equations also lead to the conclusion that the chordwise component of flow in the boundary layer can be treated as independent of the spanwise component. The momentum integral equation of the former component can be solved on accepted lines to yield the component of the drag per unit span in the chordwise direction. The drag of unit span of the wing is the resultant of this component and the spanwise component. To obtain the latter it is assumed that the form of the spanwise velocity distribution in the boundary layer is independent of the chordwise pressure distribution and everywhere satisfies a power law, of the type normally assumed to hold in the turbulent boundary layer on an unyawed flat plate in a zero external pressure gradient. This assumption, which might be based somewhat loosely, if intuitively, on the argument that the spanwise conditions of flow correspond in some respects to the simplifying conditions usually assumed in the theory from which the power law is derived, is shown by experiments to be reasonable. For the calculations discussed in this paper the law assumed is the $\frac{1}{7}^{\text{th}}$ power law. The spanwise momentum thickness at the trailing edge is then derived in terms of the chordwise momentum thickness and readily yields the spanwise component of the drag. An expression for the resultant drag coefficient is then presented in a simple and concise form. For a fully turbulent boundary layer on a flat plate at zero incidence, with the velocity distributions in both spanwise and chordwise directions satisfying the $\frac{1}{7}^{\text{th}}$ power law, the drag coefficient is reduced by yaw by the factor $\cos^{\frac{1}{2}}\Lambda$. Here it may be noted that although the flow is everywhere parallel to the undisturbed stream direction the skin friction at a point is not the same as that on an unyawed plate at the same distance measured parallel to that direction from the leading edge. Were it so, the drag coefficient would change with yaw as the factor $\cos^{\frac{1}{2}}\Lambda$.

The method has been applied to calculate the drag coefficient of a flat plate and of the N.A.C.A. 64-012 section at zero incidence for various transition positions, Reynolds numbers and angles of yaw. In the case of the flat plate (Fig. 2*b*) the

factor describing the variation of the drag coefficient with yaw changes steadily from $\cos^{\frac{1}{2}}\Lambda$ to $\cos^{\frac{3}{2}}\Lambda$ as the transition point moves back from the leading to the trailing edge, and there is no noticeable effect of Reynolds number on this factor within the range 10^6 to 10^8. In the case of the 12 per cent. thick wing section (Fig. 2*a*) the factor remains very closely $\cos^{\frac{1}{2}}\Lambda$ for transition positions from the leading edge to 0.5*c*, and the effect of Reynolds number on this factor is very slight.

Preliminary experiments made on a flat plate at a fairly low Reynolds number (about 10^6) tend to confirm the assumptions and conclusions of the theory for angles of yaw up to 45°, but further experimental work at higher Reynolds numbers is desirable.

Notation

The letters L.E. and T.E. refer to leading edge and trailing edge. Suffix "t" refers to a time mean.

x, y	curvilinear orthogonal co-ordinates on the surface of a body (y is in spanwise direction for yawed infinite span wing)	*See* Section 2.1, and Fig. 1
z	normal distance from the body	
u, v, w	velocity components in the boundary layer in the x, y, z directions, respectively	
U_1, V_1	velocity components just outside the boundary layer in x, y directions, respectively	
$\mathbf{v}$	velocity vector $=(u, v, w)$	
$\boldsymbol{\omega}$	curl $\mathbf{v}$	
Q_0	undisturbed stream velocity	
U_0, V_0	components of Q_0 in direction of chord and span respectively, of yawed infinite wing	
Λ	angle of yaw of wing	
u', v', w'	turbulent fluctuation components of velocity in x, y, z directions respectively	
c	chord of wing, measured normal to span	
p	pressure	
ρ	density	
μ	coefficient of viscosity	
ν	kinematic viscosity $=\mu/\rho$	
D	drag of unit span of the wing	
X	component of D in chordwise direction	
Y	component of D in spanwise direction	
$C_D[\alpha, \beta]$	drag coefficient at a Reynolds number α and an angle of yaw β	

R	Reynolds number $= Q_0 c/\nu$
δ	boundary layer thickness
δ_x^*	$\int_0^\delta \left(1-\frac{u}{U_1}\right) dz$
δ_y^*	$\int_0^\delta \left(1-\frac{v}{V_1}\right) dz$
θ_{xx}	$\int_0^\delta \frac{u}{U_1}\left(1-\frac{u}{U_1}\right) dz$
θ_{yy}	$\int_0^\delta \frac{v}{V_1}\left(1-\frac{v}{V_1}\right) dz$
θ_{xy}	$\int_0^\delta \frac{v}{U_1}\left(1-\frac{u}{U_1}\right) dz$
θ_{yx}	$\int_0^\delta \frac{u}{V_1}\left(1-\frac{v}{V_1}\right) dz$
H_x	δ_x^*/θ_{xx}
H_y	δ_y^*/θ_{yy}
τ_{xz}	component of shear stress in chordwise (x) direction
τ_{yz}	component of shear stress in spanwise (y) direction
$(\tau_{xz})_0$	value of τ_{xz} at surface
$(\tau_{yz})_0$	value of τ_{yz} at surface
κ_x, κ_y	curvature of lines $y=$constant, $x=$constant, respectively
n	$(H_x+5)/2$ at the trailing edge
K	$(V_1/U_1)(\theta_{yx}/\theta_{xx})$
λ	$[-\delta^2/(\mu U_1)]\,\partial p/\partial x$
$F(z/\delta)$	$2(z/\delta)-2(z/\delta)^3+(z/\delta)^4$
$G(z/\delta)$	$[z/(6\delta)][1-z/\delta]^3$
ζ	variable of integration
η	$z\sqrt{[U_0/(\nu x)]}$
ψ	stream function
$f(\eta)$	$\psi/\sqrt{(\nu x U_0)}$
ϕ	function defined by $v=\partial\phi/\partial z$
$g(\eta)$	$\phi/\sqrt{(\nu x U_0)}$

2. Boundary Layer Equations

2.1. *Laminar boundary layer*

The equations of motion of a steady viscous incompressible fluid with negligible body forces are, in the vector notation of Ref. 5,

$$-\mathbf{v}\times\boldsymbol{\omega}=-\operatorname{grad}(p/\rho+\tfrac{1}{2}\mathbf{v}^2)-\nu\operatorname{curl}\boldsymbol{\omega}. \quad . \quad . \quad . \quad . \quad (1)$$

The equation of continuity is

$$\operatorname{div}\mathbf{v}=0. \quad . \quad . \quad . \quad . \quad . \quad . \quad . \quad (2)$$

Consider the flow past a surface and take x, y, z as orthogonal curvilinear co-ordinates, such that z is the normal distance from the surface and the lines $x=$constant, $y=$constant, define parallel networks on the surface. The usual assumptions will now be made for the flow inside the boundary layer, namely that the rates of change of the velocity components normal to the surface are large compared with the corresponding rates of change parallel to the surface and that the boundary layer thickness is small compared with a representative linear dimension of the surface. It will be assumed further that, if κ_x and κ_y are the curvatures of the lines $y=$constant and $x=$constant, then the quantities $\kappa_x\delta$, $\kappa_y\delta$, $\delta^2\partial\kappa_x/\partial x$, $\delta^2\partial\kappa_y/\partial y$, $\delta^2\partial\kappa_x/\partial y$, $\delta^2\partial\kappa_y/\partial x$, $\delta^3\partial^2\kappa_x/\partial y^2$, $\delta^3\partial^2\kappa_y/\partial x^2$, $\delta^3\partial^2\kappa_x/\partial x\,\partial y$, and $\delta^3\partial^2\kappa_y/\partial x\,\partial y$ are all small compared with unity, where δ is the boundary layer thickness.

With these assumptions the equations of motion yield the boundary layer equations:—

$$u\frac{\partial u}{\partial x}+v\frac{\partial u}{\partial y}+w\frac{\partial u}{\partial z}=-\frac{1}{\rho}\frac{\partial p}{\partial x}+\nu\frac{\partial^2 u}{\partial z^2}, \quad . \quad . \quad . \quad (3)$$

$$u\frac{\partial v}{\partial x}+v\frac{\partial v}{\partial y}+w\frac{\partial v}{\partial z}=-\frac{1}{\rho}\frac{\partial p}{\partial y}+\nu\frac{\partial^2 v}{\partial z^2}. \quad . \quad . \quad . \quad (4)$$

The equation of motion in the z direction leads to the result that the pressure may be taken as constant across the boundary layer. The equation of continuity is

$$\frac{\partial u}{\partial x}+\frac{\partial v}{\partial y}+\frac{\partial w}{\partial z}=0 \quad . \quad . \quad . \quad . \quad . \quad (5)$$

For a yawed wing of infinite span, the notation illustrated in Fig. 1 will be adopted, *i.e.* x is measured along a section profile from the leading edge in a plane normal to the span and y is measured along the span. In this case the rate of change of any quantity with respect to y is zero, and hence equations (3), (4) and (5) become

$$u\frac{\partial u}{\partial x}+w\frac{\partial u}{\partial z}=-\frac{1}{\rho}\frac{\partial p}{\partial x}+\nu\frac{\partial^2 u}{\partial z^2}, \quad . \quad . \quad . \quad . \quad (6)$$

$$u\frac{\partial v}{\partial x}+w\frac{\partial v}{\partial z}=\nu\frac{\partial^2 v}{\partial z^2}, \quad . \quad . \quad . \quad . \quad . \quad (7)$$

and

$$\frac{\partial u}{\partial x}+\frac{\partial w}{\partial z}=0. \quad . \quad . \quad . \quad . \quad . \quad (8)$$

At the surface $u=v=w=0$.

Just outside the boundary layer $u=U_1$, $v=V_1$, $\partial u/\partial z=\partial v/\partial z=0$, and the flow is irrotational, consequently

$$U_1\frac{\partial U_1}{\partial x}=-\frac{1}{\rho}\frac{\partial p}{\partial x}, \quad . \quad . \quad . \quad . \quad . \quad . \quad (9)$$

and

$$\frac{\partial U_1}{\partial y}-\frac{\partial V_1}{\partial x}=0. \quad . \quad . \quad . \quad . \quad . \quad . \quad (10)$$

Since, however, $\partial U_1/\partial y=0$ it follows that $\partial V_1/\partial x=0$, *i.e.* $V_1=\text{constant}=V_0$, where V_0 is the component of the undisturbed stream velocity along the y axis.

Equations (6), (8) and (9) and the corresponding boundary conditions are identical with those for the boundary layer over the wing in an unyawed flow and with a main stream velocity $=U_0=Q_0\cos\Lambda$. Hence, the chordwise flow in the boundary layer is independent of the spanwise flow and may be derived by any of the well-established methods. An approximate method for solving for the spanwise flow will be discussed in Section 3.

2.2 *Turbulent boundary layer*

With the usual boundary layer assumptions the equations of motion for the turbulent boundary layer in three dimensions become

$$u\frac{\partial u}{\partial x}+v\frac{\partial u}{\partial y}+w\frac{\partial u}{\partial z}=-\frac{1}{\rho}\frac{\partial p}{\partial x}+\nu\frac{\partial^2 u}{\partial z^2}-\frac{\partial}{\partial x}(u'^2)_t-\frac{\partial}{\partial y}(u'v')_t-\frac{\partial}{\partial z}(u'w')_t, \quad (11)$$

$$u\frac{\partial v}{\partial x}+v\frac{\partial v}{\partial y}+w\frac{\partial v}{\partial z}=-\frac{1}{\rho}\frac{\partial p}{\partial y}+\nu\frac{\partial^2 v}{\partial z^2}-\frac{\partial}{\partial x}(u'v')_t-\frac{\partial}{\partial y}(v'^2)_t-\frac{\partial}{\partial z}(v'w')_t, \quad (12)$$

where undashed letters now refer to time means, the dashes denote turbulent fluctuations and suffix "t" denotes a time mean. The third equation of motion may again be interpreted as indicating that the variation of pressure across the boundary layer can be neglected. The equation of continuity is

$$\frac{\partial u}{\partial x}+\frac{\partial v}{\partial y}+\frac{\partial w}{\partial z}=0. \quad . \quad . \quad . \quad . \quad . \quad . \quad (13)$$

For the yawed wing of infinite span, these equations reduce to

$$u\frac{\partial u}{\partial x}+w\frac{\partial u}{\partial z}=-\frac{1}{\rho}\frac{\partial p}{\partial x}+\nu\frac{\partial^2 u}{\partial z^2}-\frac{\partial}{\partial x}(u'^2)_t-\frac{\partial}{\partial z}(u'w')_t, \quad . \quad . \quad (14)$$

$$u\frac{\partial v}{\partial x}+w\frac{\partial v}{\partial z}=\nu\frac{\partial^2 v}{\partial z^2}-\frac{\partial}{\partial x}(u'v')_t-\frac{\partial}{\partial z}(v'w')_t, \quad . \quad . \quad . \quad (15)$$

and

$$\frac{\partial u}{\partial x}+\frac{\partial w}{\partial z}=0. \quad . \quad . \quad . \quad . \quad . \quad (16)$$

Again it may be noted from equations (14), (15) and (16) that the chordwise flow is independent of the spanwise flow and can be calculated as for the unyawed wing in the stream component normal to its span.

2.3. *Momentum integral equations*

It is usual to assume that the rates of change of the mean turbulent stresses in directions parallel to the surface can be neglected, compared with the rates of change normal to the surface. Both the laminar and turbulent boundary layer equations for general three-dimensional flow can then be written

$$u\frac{\partial u}{\partial x}+v\frac{\partial u}{\partial y}+w\frac{\partial u}{\partial z}=-\frac{1}{\rho}\frac{\partial p}{\partial x}+\frac{1}{\rho}\frac{\partial \tau_{xz}}{\partial z}, \quad . \quad . \quad . \quad (17)$$

and

$$u\frac{\partial v}{\partial x}+v\frac{\partial v}{\partial y}+w\frac{\partial v}{\partial z}=-\frac{1}{\rho}\frac{\partial p}{\partial y}+\frac{1}{\rho}\frac{\partial \tau_{yz}}{\partial z}, \quad . \quad . \quad . \quad (18)$$

where $\tau_{xz}=\mu\,\partial u/\partial z$, $\tau_{yz}=\mu\,\partial v/\partial z$, in laminar flow, and $\tau_{xz}=\mu\,\partial u/\partial z-\rho\,(u'w')_t$, $\tau_{yz}=\mu\,\partial v/\partial z-\rho\,(v'w')_t$, in turbulent flow.

Outside the boundary layer

$$U_1\frac{\partial U_1}{\partial x}+V_1\frac{\partial U_1}{\partial y}=-\frac{1}{\rho}\frac{\partial p}{\partial x}, \quad . \quad . \quad . \quad . \quad (19)$$

and

$$U_1\frac{\partial V_1}{\partial x}+V_1\frac{\partial V_1}{\partial y}=-\frac{1}{\rho}\frac{\partial p}{\partial y}. \quad . \quad . \quad . \quad . \quad (20)$$

If equations (17) and (18) are now integrated with respect to z from $z=0$ to $z=\delta$, and use is made of equations (13), (19) and (20), eventually we obtain

$$(\tau_{xz})_0=\frac{\partial}{\partial x}(\rho U_1^2\theta_{xz})+\frac{\partial}{\partial y}(\rho U_1^2\theta_{xy})+\frac{\partial U_1}{\partial x}(\rho U_1\delta_x^*)+\frac{\partial U_1}{\partial y}(\rho V_1\delta_y^*), \quad (21)$$

and

$$(\tau_{yz})_0=\frac{\partial}{\partial y}(\rho V_1^2\theta_{yy})+\frac{\partial}{\partial x}(\rho V_1^2\theta_{yz})+\frac{\partial V_1}{\partial y}(\rho V_1\delta_y^*)+\frac{\partial V_1}{\partial x}(\rho U_1\delta_x^*), \quad (22)$$

where $(\tau_{xz})_0$ and $(\tau_{yz})_0$ are the values of τ_{xz} and τ_{yz}, respectively, at the surface, and

$$\delta_x^*=\int_0^\delta\left(1-\frac{u}{U_1}\right)dz, \quad \delta_y^*=\int_0^\delta\left(1-\frac{v}{V_1}\right)dz,$$

$$\theta_{xx}=\int_0^\delta\frac{u}{U_1}\left(1-\frac{u}{U_1}\right)dz, \quad \theta_{yy}=\int_0^\delta\frac{v}{V_1}\left(1-\frac{v}{V_1}\right)dz,$$

$$\theta_{xy}=\int_0^\delta\frac{v}{U_1}\left(1-\frac{u}{U_1}\right)dz, \quad \theta_{yx}=\int_0^\delta\frac{u}{V_1}\left(1-\frac{v}{V_1}\right)dz.$$

For the yawed wing of infinite span, these equations reduce to

$$(\tau_{xx})_0 = \frac{\partial}{\partial x}(\rho U_1^2 \theta_{xx}) + \frac{\partial U_1}{\partial x}(\rho U_1 \delta_x^*), \quad . \quad . \quad . \quad (23)$$

and

$$(\tau_{yx})_0 = \frac{\partial}{\partial x}(\rho V_1^2 \theta_{yx}). \quad . \quad . \quad . \quad . \quad . \quad . \quad (24)$$

Writing $H_x = \delta_x^*/\theta_{xx}$, equation (23) can be cast in the familiar form

$$\frac{(\tau_{xx})_0}{\rho U_1^2} = \frac{\partial \theta_{xx}}{\partial x} + \frac{1}{U_1}\frac{\partial U_1}{\partial x}[H_x + 2]\theta_{xx}.$$

4. The Calculation of the Profile Drag of a Yawed Wing

3.1. *The drag components*

The drag D of unit span of the wing can be resolved into components X and Y along the x and y axis. From the foregoing it follows that X is the drag of unit span of the wing when unyawed but with the same transition position in a stream of velocity $U_0 = Q_0 \cos\Lambda$, where Q_0 is the resultant undisturbed stream velocity (*see* Fig. 1). Hence X can be calculated by any of the established methods (*see*, for example, Refs. 6, 7 and 8). It remains then to determine the spanwise component of the drag, Y. To do this, it will be noted that, since the undisturbed stream is uniform and the wing section is constant along its infinite span, Y has no form

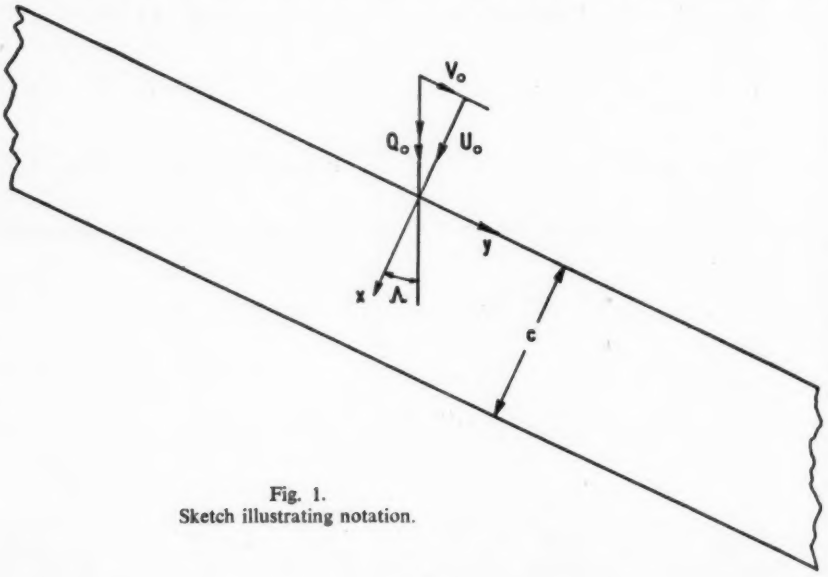

Fig. 1.
Sketch illustrating notation.

drag component but is solely the resultant of the frictional stress $(\tau_{yz})_0$. Thus, per unit span of wing, and for each surface

$$\begin{aligned} Y &= \int_0^c (\tau_{yz})_0 \, dx \\ &= \int_0^c \rho V_0^2 \frac{\partial}{\partial x}(\theta_{yz}) \, dx, \text{ from (24)}, \\ &= \rho V_0^2 [\theta_{yz}]_{\text{L.E.}}^{\text{T.E.}} \\ &= \rho V_0^2 [\theta_{yz}]_{\text{T.E.}}, \qquad . \quad . \quad . \quad . \quad . \quad . \quad . \quad (25) \end{aligned}$$

where L.E. and T.E. refer to the leading edge and trailing edge, respectively. Here it has been assumed that the momentum thickness θ_{yz} is zero at the leading edge and is continuous at the transition point, it being accepted that the stress $(\tau_{yz})_0$ could not become infinite. The problem then reduces to the determination of $[\theta_{yz}]_{\text{T.E.}}$

Now
$$\begin{aligned} \theta_{yz} &= \int_0^\delta \frac{u}{V_1}\left(1 - \frac{v}{V_1}\right) dz \\ &= \frac{U_1}{V_1} \int_0^\delta \frac{u}{U_1}\left(1 - \frac{v}{V_1}\right) dz. \\ &= \frac{U_1}{V_1} K \theta_{zz}, \text{ say}, \end{aligned} \Bigg\} \quad . \quad . \quad (26)$$

$$\text{where } K = \int_0^\delta \frac{u}{U_1}\left(1 - \frac{v}{V_1}\right) dz \Big/ \int_0^\delta \frac{u}{U_1}\left(1 - \frac{u}{U_1}\right) dz.$$

Suppose for the moment that the value of K is known at the trailing edge of the wing. From equations (25) and (26)

$$Y = \rho U_{\text{T.E.}} V_0 K_{\text{T.E.}} \theta_{zz}.$$

But (*see* Ref. 6)

$$\frac{2\theta_{zz}}{c} = \frac{X}{\frac{1}{2}\rho U_0^2 c}\left(\frac{U_0}{U_{\text{T.E.}}}\right)^n,$$

where $n = [(H_z)_{\text{T.E.}} + 5]/2$.

Hence $$Y = \frac{\sin\Lambda}{\cos\Lambda} K_{\text{T.E.}} \left(\frac{U_0}{U_{\text{T.E.}}}\right)^{n-1} X .$$

The resultant drag D is given by

$$D = X\cos\Lambda + Y\sin\Lambda ,$$

and therefore

$$C_D[R,\Lambda] = \frac{D}{\frac{1}{2}\rho Q_0^2 c} = \frac{X}{\frac{1}{2}\rho U_0^2 c}\cos^3\Lambda + \frac{Y}{\frac{1}{2}\rho U_0^2 c}\cos^2\Lambda\sin\Lambda$$

$$= \frac{X}{\frac{1}{2}\rho U_0^2 c}\left\{\cos^3\Lambda + \cos\Lambda\sin^2\Lambda K_{\text{T.E.}}\left(\frac{U_0}{U_{\text{T.E.}}}\right)^{n-1}\right\}$$

$$= C_D[R\cos\Lambda, 0]\cos\Lambda\left\{\cos^2\Lambda + \sin^2\Lambda K_{\text{T.E.}}\left(\frac{U_0}{U_{\text{T.E.}}}\right)^{n-1}\right\} . \qquad (27)$$

Here $C_D[\alpha,\beta]$ denotes the drag coefficient of the wing at a Reynolds number α and an angle of yaw β. Equation (27) enables the drag coefficient of the yawed wing to be calculated in terms of the existing results for the drag coefficient of the unyawed wing, the angle of yaw, the chordwise component of velocity just outside the boundary layer at the trailing edge and the quantities n and K at the trailing edge. The quantity n is known from the chordwise calculations; the problem is solved therefore when $K_{\text{T.E.}}$ has been determined.

3.2 *The spanwise flow in the laminar boundary layer*

It is sufficiently accurate to treat the chordwise flow in the boundary layer by the Karman-Pohlhausen method or by one of the variants based on it (*see*, for example, Ref. 9). Thus we assume

$$\frac{u}{U_1} = a_1\left(\frac{z}{\delta}\right) + b_1\left(\frac{z}{\delta}\right)^2 + c_1\left(\frac{z}{\delta}\right)^3 + d_1\left(\frac{z}{\delta}\right)^4 ,$$

and if the boundary conditions $\nu\dfrac{\partial^2 u}{\partial z^2} = \dfrac{1}{\rho}\dfrac{\partial p}{\partial x}$, at $z=0$,

and $$u = U_1 , \frac{\partial u}{\partial z} = \frac{\partial^2 u}{\partial z^2} = 0 , \text{ at } z=\delta ,$$

are satisfied, it is found that $\dfrac{u}{U_1} = F\left(\dfrac{z}{\delta}\right) + G\left(\dfrac{z}{\delta}\right)$,

where $F\left(\dfrac{z}{\delta}\right) = 2\left(\dfrac{z}{\delta}\right) - 2\left(\dfrac{z}{\delta}\right)^3 + \left(\dfrac{z}{\delta}\right)^4$, $G\left(\dfrac{z}{\delta}\right) = \dfrac{z}{6\delta}\left(1-\dfrac{z}{\delta}\right)^3$,

and $\lambda = -\dfrac{\delta^2}{\mu U_1}\dfrac{\partial p}{\partial x}$.

It then follows that

$$\theta_{xz} = \delta\left[\frac{37}{315} - \frac{\lambda}{945} - \frac{\lambda^2}{9072}\right].$$

If it is likewise assumed that

$$\frac{v}{V_1} = a_2\left(\frac{z}{\delta}\right) + b_2\left(\frac{z}{\delta}\right)^2 + c_2\left(\frac{z}{\delta}\right)^3 + d_2\left(\frac{z}{\delta}\right)^4,$$

and the boundary conditions $\nu\dfrac{\partial^2 v}{\partial z^2} = 0$, at $z = 0$,

and $$v = V_1, \frac{\partial v}{\partial z} = \frac{\partial^2 v}{\partial z^2} = 0, \text{ at } z = \delta,$$

are satisfied, it is found that

$$\frac{v}{V_1} = F\frac{z}{\delta}$$

i.e. the form of the spanwise velocity distribution is independent of the chordwise pressure distribution†. Hence, from (26)

$$K = \delta\int_0^1 [F(\zeta) + \lambda G(\zeta)]\ [1 - F(\zeta)]\, d\zeta/\theta_{xz}$$

$$= \left[\frac{37}{315} + \frac{11\lambda}{3024}\right] \Big/ \left[\frac{37}{315} - \frac{\lambda}{945} - \frac{\lambda^2}{9072}\right]$$

$$= K(\lambda), \text{ say.} \qquad (28)$$

The value of H_z is given by

$$H_z = \left(\frac{3}{10} - \frac{\lambda}{120}\right) \Big/ \left(\frac{37}{315} - \frac{\lambda}{945} - \frac{\lambda^2}{9072}\right) \qquad (29)$$

The usual methods of solution for the chordwise flow yield λ as a function of x, and hence the value of K and H_z (and therefore n) can be determined at the trailing edge from equations (28) and (29), assuming that the flow remained laminar to the

†Sears[2] has calculated by a more accurate method the spanwise velocity profiles for a simple case of an external chordwise pressure gradient leading to chordwise separation. The spanwise profiles show small changes of form up to a point near the separation, after which the change of form becomes more marked. These changes are much less severe than the corresponding changes of form undergone by the chordwise profiles.

trailing edge and was not too near separation anywhere for the foregoing method to be seriously in error. In applying equation (27) it is implicitly assumed that the solution of the momentum integral equation for the wake developing from completely laminar boundary layers follows exactly the lines of the solution for the case when the boundary layers are turbulent at the trailing edge. On the face of it this assumption seems plausible enough, but in any case the problem of the wing with completely laminar boundary layers is at present of little more than academic interest.

It is noted that for a flat plate at zero incidence with completely laminar boundary layers the foregoing leads to $v/V_0 = u/U_0$ or $K=1$. Since $U_{T.E.} = U_0$, it follows from (27) that

$$\begin{aligned} C_D[R, \Lambda] &= \cos\Lambda\, C_D[R\cos\Lambda, 0] \\ &= \cos^4\Lambda\, C_D[R, 0] \\ &= C_D[R/\cos\Lambda, 0]. \end{aligned} \qquad (30)$$

These results also follow directly from exact solutions of the boundary layer equations as can be seen from the following argument. The equations of motion are now

$$\left.\begin{aligned} u\frac{\partial u}{\partial x} + w\frac{\partial u}{\partial z} &= \nu\frac{\partial^2 u}{\partial z^2}, \\ u\frac{\partial v}{\partial x} + w\frac{\partial v}{\partial z} &= \nu\frac{\partial^2 v}{\partial z^2}, \end{aligned}\right\} \qquad (31)$$

and the equation of continuity is

$$\partial u/\partial x + \partial w/\partial z = 0.$$

Proceeding along classic lines, from the equation of continuity the existence of a stream function ψ is inferred such that $u = \partial\psi/\partial z$, $w = -\partial\psi/\partial x$, and assuming that $\psi = f(\eta)\sqrt{(\nu x U_0)}$, where $\eta = z\sqrt{[U_0/(\nu x)]}$ we derive the Blasius equation for $f(\eta)$ from the first equation of (31), namely

$$ff'' + 2f''' = 0. \qquad (32)$$

Writing $v = \partial\phi/\partial z$, and assuming ϕ is of the form $\phi = g(\eta)\sqrt{(\nu x U_0)}$, the second equation of (31) reduces to

$$\left.\begin{aligned} fg'' + 2g''' &= 0, \\ v &= U_0 g'. \end{aligned}\right\} \qquad (33)$$

with

From (32) and (33) it is seen that

$$f'''/f''=g'''/g'',$$

and hence $f'=\text{constant}\times g'+\text{constant}$. But $f'=u/U_0$, and $g'=v/U_0$, and since $u=0$, $v=0$, when z=0, and $u=U_0$, $v=V_0$, when $z=\infty$, we obtain finally

$$\frac{u}{U_0}=\frac{v}{V_0}.$$

As already noted, it follows that in this case the resultant flow in the boundary layer is everywhere parallel to the undisturbed flow. Equation (30) indicates that the drag coefficient is the same as that of an unyawed wing with chord equal to the distance from leading edge to trailing edge measured parallel to the direction of the undisturbed flow (*i.e.* $c/\cos\Lambda$) in a stream of velocity Q_0. This result is peculiar to laminar flow in the boundary layer and follows from the fact that for an unyawed wing $C_D \propto 1/R^{\frac{1}{2}}$. Any other C_D, R relation would not lead to this result even with the flow in the boundary layer everywhere parallel to the undisturbed stream flow.

3.3. *The spanwise flow in the turbulent boundary layer*

To obtain the value of $K_{T.E.}$ when the boundary layer is partly or wholly turbulent the following assumptions will be made:—

(*i*) The distribution of v/V_0 is the same for all x where the boundary layer is turbulent and is independent of the chordwise pressure gradient and therefore of the distribution of u/U_1.

(*ii*) The distribution of v/V_0 is then given by $v/V_0=(z/\delta)^m$, where m will be taken to be $\frac{1}{7}$.

It is highly unlikely that these assumptions describe exactly what happens in practice, but experimental evidence tending to indicate that they are sufficiently close to the truth for our purposes will be discussed subsequently (Section 5). It may be noted, however, that in the usual argument underlying the derivation of the power or "log" laws for the velocity distribution in the turbulent boundary layer on a flat plate, the development of the boundary layer with distance from the leading edge plays no direct part. From this point of view, the argument might be expected to apply rather more readily to the spanwise flow in the boundary layer of a yawed wing than in the accepted case of the chordwise flow in the boundary layer of an unyawed wing.

With these assumptions we can write

$$\frac{\theta_{yx}}{\theta_{xx}}=\frac{U_1}{V_0}\int_0^{\delta/\theta_{xx}}\frac{u}{U_1}\left[1-\left(\frac{z}{\theta_{xx}}\right)^{\frac{1}{7}}\left(\frac{\theta_{xx}}{\delta}\right)^{\frac{1}{7}}\right]d\left(\frac{z}{\theta_{xx}}\right).$$

From the evidence marshalled in Ref. 7 it may be assumed that u/U_1 is a function of z/θ_{xx} and H_x only, while θ_{xx}/δ is a function of H_x only. Hence we can write

$$\frac{\theta_{yx}}{\theta_{xx}}=\frac{U_0}{V_0}\left(\frac{U_1}{U_0}\right)K,$$

where K is now a function of H_x only, given by

$$K=K(H_x)=\int_0^{\delta/\theta_{xx}}\frac{u}{U_1}\left[1-\left(\frac{z}{\theta_{xx}}\right)^{\frac{1}{7}}\left(\frac{\theta_{xx}}{\delta}\right)^{\frac{1}{7}}\right]d\left(\frac{z}{\theta_{xx}}\right) \quad . \quad . \quad (34)$$

The function $K(H_x)$ can be readily determined using the curves of Ref. 7. The value of H_x can either be assumed to be a constant over the wing as in the method of profile drag calculation described in Ref. 6, or it can be calculated as part of the chordwise profile drag calculations as discussed in Ref. 7. Hence the value of H_x at the trailing edge can be determined, and therefore $K_{T.E.}$ can be calculated. Sample values of K are as follows:—

$$H_x=1.29,\ K=1;\quad H_x=1.4,\ K=0.910;\quad H_x=1.5,\ K=0.777.$$

Having determined K and H_x (and therefore $n=(H_x+5)/2$) at the trailing edge, the drag coefficient can be determined from equation (27).

For a flat plate at zero incidence it is reasonable to assume $u/U_0=v/V_0$, and hence $K=1$. In this case (27) reduces to

$$C_D[R,\Lambda]=C_D[R\cos\Lambda,0]\cos\Lambda. \quad . \quad . \quad . \quad (35)$$

For a fully turbulent boundary layer on the plate the $\frac{1}{7}^{\text{th}}$ power law leads to

$$C_D[R,0]=\text{constant}/R^{\frac{1}{5}}$$

Hence
$$C_D[R,\Lambda]=C_D[R,0]\cos^{\frac{1}{5}}\Lambda. \quad . \quad . \quad . \quad (36)$$

To illustrate the remarks made at the end of Section 3.2 it may be noted that in this case the drag coefficient of an unyawed flat plate with chord $=c/\cos\Lambda$ would be

$$C_D[R/\cos\Lambda,0]=C_D[R,0]\cos^{\frac{1}{5}}\Lambda \neq C_D[R,\Lambda],$$

in spite of the fact that the flow is everywhere parallel to the undisturbed stream direction.

4. Specimen Calculations and Results

The method described has been used to calculate the profile drag coefficient of a yawed wing of section N.A.C.A. 64-012 at zero incidences for angles of yaw up to 45°, for Reynolds numbers of 10^6, 10^7 and 10^8 and for various transition

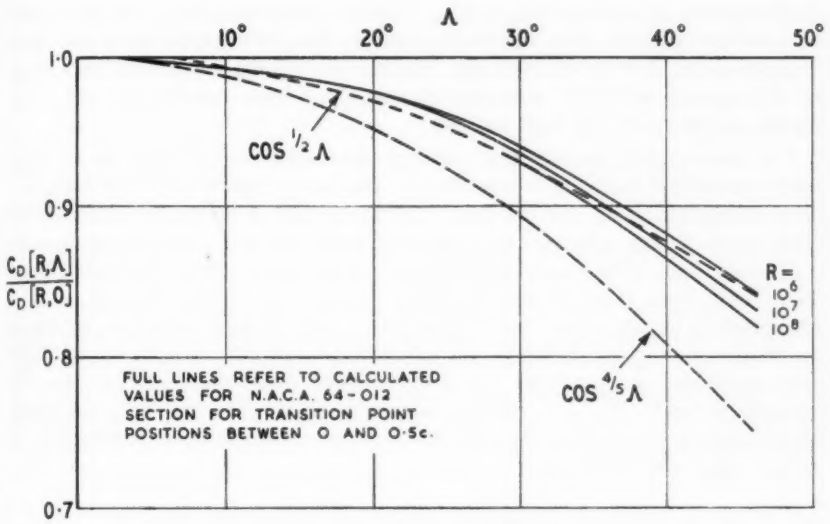

(a) N.A.C.A. 64-012 SECTION AT ZERO INCIDENCE

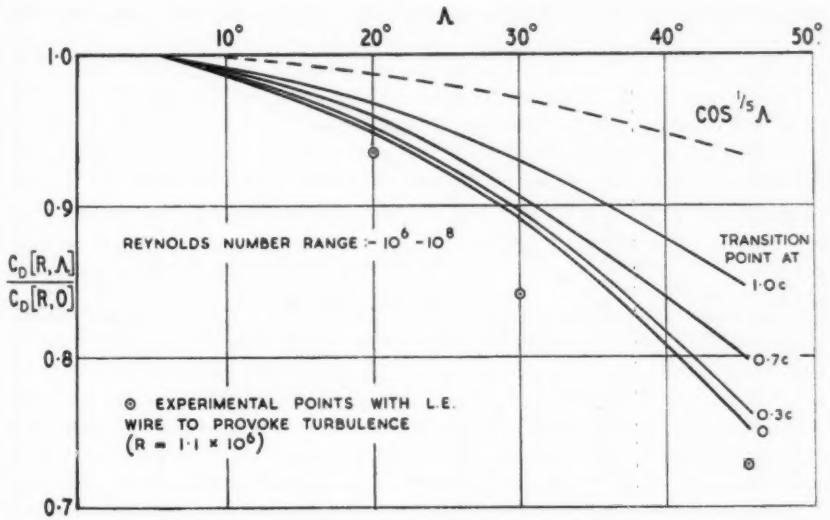

(b) FLAT PLATE

Fig. 2.

Calculated values of $C_D(R, \Lambda)/C_D(R, 0)$.

positions from the leading edge to 0.5c. Similar calculations, but covering a range of transition positions from the leading edge to the trailing edge, have also been made for a flat plate at zero incidence. For the aerofoil the calculations were made on the assumption that H_x was constant over the section and equal to 1.4. The results are shown in Fig. 2 (*a*) and (*b*).

It is of interest to note that although the variation with yaw of the drag coefficient of the flat plate is described by the factor $\cos^{\frac{1}{2}} \Lambda$ when the boundary layer is fully turbulent, and changes to the factor $\cos^{\frac{1}{2}} \Lambda$ as the transition moves back to the trailing edge, the corresponding factor for the wing section remains very closely $\cos^{\frac{1}{2}} \Lambda$ for transition positions between 0 and 0.5 c. The latter factor shows only slight variation with Reynolds numbers. It appears that for a wing, where there is usually a small positive pressure at the trailing edge helping to reduce the chordwise drag, the factor $(U_0/U_{\text{T.E.}})^{n-1}$ in equation (27) weights the spanwise drag component as compared with the chordwise drag component, so that the resultant factor $C_D[R, \Lambda]/C_D[R, 0]$ is somewhat higher than that for a flat plate. More extensive calculations are required to throw additional light on the effect of section shape and thickness.

5. Some Experimental Results

A few preliminary experiments have been made to check some of the assumptions of the theory and the results. The experiments were made on a flat

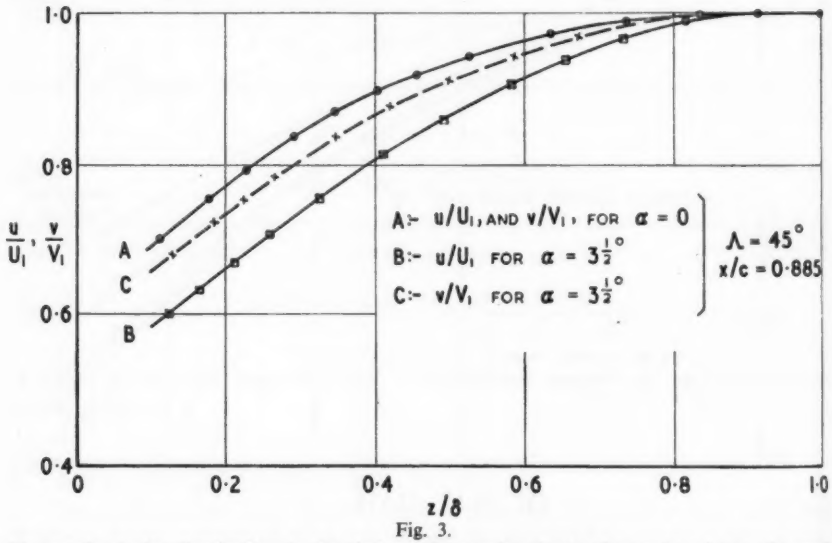

Fig. 3.

Measured velocity distributions in chordwise and spanwise planes of boundary layer of yawed flat plate at zero incidence and at incidence of 3½°.

plate of 19 in. chord extending across an open jet tunnel (jet dimensions 3 ft. 6 in. × 2 ft. 6 in.) of top speed about 125 ft./sec. giving a Reynolds number of about 1.2×10^6. It was intended to check (*a*) whether the flow in the turbulent boundary layer of the yawed plate at zero incidence was everywhere parallel to the undisturbed stream direction, (*b*) whether, with the plate at incidence, the spanwise velocity distribution was independent of the chordwise pressure gradient, and (*c*) whether the drag coefficient at zero incidence with a fully turbulent boundary layer obeyed the law given by equation (35).

Unfortunately, at the low Reynolds numbers of the tests it was impossible to secure a fully turbulent boundary layer or a sharp transition without the aid of a turbulence wire of such a size that its drag coefficient was an appreciable and not accurately known fraction of that of the plate. The experiments were made with the plate at zero incidence and at $3\frac{1}{2}°$ incidence with various angles of yaw up to 45°, and consisted of velocity and yawmeter traverses through the boundary layer at various stations aft of the leading edge. From these traverses the spanwise and chordwise velocity traverses were deduced as well as the drag coefficient of the part of the plate ahead of the traverse station.

The yawmeter traverses made at zero incidence with various angles of yaw showed no measurable deviation anywhere in flow direction from that of the undisturbed stream, thus checking the assumption that at zero incidence the chordwise and spanwise velocity distributions in the boundary layer were similar. Some of the spanwise and chordwise velocity distributions measured at $x/c = 0.855$ at 45° yaw and 0° and $3\frac{1}{2}°$ incidence are shown in Fig. 3. It will be seen that while the chordwise distribution shows a marked change of shape with change of incidence, the spanwise distribution shows comparatively little change. The latter falls between a $\frac{1}{5}^{\text{th}}$ and $\frac{1}{7}^{\text{th}}$ power law for regions in the boundary layer near the surface, but fits a somewhat smaller power than $\frac{1}{7}^{\text{th}}$ in the outer part of the layer.

Because of the lack of measurements very near the surface it is difficult to estimate the corresponding values of $H_v = (\delta_v^*/\theta_{vv})$ with satisfactory accuracy but the value appears to be about 1.4.

In this connection it may be noted that similar velocity traverses were made in the turbulent boundary layer of a yawed wing of finite span and are reported in Ref. 10. The wing was of elliptical plan form and of aspect ratio about 5.4; it was tested for an angle of yaw of 25° and at angles of incidence of 12° and 14°, at which latter incidence part of the wing was stalled. Nevertheless, even under these extreme conditions the velocity profiles of the spanwise flow showed themselves to be very nearly independent of the chordwise pressure gradients. An indication of this is the fact that the value of H_v for the spanwise profiles rarely deviated from a value within the range 1.3 to 1.5, while the corresponding values of H_r ranged from about 1.7 to 6.7. The evidence therefore tends to support the assumption that the form of the spanwise velocity distribution is relatively insensitive to the chordwise pressure gradients.

The measured ratios of the drag coefficients $C_D[R, \Lambda]/C_D[R, 0]$ are shown in Fig. 2(*b*) for comparison with the theory. It will be seen that the experimental results show an even greater reduction of drag coefficient with yaw than is given by the theoretical $\cos^{\frac{1}{2}} \Lambda$ law. This may well have been due to the drag contribution of the transition wire, which is almost entirely form drag and would vary as $\cos^3 \Lambda$.

It is of interest to note that the theory as developed in this paper leads to the following result for thickness at a given chordwise position of the fully turbulent boundary layer:—

$$\delta[R, \Lambda]/\delta[R, 0] = \cos^{-\frac{1}{2}} \Lambda,$$

where $\delta[\alpha, \beta]$ is the boundary layer thickness at the specified position for a Reynolds number equal to α and a yaw of angle β. This relation is shown in Fig. 4 for comparison with the measured values. The very close agreement between theory and experiment in this instance is probably in part fortuitous, but it is clear that the assumptions of the theory cannot be seriously wrong. For comparison the factor $\cos^{-\frac{1}{2}} \Lambda$ is also shown; this defines what the ratio $\delta[R, \Lambda]/\delta[R, 0]$ would

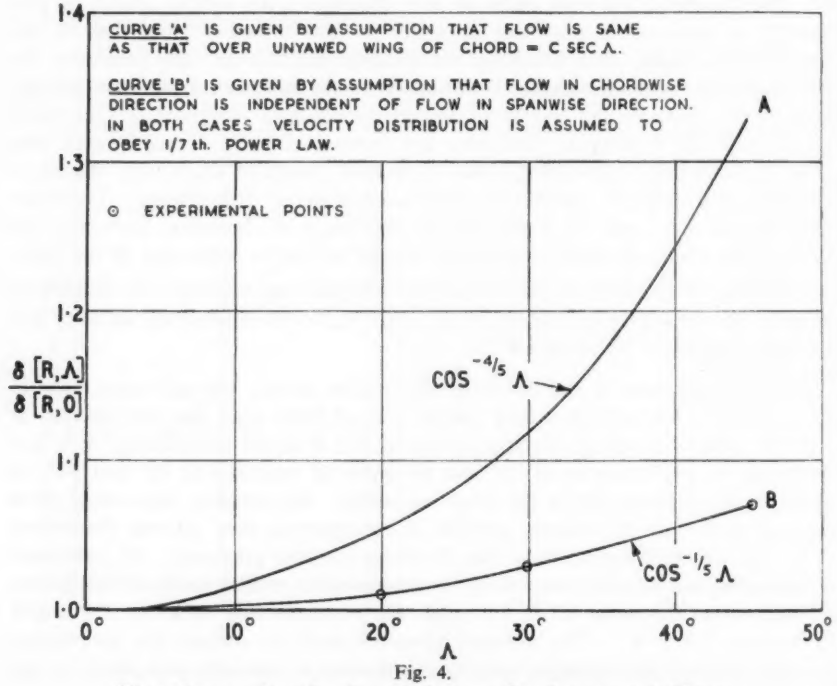

Fig. 4.

Effect of yaw on boundary layer thickness on flat plate at zero incidence.

be if the development of the boundary layer on the plate depended solely on the distance from the leading edge measured in the direction parallel to the undisturbed stream and was otherwise unaffected by yaw.

These experiments cannot be regarded as completely conclusive and further work is required, particularly at higher Reynolds numbers, but the results indicate that the assumptions made in the theory developed here are unlikely to lead to serious errors.

REFERENCES

1. PRANDTL, L. (1946). On Boundary Layers in Three-dimensional Flow. Volkenröde R. and T. No. 64, File No. B.I.G.S. 84, 1946.
2. SEARS, W. R. (1948). Boundary Layer of Yawed Cylinders. *Journal Aeronautical Sciences*, Vol. 15, January 1948, pp. 49-52.
3. WILD, J. M. (1949). Boundary Layer of Yawed Infinite Wings. *Journal Aeronautical Sciences*, Vol. 16, January 1949, pp. 41-45.
4. JONES, R. T. (1947). Effect of Sweepback on Boundary Layer and Separation. N.A.C.A. T.N. No. 1402, 1947.
5. GOLDSTEIN, S. (Editor) (1938). *Modern Developments in Fluid Dynamics*, Vol. I, Ch. III. Clarendon Press, Oxford, 1938.
6. SQUIRE, H. B. and YOUNG, A. D. (1937). The Calculation of the Profile Drag of Aerofoils. R. & M. 1838, 1937.
7. VON DOENHOFF, A. E. and TETERVIN, N. (1943). Determination of General Relations for the Behaviour of Turbulent Boundary Layers. N.A.C.A. Report No. 772, 1943.
8. NITZBERG, G. E. (1944). A Concise Theoretical Method for Profile Drag Calculation. N.A.C.A. A.C.R. No. 4B05, 1944.
9. YOUNG, A. D. (1949). Skin Friction in the Laminar Boundary Layer in Compressible Flow. *The Aeronautical Quarterly*, Vol. 1, August 1949, pp. 137-164.
10. KUETHE, A. M., MCKEE, P. B. and CURRY, W. H. (1949). Measurements in the Boundary Layer of a Yawed Wing. N.A.C.A. T.N. No. 1946, 1949.

Beams on Cross-Girders with Clamped Ends

J. M. KLITCHIEFF

(Professor of Applied Mechanics, The Technical University, Belgrade)

1. Introduction

In a previous paper[1] it was assumed that the cross-girders are freely supported at their ends. In practice these ends can often be considered as clamped ("built-in"), for example, a span of continuous bottom-girders of a ship between two transverse bulkheads.

In the following discussion it is assumed that the ends of the cross-girders are clamped, conditions at the ends of the main beams remaining arbitrary, as in Ref. 1.

Notation

$m-1$	total number of lateral loads, or of beams
x	distance of cross-section considered measured from left-hand end of cross-girder
L	length of cross-girder
l	length of beam
I	moment of inertia of cross-section of beam
J	moment of inertia of cross-section of cross-girder
$i=1,2,\ldots,m-1$	number corresponding to a particular lateral load or beam
ξ	value of x at point of application of load (*see* Fig. 1)
R	applied load (*see* Fig. 1)
M	total bending moment
M_i	bending moment due to pressure of beam number i
u	deflection of cross-girder
u_i	value of u at beam number i
$C_n, C'_n, C''_n \ldots$	coefficients of trigonometric series representing deflection curve of girder
E	Young's modulus

Paper received March 1951.

[The Aeronautical Quarterly, Vol. III, November 1951]

n, k, j	integers
R_i	pressure exerted by beam number i on the girder
Q	given lateral load acting on one beam
γ, β	coefficients in the relation $u_i = B(\gamma Q - \beta R_i)$
B	$l^3/(EI)$
B'	$L^3/(EJ)$
Ω	$[m/(8\beta\pi^4)](B'/B)$
δ	$[m/(8\beta\pi^4)]\gamma Q B'$
ϕ_n	defined by equation (16)
S	$\sum_{k=1}^{\infty}{}' C_k$
S_n	$\sum_{j=-\infty}^{\infty}{}' C_{\lvert n+2jm\rvert}$
S', S''	$\sum_{k=1}^{\infty}{}' C'_k$, $\sum_{k=1}^{\infty}{}' C''_k$ — and so on
S'_n, S''_n	$\sum_{j=-\infty}^{\infty} C'_{\lvert n+2kj\rvert}$, $\sum_{j=-\infty}^{\infty} C''_{\lvert n+2kj\rvert}$ — and so on

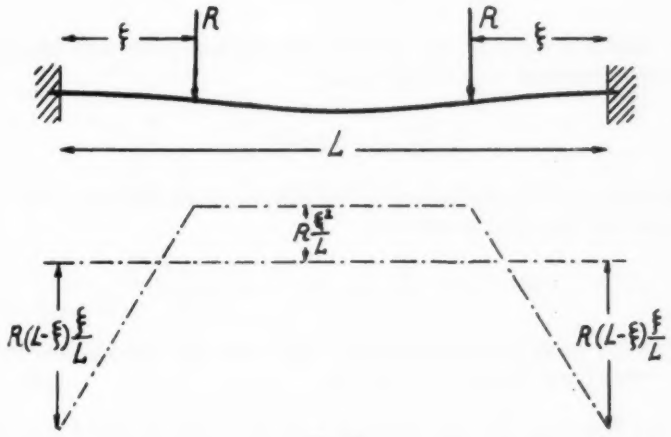

Fig. 1.

R'_i pressure exerted by beam number i on girders I and V

R''_i pressure exerted by beam number i on girders II and IV

$2R''_i$ pressure exerted by beam number i on central girder

} Assuming five girders numbered I-V as in Ref. 1

M'_i bending moment in first girder due to the pressures R'_i exerted by the beams i and $12-i$ (assuming eleven beams as in Ref. 1)

Σ' summation, in which the terms corresponding to the values of n which are multiples of m ($n=jm$), are not included

2. Built-in Cross-Girders

If a girder with clamped ends carries two equal and symmetrically situated loads (Fig. 1), the expression for the bending moment

$$M=\begin{cases} -R\left[\xi\left(1-\frac{\xi}{L}\right)-x\right], & \text{for } 0<x<\xi, \\ \frac{R\xi^2}{L}, & \text{for } \xi<x<L-\xi, \\ -R\left[\xi\left(1-\frac{\xi}{L}\right)-\left(L-x\right)\right], & \text{for } l-\xi<x<L. \end{cases}$$

can be developed in a Fourier series

$$M=-\frac{RL}{\pi^2}\sum_{n=1}^{\infty}\frac{1}{n^2}\left(1-\cos 2n\pi\frac{\xi}{L}\right)\cos 2n\pi\frac{x}{L}.$$

The deflection curve of any symmetrically loaded girder with clamped ends can also be represented by a Fourier series

$$u=\sum_{n=1}^{\infty}C_n\left(1-\cos 2n\pi\frac{x}{L}\right), \quad . \quad . \quad . \quad . \quad (1)$$

the coefficients C_n being determined by the distribution of the load. Thus, instead of equation (14) of Ref. 1, in this case

$$R_i=\frac{\gamma}{\beta}Q-\frac{1}{\beta B}\sum_{k=1}^{\infty}C_k\left(1-\cos 2k\pi\frac{i}{m}\right) \quad . \quad . \quad . \quad (2)$$

and the bending moment due to pressures exerted by a pair of symmetrically situated beams, number i and number $m-i$ will be

$$M_i=-\frac{L}{\pi^2}\left[\frac{\gamma}{\beta}Q-\frac{1}{\beta B}\sum_{k=1}^{\infty}C_k\left(1-\cos 2k\pi\frac{i}{m}\right)\right]\sum_{n=1}^{\infty}\frac{1}{n^2}\left(1-\cos 2n\pi\frac{i}{m}\right)\cos 2n\pi\frac{x}{L}.$$

If the total number of beams is an *even* one, the bending moment due to pressures exerted by all of them, is

$$M=\sum_{i=1}^{\frac{1}{2}(m-1)} M_i=-\frac{L}{\pi^2}\left[\frac{\gamma}{\beta}Q\sum_{n=1}^{\infty}\frac{1}{n^2}\sum_{i=1}^{\frac{1}{2}(m-1)}\left(1-\cos 2n\pi\frac{i}{m}\right)\cos 2n\pi\frac{x}{L}-\right.$$

$$\left.-\frac{1}{\beta B}\sum_{k=1}^{\infty}C_k\sum_{i=1}^{\frac{1}{2}(m-1)}\left(1-\cos 2k\pi\frac{i}{m}\right)\sum_{n=1}^{\infty}\frac{1}{n^2}\left(1-\cos 2n\pi\frac{i}{m}\right)\cos 2n\pi\frac{x}{L}\right]. \quad . \quad . \quad . \quad . \quad . \quad . \quad (3)$$

Using the known expression for the sum of trigonometric polynomials

$$\tfrac{1}{2}+\sum_{k=1}^{n}\cos k\theta=\tfrac{1}{2}\frac{\sin(n+\frac{1}{2})\theta}{\sin\frac{1}{2}\theta},$$

it can be proved that

$$\sum_{i=1}^{\frac{1}{2}(m-1)}\left(1-\cos 2n\pi\frac{i}{m}\right)=\left\{\begin{array}{l}0 \text{ if } n \text{ is a multiple of } m,\\ \tfrac{1}{2}\,m \text{ for all other values of } n,\end{array}\right\} \quad . \quad (4)$$

and that

$$\sum_{i=1}^{\frac{1}{2}(m-1)}\left(1-\cos 2k\pi\frac{i}{m}\right)\left(1-\cos 2n\pi\frac{i}{m}\right)=\left\{\begin{array}{l}0 \text{ if } n \text{ or } k \text{ is a multiple of } m,\\ \tfrac{3}{4}\,m \text{ if } k=|n\pm 2jm|,\ (j=0,1,2\ldots),\\ \tfrac{1}{2}\,m \text{ for all other values of } k.\end{array}\right\}$$

. . . . . (5)

Thus, expression (3) becomes

$$M=-\frac{L}{\pi^2}\frac{m}{2}\left[\frac{\gamma}{\beta}Q\sum_{n=1}^{\infty}{}'\frac{1}{n^2}\cos 2n\pi\frac{x}{L}-\right.$$

$$\left.-\frac{1}{\beta B}\left(\sum_{k=1}^{\infty}C_k\sum_{n=1}^{\infty}{}'\frac{1}{n^2}\cos 2n\pi\frac{x}{L}+\frac{1}{2}\sum_{j=-\infty}^{\infty}{}'C_{|n+2jm|}\sum_{n=1}^{\infty}{}'\frac{1}{n^2}\cos 2n\pi\frac{x}{L}\right)\right], \quad . \quad . \quad . \quad . \quad . \quad . \quad (6)$$

where the terms corresponding to the values of n which are multiples of m ($n=jm$), are not included in Σ'.

If the total number of beams is an *uneven* one, the left hand side of (4) must be replaced by

$$\sum_{i=1}^{\frac{1}{2}m}\left(1-\cos 2n\pi\frac{i}{m}\right)-\tfrac{1}{2}(1-\cos n\pi), \quad . \quad . \quad . \quad (7)$$

and the left hand side of (5) by

$$\sum_{i=1}^{\frac{1}{2}m}\left(1-\cos 2i\pi\frac{k}{m}\right)\left(1-\cos 2i\pi\frac{n}{m}\right)-\tfrac{1}{2}(1-\cos k\pi)(1-\cos n\pi). \quad . \quad (8)$$

It can be proved in a similar manner that these sums are also equal to the values given by the right hand side of (4) and (5) respectively.

Thus the expression (6) holds for *any* number of beams. Introducing it into the differential equation of the deflection curve of the girder it becomes

$$\frac{C_n}{\delta}+\frac{\Omega}{n^4}\left(\frac{S}{\delta}+\tfrac{1}{2}\frac{S_n}{\delta}\right)=\frac{1}{n^4}, \quad . \quad . \quad . \quad . \quad . \quad (9)$$

where

$$S=\sum_{k=1}^{\infty}{}'C_k,\quad S_n=\sum_{j=-\infty}^{\infty}{}'C_{|n+2jm|}, \quad . \quad . \quad . \quad . \quad (10)$$

and

$$\Omega=\frac{m}{8\beta\pi^4}\frac{B'}{B},\quad \delta=\frac{m}{8\beta\pi^4}\gamma Q B'. \quad . \quad . \quad . \quad . \quad (11)$$

With $n=1, 2, \ldots, m-1, m+1, m+2, \ldots$ equation (9) represents a system of an infinite number of linear equations for calculating the coefficients C_n. In every particular case it can easily be solved by the method of successive approximations. It can be solved in the general form also; the corresponding method is developed in the Appendix, mainly as a demonstration of the convergency of the series (1).

3. Several Built-in Cross-Girders.

The method described in Section 2 will be applied to the example discussed in Section 4 of Ref. 1, but assuming now that the ends of the cross-girders are clamped.

Equations (19) of Ref. 1 must be replaced in this case by

$$\left.\begin{aligned}
R'_i&=\frac{1}{26}\left[\frac{118}{24}Q-\frac{6^4}{B}\sum_{k=1}^{\infty}\left(44C'_k-46C''_k+18C'''_k\right)\left(1-\cos k\pi\frac{i}{6}\right)\right],\\
R''_i&=\frac{1}{26}\left[\frac{100}{24}Q-\frac{6^4}{B}\sum_{k=1}^{\infty}\left(-46C'_k+80C''_k-46C'''_k\right)\left(1-\cos k\pi\frac{i}{6}\right)\right],\\
R'''_i&=\frac{1}{26}\left[\frac{53}{24}Q-\frac{6^4}{B}\sum_{k=1}^{\infty}\left(18C'_k-46C''_k+31C'''_k\right)\left(1-\cos k\pi\frac{i}{6}\right)\right],
\end{aligned}\right\} \quad (12)$$

and the bending moment in the *first* girder, due to the pressures R_i exerted by the beams numbered i and $12-i$, is

$$M'_i = -\frac{L}{\pi^2}\frac{1}{26}\Big[\frac{118}{24}Q\sum_{n=1}^{\infty}\frac{1}{n^2}\Big(1-\cos n\pi\frac{i}{6}\Big)\cos 2n\pi\frac{x}{L} -$$

$$-\frac{6^4}{B}\sum_{k=1}^{\infty}\Big(44\,C'_k-46\,C''_k+18\,C'''_k\Big)\Big(1-\cos k\pi\frac{i}{6}\Big)\sum_{n=1}^{\infty}\frac{1}{n^2}\Big(1-\cos n\pi\frac{i}{6}\Big)\cos 2n\pi\frac{x}{L}\Big].$$

Thus, the total bending moment due to the pressures exerted on the first girder by all beams becomes

$$M' = -\frac{L}{\pi^2}\frac{1}{26}\sum_{n=1}^{\infty}{}'\Big[\frac{118}{4}Q-\frac{6^5}{B}\sum_{k=1}^{\infty}\Big(44\,C'_k-46\,C''_k+18\,C'''_k\Big)+$$

$$+\tfrac{1}{2}\sum_{j=-\infty}^{\infty}{}'\Big(44\,C'_{|n+24j|}-46\,C''_{|n+24j|}+18\,C'''_{|n+24j|}\Big)\Big]\frac{1}{n^2}\cos 2n\pi\frac{x}{L}.$$

From the differential equation for the deflection curve of the first girder, it follows that

$$C'_n n^2 EJ\Big(\frac{2n\pi}{L}\Big)^2 = \frac{L}{\pi^2}\frac{1}{26}\Big\{\frac{118}{4}Q-\frac{6^5}{B}[44\,(S'+\tfrac{1}{2}S'_n)-46\,(S''+\tfrac{1}{2}S''_n)+18\,(S'''+\tfrac{1}{2}S'''_n)]\Big\}, \qquad (13)$$

with the notation

$$S'=\sum_{k=1}^{\infty}C'_k,\quad S''=\sum_{k=1}^{\infty}C''_k,\quad S'''=\sum_{k=1}^{\infty}C'''_k,$$

$$S'_n=\sum_{j=-\infty}^{\infty}{}'C'_{|n+24j|},\quad S''_n=\sum_{j=-\infty}^{\infty}{}'C''_{|n+24j|},\quad S'''_n=\sum_{j=-\infty}^{\infty}{}'C'''_{|n+24j|}.$$

Equation (13) and two similar equations for the second and third girder can be written in the form

$$\left.\begin{aligned}
&C'_n+\frac{6^5}{104\,\pi^4}\frac{B'}{B}\frac{1}{n^4}[44\,(S'+\tfrac{1}{2}S'_n)-46\,(S''+\tfrac{1}{2}S''_n)+18\,(S'''+\tfrac{1}{2}S'''_n)]=\frac{B'}{104\,\pi^4}\frac{118}{4}Q\frac{1}{n^4},\\
&C''_n+\frac{6^5}{104\,\pi^4}\frac{B'}{B}\frac{1}{n^4}[-46\,(S'+\tfrac{1}{2}S'_n)+80\,(S''+\tfrac{1}{2}S''_n)-46\,(S'''+\tfrac{1}{2}S'''_n)]=\frac{B'}{104\,\pi^4}\frac{100}{4}Q\frac{1}{n^4},\\
&C'''_n+\frac{6^5}{104\,\pi^4}\frac{B'}{B}\frac{1}{n^4}[18\,(S'+\tfrac{1}{2}S'_n)-46\,(S''+\tfrac{1}{2}S''_n)+31\,(S'''+\tfrac{1}{2}S'''_n)]=\frac{B'}{104\,\pi^4}\frac{53}{4}Q\frac{1}{n^4}.
\end{aligned}\right\} \qquad (14)$$

This system of equations, as system (9), can be solved easily in every particular case by the method of successive approximations. For example, for $B'/B=0.438$,

$$C'_1=49.1\frac{QB'}{416\pi^4},\quad C''_1=77.5\frac{QB'}{416\pi^4},\quad C'''_1=84.8\frac{QB'}{416\pi^4},$$

$$C'_2=3.8\frac{QB'}{416\pi^4},\quad C''_2=5.1\frac{QB'}{416\pi^4},\quad C'''_2=5.0\frac{QB'}{416\pi^4},$$

$$C'_3=0.6\frac{QB'}{416\pi^4},\quad C''_3=0.9\frac{QB'}{416\pi^4},\quad C'''_3=1.0\frac{QB'}{416\pi^4}.$$

The method for solving equations (14) in the general form is similar to that given in the Appendix for system (9).

APPENDIX

Solution of the System of Equations (9) in the General Form

It may be noted that

$$S_{n+m}=C_{n+m}+C_{n+2m}+\ldots+C_n+C_{|n-m|}+C_{|n-2m|}+\ldots=S_n,$$

$$S_{|n-m|}=C_{|n-m|}+C_{|n-2m|}+\ldots+C_n+C_{n+m}+C_{n+2m}+\ldots=S_n,$$

and that generally $S_{|n\pm 2jm|}=S_n$.

Thus, replacing n in equation (9) successively by $n+2m$, $n+4m$, ..., $|n-2m|$, $|n-4m|$, ... and adding all the equations obtained to equation (9), gives

$$S_n+\Omega(S+\tfrac{1}{2}S_n)\sum_{j=-\infty}^{\infty}\frac{1}{(n+2jm)^4}=\delta\sum_{j=-\infty}^{\infty}\frac{1}{(n+2jm)^4},$$

or

$$S+\tfrac{1}{2}S_n=\frac{S+\frac{1}{2}\delta\phi_n}{1+\frac{1}{2}\Omega\phi_n}, \qquad (15)$$

where

$$\phi_n=\sum_{j=-\infty}^{\infty}\frac{1}{(n+2jm)^4}=\frac{\pi^4}{48m^4}\left(1+\cot^2\frac{n\pi}{2m}\right)\left(1+3\cot^2\frac{n\pi}{2m}\right). \qquad (16)$$

Introducing expression (15) into equation (9) it becomes

$$C_n + \frac{\Omega}{n^4}\frac{S+\frac{1}{2}\delta\phi_n}{1+\frac{1}{2}\Omega\phi_n} = \frac{\delta}{n^4}.$$

Adding together all such equations for $n=1, 2, \ldots$ gives

$$S+\Omega S \sum_{n=1}^{\infty}{}' \frac{1}{n^4(1+\frac{1}{2}\Omega\phi_n)} + \tfrac{1}{2}\Omega\delta \sum_{n=1}^{\infty}{}' \frac{\phi_n}{n^4(1+\frac{1}{2}\Omega\phi_n)} = \delta \sum_{n=1}^{\infty}{}' \frac{1}{n^4},$$

or

$$\frac{S}{\delta}\left[1+\Omega \sum_{n=1}^{\infty}{}' \frac{1}{n^4(1+\frac{1}{2}\Omega\phi_n)}\right] = \sum_{n=1}^{\infty}{}' \frac{1}{n^4(1+\frac{1}{2}\Omega\phi_n)} \quad . \quad . \quad (17)$$

First, the value of S given explicitly by equation (17) must be introduced into (15), then the expression obtained for $S+\frac{1}{2}S_n$ is introduced into (9), which then gives the value of C_n explicitly.

The solution of the problem in its general form can be reduced to the solution of three independent systems of equations, the number of unknowns in every system being equal to the number of unsymmetrical cross-girders only, instead of being equal to the number of intersections, as it would be if the usual method were applied.

Reference

1. Klitchieff, J. M. (1950). Beams on Elastic Supports and on Cross-Girders. *The Aeronautical Quarterly*, Vol. II, November 1950.

A Direct Aerodynamic Proof of the Biot-Savart Law

J. LOCKWOOD TAYLOR
(Institutt for Flyteknikk, Norges Tekniske Hogskole)

The expression for the induced velocity of a vortex element,

$$dq = \frac{Kh \,.\, ds}{4\pi r^3}$$

in Glauert's notation (where K is the strength of the vortex, **h** the length of the normal, and **r** the distance from the field point to the element, of length **ds**) which is often known as the Biot-Savart law, and is of fundamental importance in aerodynamics, is frequently left unproved in textbooks. Sometimes reference is made to the electro-magnetic analogy, or to a standard treatise such as Lamb. One well-known work implies that the law is the solution of an integral equation derived from the known induced velocity of an infinite straight-line vortex, but this is misleading, since there is an infinite number of solutions, of which only one is correct. Another textbook gives a lengthy argument starting from the replacement of a line vortex by a sheet of sources and sinks, which is probably not too convincing to the average student. Lamb himself gives a long and rather involved proof based on Helmholtz and Stokes, with appeals to the Theory of Attractions, with which few are likely to be familiar. A simple and direct proof from fluid mechanics seems therefore worth while.

If the law can be established for an elementary square or rectangle, *i.e.* if it can be shown that the total induced velocity of a line vortex of this form is the same as would be obtained by summing the elements **dq** (or their components, since **q** is a vector) then it can be regarded as proved for a closed line vortex of any form, plane or not, since it is well known that the area or surface enclosed can be cut up into rectangles, and that the sum of these rectangles, regarded as line vortices, is equivalent to the original contour enclosing them. It is very easy to prove the law for a rectangular line vortex, since a direct solution for the velocity field and potential can be written down.

Consider first the velocity potential represented by

$$\phi = \tan^{-1} \frac{xy}{zr}$$

Received November 1951.
[The Aeronautical Quarterly, Vol. III, November 1951]

in the usual Cartesian co-ordinates, with $r^2=x^2+y^2+z^2$. Near the x-axis, $y=z=0$ nearly and $|x|=r$ very nearly, so that

$$|\phi|=\tan^{-1}\frac{y}{z}$$

as for a two-dimensional vortex, but since **r** is always positive, the sign of ϕ changes with **x**, so that the direction of the vorticity is reversed at the origin. Similarly along the y-axis. Hence altogether the expression for ϕ applies to a cruciform vortex, with a reversal in sign at the origin, where the two lines intersect.

Now consider

$$\phi=\tan^{-1}\frac{x_1 y_1}{zr_1}-\tan^{-1}\frac{x_2 y_2}{zr_2}+\tan^{-1}\frac{x_3 y_3}{zr_3}-\tan^{-1}\frac{x_4 y_4}{zr_4},$$

where the suffixes 1, 2, 3, 4 refer to the successive corners of a rectangle. The outlying parts of the four cruciform line vortices cancel each other, leaving the required solution for a rectangular line vortex. It is a matter of simple algebra to verify that the induced velocities according to the expression for ϕ just given are in fact in accordance with the Biot-Savart law. The general proof for any vortex follows, as previously indicated. If it be argued that the proof applies strictly to the whole vortex only, and not to the element, this is quite correct: the law itself applies only to the vortex as a whole (although it is stated for the element), since the element **ds** can exist only as part of the whole vortex.

A REVIEW

Laws of Free Turbulence *H. Reichardt. V.D.I. Forschungsheft No.* 414, *2nd impression. Deutscher Ingenieur-Verlag, G.M.B.H., Dusseldorf.* 1951. 30 *pp. Illustrated.* 12.50 *Dm.*

The first impression of this paper appeared in 1942 (*see* R.T.P. Trans. 1752). This present edition includes all the original data with only slight modifications and additions. For example, a new chapter on momentum and heat exchange is included.

Free turbulence problems consist of those cases of turbulent flow in which wall effects are not present. The more important cases are those of free jets and wakes.

The analysis of such problems can be divided into either the phenomenological or the statistical approach. In this paper the statistical nature of the turbulent flow is not discussed. The former approach, which was originated by Reynolds, owes its main impetus to the "mixing length" concept by Prandtl and the later developments due to Prandtl, Taylor and Kármán. Their respective theories, namely the momentum, vorticity and similarity theories, enabled mean velocity and temperature distributions to be predicted with reasonable certainty. It was noticeable however, that systematic changes from the predicted values, especially in the first and second derivatives of the main mean velocity, did occur and such changes could not be dismissed as being due to experimental errors. Recent measurements have shown that the distributions and magnitudes of the turbulent velocities which are assumed in the "mixing length" theories are often incorrect and misleading. What is more important is the fact stated by Reichardt that all the main results in these "mixing length" theories can be deduced from dimensional considerations alone.

Reichardt introduces a new theory of turbulence which is based on the results obtained from careful measurements of mean velocity and velocity gradient under conditions of free turbulence. The main objection to this inductive approach is naturally the fact that since the theory is based on distributions of mean velocity the results can hardly be expected to predict accurate distributions of turbulent velocity and to throw light on the physics of the turbulence producing the phenomenon.

From the hydrodynamical equations of motion and continuity, and assuming that the longitudinal mean velocity distribution can be represented by the error law function, Reichardt derives expressions for the mean lateral velocity, the turbulent shear stress (or Reynolds stress) and the mean transport of longitudinal momentum in the transverse direction. Direct comparison with measured results leads to a general theorem which states that "The mean flux of the longitudinal momentum which wanders in the transverse direction is equal to the mean longitudinal momentum gradient in this direction multiplied by a function, having the units of a length, which is independent of this direction." This function, which is analogous to the "mixing length," but unlike it, has no direct physical significance. This theorem, together with certain predictions from the theory cannot be accepted without further experimental verification.

In conclusion it should be stated that Reichardt's theory, although in many ways more logical than the early mixing length theories, still has many serious objections. At the best it may be regarded as an empirical theory for the determination of the distributions of mean velocity under conditions of free turbulence.